ENVIRONMENTAL PHOTOOXIDATION AND MIXTURE TOXICITY OF POLYCYLIC AROMATIC HYDROCARBONS

by

Brendan McConkey

A thesis

presented to the University of Waterloo

in fulfilment of the thesis requirement for the degree of

Doctor of Philosophy

in

Biology

Waterloo, Ontario, Canada, 1999

© Brendan McConkey 1999

The University of Waterloo requires the signatures of all persons using or photocopying this thesis. Please sign below, and give address and date.

ABSTRACT

Exposure of polycyclic aromatic hydrocarbons (PAHs) to light has been shown to result in an increase in toxicity of PAHs to aquatic organisms. The observed increase in toxicity is a general phenomenon, and has been observed in bacteria, plants, invertebrates and fish. Two mechanisms of action for this increase in toxicity are photosensitization (production of singlet oxygen) and photooxidation, whereby the oxidation products are more toxic than the parent PAHs. Either may have the greater effect, depending on the organism and the exposure history. Previously, specific toxic products of PAH photooxidation have not been well characterised. Furthermore, PAHs and PAH photoproducts exist almost exclusively as complex mixtures in environmental compartments, and methods for addressing mixture toxicity are required.

PAH photoproducts were generated by exposing PAHs, either in solution or in bound phase, to natural sunlight or a light source mimicking solar radiation. The generated photooxidation products were identified by GC/MS, HPLC/diode array, and/or by comparison with authentic standards. Photooxidation experiments were conducted with two to five ring PAHs, specifically naphthalene, phenanthrene, fluoranthene, pyrene, benzo(a)anthracene, benzo(b)anthracene, chrysene, and benzo(a)pyrene. The toxicity of observed photoproducts was addressed either by the use of toxicity assays, or reference to published toxicity data. The primary organism used to estimate the relative toxicity of PAH photoproducts and intact PAHs was the luminescent marine bacteria, *Photobacterium phosphoreum*. It was found in many cases that the products of PAH photooxidation were more toxic than the intact PAHs. The observed toxicity was further corroborated by toxicity assessment using other species as test organisms. PAH quinones were identified as a class of compounds frequently having greater toxicity than the intact PAHs. Some observed photoproducts were also previously identified as toxicants or mutagens, resulting from metabolism of PAHs in mammalian systems.

Two factors influencing the photodegradation rates of PAHs were identified. The ability of PAHs to generate singlet oxygen by photosensitization reactions was related to PAH reaction rates, as was the change in the delocalization energy of PAH electronic orbitals on oxidation. Changes in delocalization energy were also used to predict thermodynamically favoured oxidation products.

PAHs occur in environmental compartments as complex mixtures, and each PAH may produce several major photoproducts. Thus, a means to assess the toxicity of a mixture of PAHs and PAH photoproducts is needed. 'Fractional simplex designs' were generated to address the toxicity of complex mixtures. These designs provide a means to screen for interactions and to investigate the behaviour of many-component mixtures as a whole, without extensive data requirements. One of these designs was used to investigate interactions within a group of PAHs and PAH photoproducts, using the *P. phosphoreum* toxicity assay. For the given mixture of chemicals and the bacterial toxicity assay, a concentration additive model of interaction was found to be a good descriptor of the data set, though a trend to slightly greater than additive interaction was observed for some mixtures.

ACKNOWLEDGEMENTS

also to Craig, Bill, and Sue for their input along the way. I wish you all the best, and I'm sure our paths will cross many times to come.

Table of Contents

List of Tables

List of Figures

CHAPTER 1

INTRODUCTION

The field of environmental toxicology has developed over the last several decades in response to increasing public awareness of environmental issues. As members of a modern, industrialised society, we are in the position of being able to consciously influence what impacts we have on the environment around us, and to what degree. Unfortunately, the myopic tendencies of our society usually cause us to underestimate the long-term impacts that we have on our environment in favour of more immediate economic gains – we tend to live off the capital of environmental resources, instead of living off the interest. This comes at the expense of most other organisms with which we share our environment.

Impacts on ecosystems can be divided into two broad, non-exclusive categories: loss of habitat specific to a given ecosystem, and degradation of habitat. Loss of habitat may be the result of harvesting of natural resources such as forests or mineral deposits to fuel the economy, or through encroachment by urban sprawl. Degradation of habitat may occur via the introduction of chemical and physical agents that impair ecosystem function, or by the repositioning of chemical or physical agents currently within an ecosystem. Habitat loss and degradation are recognised as harmful, and efforts are taken by society to reduce environmental impact. Resource management and urban planning tangentially address habitat loss, and environmental toxicology addresses degradation of habitat by chemical or physical agents.

Environmental toxicology can be defined as the study of the impacts of contaminants on the structure and function of ecological systems (Landis and Yu 1995), at various levels of organisation from genetic and molecular, through individual organisms, to populations, communities and ecosystems (Rand et al. 1995). Environmental toxicology is a multidisciplinary science, borrowing from a variety of disciplines including chemistry, biology, physics, limnology, ecology, mathematics and statistics. This thesis is a reflection of the interdisciplinary nature of the field, and draws from several fields of study, as required to address specific questions. Here, the

theme uniting these disciplines is the environmental fate and toxicology of polycyclic aromatic hydrocarbons and their degradation products.

Polycyclic aromatic hydrocarbons (PAHs) are widely distributed environmental contaminants, occurring in sediment, freshwater, atmospheric and marine environments. Deleterious environmental impacts due to PAHs are recognised as an issue of environmental importance. The toxicity of this family of compounds is a complex problem, as there is no one dominant mode of action. Depending on the organism and the environment in which it is exposed to PAHs, there are several possible modes of toxic action by which PAHs may have effects.

One possible source of toxicity associated with PAHs is through the formation of oxidation products by exposure of PAHs to light. These photochemical reactions can occur in both the atmosphere and within aquatic systems. The photochemical reactions of PAHs, the toxicity of the photoproducts, and methods of assessing the toxicity of complex mixtures are addressed in this thesis. As PAHs and PAH photoproducts occur almost exclusively as mixtures in natural systems, an effort was made to address the means by which the toxicity of complex mixtures may be assessed. This resulted in the generation of novel experimental designs to investigate interactions within multi-component mixtures.

1.1 Chemical properties, Sources, and Occurrence of PAHs

Polycyclic aromatic hydrocarbons (PAHs) are a class of hydrocarbons containing two or more fused benzene rings (Neff 1979). The most frequently occurring PAHs contain two to five aromatic rings. Sample structures of some of the more common PAHs are shown in Figure 1.1. Polycyclic aromatic compounds containing nitrogen, sulphur, or oxygen, which are functionally and chemically related to PAHs, are sometimes included within the PAH family (Varanasi, 1989). Oxygenated polycyclic aromatics (oxyPAHs) are frequent products of PAH photoreactions, and specific oxyPAHs will be discussed in detail in later chapters.

PAHs are only slightly soluble in water, and will partition out of the water phase and into both sediments and the lipids within organisms. One means of estimating the tendency of a

2

Naphthalene   Fluorene   Anthracene   Phenanthrene

Benzo[b]anthracene   Benzo[a]anthracene   Chrysene

Pyrene   Fluoranthene   Benzo[b]fluoranthene   Benzo[k]fluoranthene

Benzo[a]pyrene   Benzo[e]pyrene   Dibenzo[a,i]anthracene

Perylene   Indeno[123-cd]pyrene   Benzo[ghi]perylene
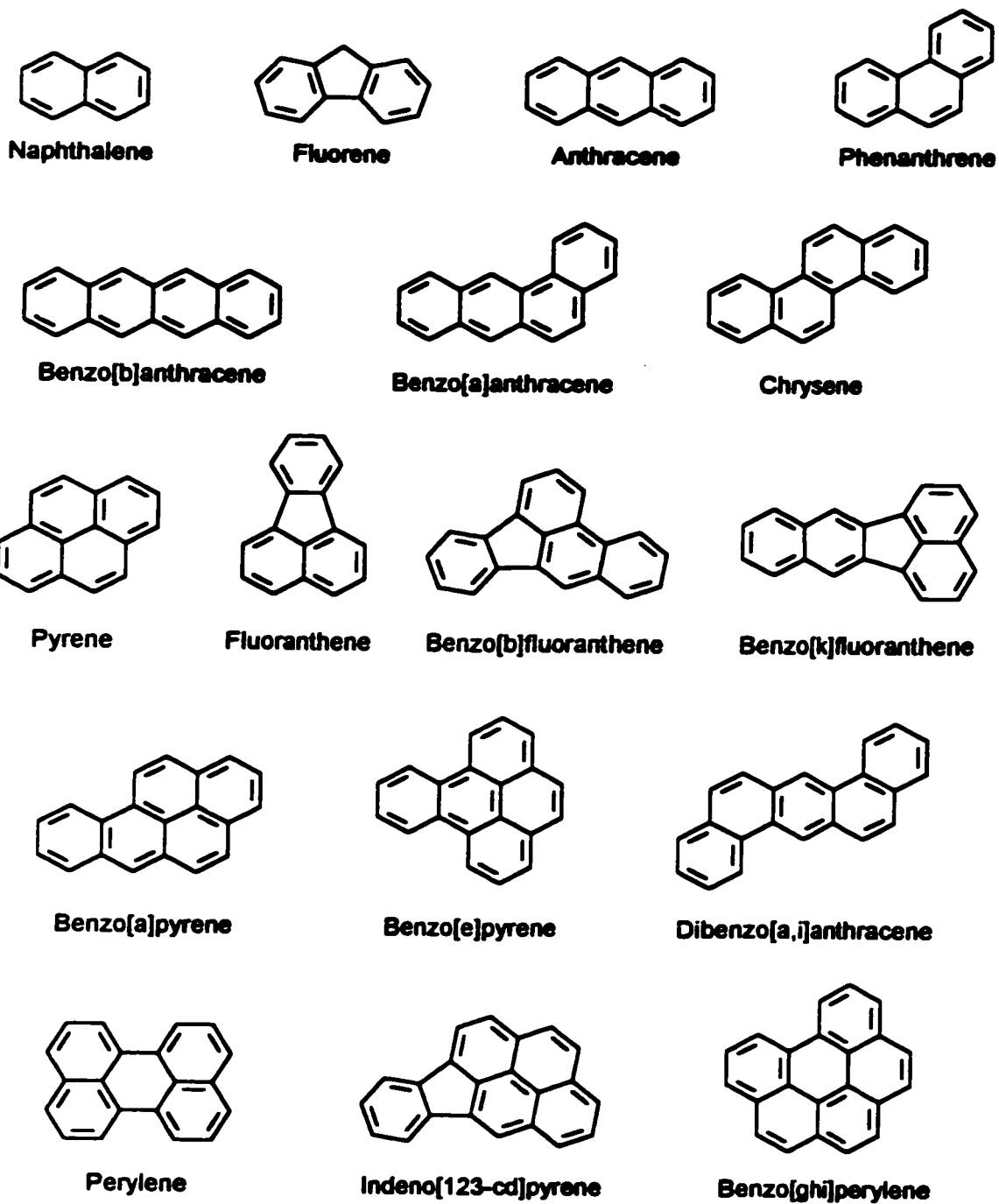
Figure 1.1: Chemical structures of some commmon PAHs.

chemical to partition into lipids is via the octanol/water partition coefficient, or K_{ow}. The K_{ow} of a substance is the ratio of its concentrations (at equilibrium) when the substance is distributed between two immiscible liquids, octanol and water. Higher K_{ow} values imply that the chemical will partition into lipids within organisms to a greater degree, and thus can be more available to elicit a toxic effect (Lipnick 1995). Both the solubility and the octanol/water partition coefficient are dependent on the structure and molecular weight of the PAH, with a general trend towards decreasing aqueous solubility and increasing K_{ow} with increasing molecular weight (Table 1.1). The chemical properties of PAHs have a large influence on their interactions of PAHs with biota. An exception to the increased uptake by organisms with increasing K_{ow} occurs for the high molecular weight PAHs, as uptake of some of the larger PAHs does not occur with a high efficiency in some organisms (van Brummelen et al. 1996).

Table 1.1: Physiochemical properties of representative PAHs. K_{ow} is the octanol/water partition coefficient.

Compound	Molecular weight	Solubility, mg/L[1]	Log K_{ow} range[2]
Naphthalene	128	31.7 ± 0.2	3.3 – 3.5
Fluorene	166	1.98 ± 0.04	3.8 – 4.2
Anthracene	178	0.073 ± 0.005	4.4 – 4.7
Phenanthrene	178	1.290 ± 0.070	4.4 – 4.6
Fluoranthene	202	0.260 ± 0.020	5.1 – 5.3
Pyrene	202	0.135 ± 0.005	4.8 – 5.3
Benzo[a]anthracene	228	0.014 ± 0.0002	5.6 – 5.9
Chrysene	228	0.002 ± 0.0002	5.6 – 5.8
Benzo[a]pyrene	252	0.003 ± 0.001	6.0 – 6.1
Benzo[k]fluoranthene	252	0.0017	6.0 – 6.1

[1] from Mackay and Shiu 1977, Neff 1985

[2] from van Brummelen 1995

PAHs in the absence of light are relatively inert compounds. However, due to the highly conjugated aromatic structure of PAHs they readily absorb UV or visible light, changing the

electronic configuration of the molecule to an unstable excited state (Gilbert and Baggott 1991). This changes the chemistry of PAHs significantly as the electronically excited states of PAHs, while short lived, are far more reactive than the ground state (Malkin 1992) .

The major source of environmental PAHs is the incomplete combustion or cracking of organic material (Suess, 1976; Neff, 1985). Sources of PAHs include industrial activity, automobiles, volcanoes, and forest fires. Biosynthesis of PAHs can also occur to a small degree (Graf and Diel 1966; Borneff et al. 1968), but by far the largest sources are anthropogenic. It has been estimated that 230,000 tons of PAH enter aquatic environments each year (Newsted and Giesy 1987; Eisler, 1987). Contributors to the aquatic environment include surface runoff, atmospheric deposition, industrial effluents, and petroleum spillage (Neff 1985; Wan 1994). Due to their highly hydrophobic nature, PAHs in aquatic environments will accumulate in sediments at levels in the ppm range (Environment Canada 1994). Concentrations seen in the water column are usually in the range of parts per trillion to parts per billion (Arfsten et al. 1996). The concentration bound to particulate matter can be much higher.

Overall environmental levels of PAHs have increased dramatically since the industrial revolution. Historical records of PAH concentrations obtained from different environmental compartments show that concentrations are correlated to industrial activity, using net world petroleum production as an index (Jones et al. 1989; Sanders et al. 1993; Kawamura et al. 1994). Even in compartments far removed from human activity, a large increase in PAH concentration has been observed since the industrial revolution. In the study by Kawamura et al (1994), a 203 meter ice core obtained from a Greenland glacier provided a record of atmospherically deposited PAHs dating back to the 16th century. It showed an almost exponential increase in PAH concentration from the 1930s onwards, with a 50-fold increase relative to the 18th century.

1.2 Photochemistry of PAHs

In the absence of light or other activating processes, PAHs are relatively unreactive molecules. The conjugated aromatic structure of PAHs gives them a high degree of resonance stabilisation

and low energy in the ground state, making them resistant to chemical attack. In the presence of light, the reactivity of PAHs varies tremendously, and is dependent on the wavelength of incident light and the structure of the PAH in question. Upon absorbing a photon of light, the molecule undergoes a transition to an electronically excited state. The molecule can then dissipate the absorbed energy and return to ground state via fluorescence (in which a photon of light is emitted), or through internal conversion where the energy is dissipated as heat. Alternatively, the excited state molecule may undergo an intersystem crossing from a singlet to a triplet state, or vice versa. From the new energy state, the molecule can return to ground state by emitting a photon (phosphorescence) or dissipate the energy as heat via intersystem degradation. Monomolecular excited state transitions may be graphically represented as a Jablonski diagram (Figure 1.2). Bimolecular reactions from excited states also occur and in some cases have a very high yield.

The relative abundance and probability of transitions between the electronically excited singlet and triplet states are fundamental to the understanding of the photochemical reactivity of PAHs. In any photochemical process, the absorption of a photon of light causes an electron to undergo a state transition from a lower energy quantum state to a higher energy state. While molecules can absorb light from states other than the ground state under certain conditions, these transitions are not particularly relevant to environmental photochemistry. It will be assumed here that photon absorption occurs from the ground state.

Briefly, singlet and triplet states describe the quantum spin of the electrons in the highest occupied electronic states. Each electron has two possible spin states, spin up ($\uparrow$) or spin down ($\downarrow$). Each electron in a molecule may be described by a spatial function ψ and a spin function χ, where each function may be symmetric (ψ_s and χ_s) or antisymmetric (ψ_a and χ_a). As first recognised by Heisenberg (1926), two indistinguishable electrons within a molecule must have a total wave function that is antisymmetric ($\psi_s \chi_a$ or $\psi_a \chi_s$). The most important implication of this with respect to molecular structure is the Pauli exclusion principle, which stipulates that no two electrons within a molecule can exist in identical states (Pauli 1924). Thus, two electrons must
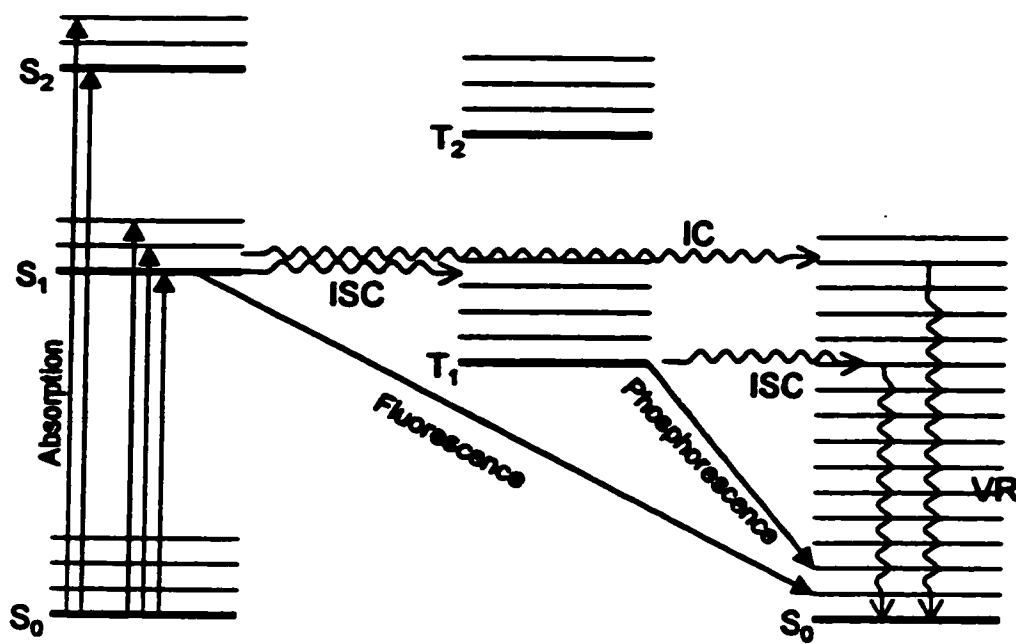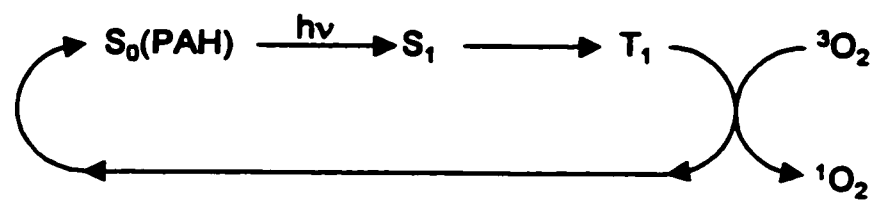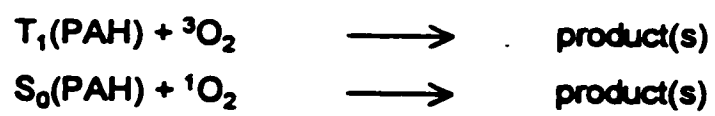
Figure 1.2: Mono- and bi-molecular photochemical reactions of PAHs. The Jablonski diagram (top) shows the monomolecular reactions of PAHs. Ground state PAH (S_0) absorbs a photon and forms an excited singlet state (S_1, S_2). It can then undergo fluorescence, phosphorescence, intersystem crossing (ISC) to a triplet state (eg. T_1), internal conversion, or vibrational relaxation. Non-radiative processes are designated by wavy lines. Two general types of oxygen dependent bimolecular reactions occur (bottom): the transfer of energy to oxygen forming singlet state oxygen (sensitization), or reaction of the PAH with oxygen to form a new compound (photooxidation).

7

have either different spatial functions or opposite spins. Given two electrons of an organic molecule, if they are in the highest occupied molecular orbital (HOMO) and have the same spatial function, the electron spins are necessarily antiparallel ($\uparrow\downarrow$). When the electrons in the two highest states have different spatial functions and are of the same spin, the molecule is in a triplet state. There are actually three parallel spin states allowed quantum mechanically for a pair of electrons: $\uparrow\uparrow$, $\downarrow\downarrow$, and $1/\sqrt{2}$ ($\uparrow\downarrow - \downarrow\uparrow$). If the emission spectra of a triplet atom is observed in the presence of a magnetic field, these three states show up as three closely spaced bands (hence the name triplet). Most organic molecules have a ground state as a singlet state (Gilbert and Baggott 1991). A notable exception to this is oxygen, which has a triplet ground state.

The singlet and triplet states of molecules have remarkably different properties. Direct transitions from singlet to triplet states by absorption of a photon are forbidden by quantum mechanics, as they require an electron to undergo a change in spin while changing orbitals. Thus direct transitions from ground state to excited triplet states tend to occur with a very low quantum yield. However, in some molecules (such as PAHs), population of triplet states from excited singlet states do occur with a high quantum yield. Typically a triplet state is generated after a molecule in ground state absorbs a photon to form an excited singlet state. The singlet state decays into a triplet state via an intersystem crossing to a vibrational level of a triplet state, which then undergoes an internal conversion to the lowest excited triplet state. Since changes in electron spin are forbidden by quantum mechanics, transitions from an excited triplet state to singlet ground state are orders of magnitude more long lived than excited singlet states (Malkin 1992). Furthermore, as the triplet states are longer lived, the probability of a chemical reaction from the triplet state is greater than that from the singlet state.

Another outcome of the antisymmetry requirement for a pair of electrons is the *exchange energy*, or the energy difference between the singlet and triplet states. The singlet state electrons have a symmetric space function ψ_s, and will tend to be close together, whereas the triplet state electrons have an anti-symmetric space function ψ_a, and will tend to avoid each other. As electrons are negatively charged, there is a Coulomb charge repulsion between them and there is

8

more energy in the singlet state, where the electrons are close together, than in the triplet state, where they are farther apart (French and Talyor, 1978). This difference in energy is defined as the exchange energy, and is the reason for triplet states being of lower energy than the corresponding singlet states.

In addition to the monomolecular interconversions of excited state molecules, bimolecular reactions also occur from the excited states. Quenching occurs when an excited state of a molecule interacts or reacts with a second molecule, the quencher. The excited state may transfer its energy to the quencher and return intact to ground state, or it may react directly with the quencher to form a new chemical species (Malkin 1992). If oxygen is the quencher, these two types of reactions summarise two possible mechanisms of PAH toxicity. In the first, photosensitization, triplet state PAH transfers its energy to molecular oxygen, resulting in ground state PAH and the highly reactive singlet oxygen (Landrum et al. 1986; Arfsten et al. 1996). In the second, the PAH is oxidised from an excited state, resulting in a different chemical species which can have greatly altered biological effects than the parent PAH (Huang et al. 1997; Krylov et al. 1997) (Figure 1.2).

1.3 Photoreactions of PAHs

The process of sensitisation, where triplet state PAHs transfer energy to singlet oxygen, has been discussed. There are a number of specific bimolecular reactions in which PAHs result in the formation of photoproducts. PAHs may undergo addition reactions with molecular oxygen in the presence of light via reaction with singlet state oxygen. The excited state PAH forms singlet oxygen, which can then react with the ground state PAH via a 1,4-photocycloaddition across a ring or a 1,2-photocycloaddition to a double bond, resulting in endoperoxides (Gilbert and Baggott 1991; Malkin 1992). These reactions are typified by the reactions of anthracene and phenanthrene with molecular oxygen (Figure 1.3). It is also possible that this reaction may occur directly from the reaction of ground state oxygen with an excited state PAH. 1,4-photocyclo-additions are dependent upon the rate of formation of singlet oxygen by the PAH, and the relative

9

Anthracene 1,4-photocycloaddition
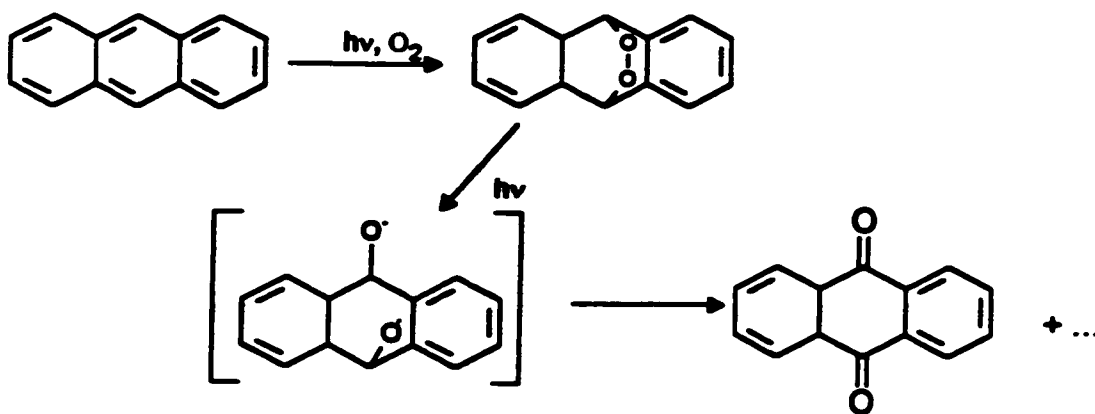
Phenanthrene 1,2-photocycloaddition
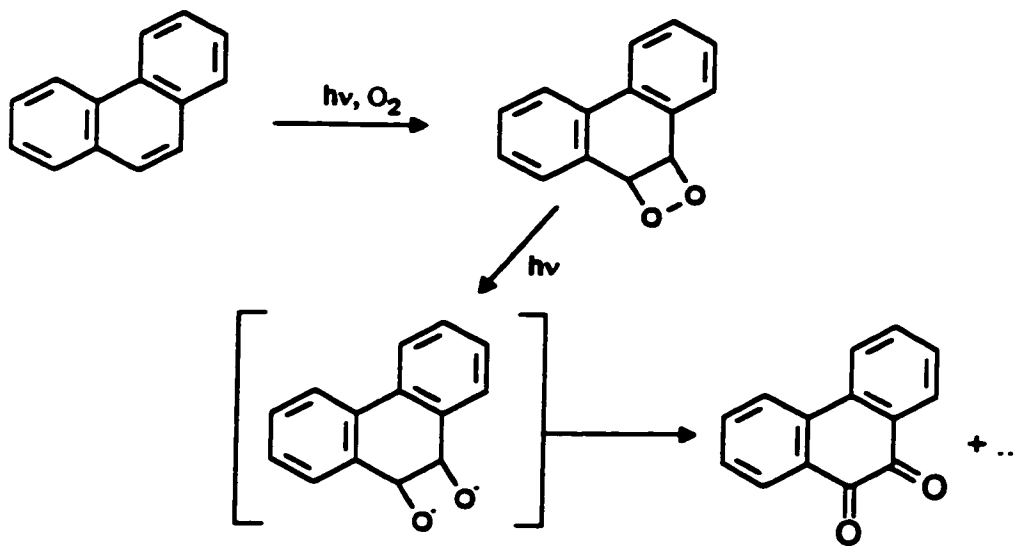
Figure 1.3: Photocycloaddition reactions of anthracene and phenanthrene. Due to the different electron configurations of the two molecules, the most reactive sites differ and will favour different types of initial photoreactions. Both reactions proceed via an unstable endoperoxide, which disassociates to form a diradical intermediate. In each case, the resulting quinone is two electrons more reduced than the intermediate endoperoxide.

reactivity of the rings within the PAH. Linearly annealated PAHs (napthalene, anthracene, naphthacene, pentacene) show increasing reactivity with increasing number of rings (Wiberg 1997). Pentacene (5 rings) is reactive with oxygen at room temperature and does not require photoactivation; hexacene (6 rings) is unstable and will decompose at room temperature. The reactivity is due to the radical character of opposing carbons in the center ring(s). The analogous series of PAHs annealated at obtuse angles (phenanthrene, chrysene, picene) have comparable total energy as the corresponding linear PAHs, but the non-linear structure tends to reinforce the double bond character of the external bonds rather than the radical character of the opposing carbons, and are more stable against oxygen additions. [1,2]-photocycloadditions across bonds with a strong double bond character (and associated electron density) are more likely to occur within this group of PAHs, and at a slower rate than the oxidation of the linear PAHs (Wiberg 1997).

Another type of reaction with oxygen that is particularly important for the condensed non-linear PAHs such as pyrene, benzo(a)pyrene, and fluoranthene, is the abstraction of a hydrogen atom from the hydrocarbon by singlet oxygen (Payne and Phillips 1985; Malkin 1992). The resulting PAH radical is likely to further react with oxygen or other available molecules, resulting in hydroxyPAHs, quinones, or ring fragmentation products.

Within a mixture of PAHs and other hydrocarbons, numerous other reactions can occur. In the presence of phenolics, which frequently co-exist with PAHs and are also PAH degradation products, additional free radical reactions can be initiated by light. The photoactivation of phenolics results in the generation of radical species capable of hydrogen abstraction from hydrocarbons and from water. This subject has been addressed in a review of the photochemistry of petroleum in water (Payne and Phillips 1985).

1.4 Mechanisms of PAH Toxicity

There are several possible modes of action by which PAHs can affect an organism. Each of the various modes of action may be significant, depending upon the organism, internal concentrations

11

of PAH, and the external environment. The possible effects may be categorised into five non-exclusive modes of action: non-polar narcosis, genotoxicity, endocrine and immune effects, photosensitization, and toxicity via photooxidation products. It is likely that several of these modes can operate simultaneously within an organism, though there is usually a dominant mode of action eliciting the observed effects.

1.4.1 Non-polar narcosis

Non-polar narcosis is sometimes referred to as baseline toxicity, in which toxic effects are the result of accumulation of chemical in the biological membranes of an organism (McCarty et al. 1992; Rand et al. 1995). The structure of the cell membrane is disturbed by the presence of the toxicant, and at high enough concentrations the biological function of the membrane is sufficiently impaired to cause death of the organism (Lipnick 1995; van Wezel et al. 1996). Effects are caused when the molar concentration of chemical within the membrane reaches a threshold level (approximately 2 to 8 mmol/kg for fish) and is similar for any chemical acting via this mode of action alone (McCarty et al. 1992). As PAHs are highly lipophilic and will concentrate in membranes, low environmental concentrations of PAHs can result in sufficient accumulation of PAHs in organisms to cause acute toxic effects. It should be noted that PAHs are only marginally soluble in water, and thus it is an infrequent case where dissolved PAHs will be at high enough concentrations to cause non-polar narcosis via water exposure alone. However, there can be narcotic effects from exposure to PAHs in food or sediments. The other modes of action are more specific to certain organisms and environmental conditions, and can occur at much lower concentrations (Rand et al. 1995).

1.4.2 Genotoxicity

Once incorporated into an organism's tissues, PAHs can undergo biochemical activation to carcinogenic or mutagenic compounds. The best and most studied of these reactions is the enzymatic transformation of benzo(a)pyrene to its 7,8-diol-9,10-epoxide, which covalently binds

12

to the DNA base guanine (Timbrell 1991). The DNA adduct formed can eventually result in carcinogenesis or teratogenesis, leading to the death of the organism. The enzyme family responsible for the activation of PAHs to carcinogens is the mixed function oxygenase (MFO) system (Payne et al. 1987; Livingstone et al. 1989). In particular, P450 enzymes add an oxygen to the PAHs as an initial step towards the metabolism or elimination of the PAH. Some of the reactive intermediates formed, such as BAP-7,8-diol-9,10-epoxide, can intercalate with DNA or form covalent bonds with protein. A number of reviews have been published on mechanisms of P450 metabolism (Livingstone et al. 1989; Varanasi 1989; Bucheli and Fent 1995; Di Giulio et al. 1995). Interestingly, the levels of PAHs from organisms at contaminated sites can be lower than those from cleaner sites, due to induction of the MFO system. Van der Oost et al. (1994) found increased excretion of 1-hydroxypyrene and increased numbers of DNA adducts in organisms at a PAH contaminated site, but no increase in the tissue levels of pyrene as compared to uncontaminated sites. An increased rate of mutations has been observed in fish from contaminated sites (Malins et al. 1988; Baumann 1989; Landahl et al. 1990) and also in beluga whales exposed to PAHs (De Guise et al. 1994).

This type of toxicity is specific to certain PAHs and certain classes of organisms. Some PAHs such as benzo(a)pyrene are potent pro-carcinogens, while others such as phenanthrene show little or no carcinogenic activity. Organisms have an equally great variability in susceptibility. For the requisite formation of the activated metabolites, the organism must have a well developed MFO system capable of forming the active metabolites in sufficient quantity. The life span of the organism is also a factor; organisms with a relatively short lifetime are unlikely to exhibit genotoxic effects, as the time required for these effects to appear is comparable to the lifespan of the organism. Thus, aquatic invertebrates are unlikely to exhibit genotoxic effects, whereas larger more complex species such as fish or marine mammals will be more likely to show genotoxicity.

13

1.4.3 Endocrine disruption and immunotoxic effects

The potential for PAHs to have estrogenic or antiestrogenic activity has recently been reviewed (Santodonato 1997). Specifically, the author reviewed the effect of PAHs on the human endocrine system and the role played by the PAHs in carcinogenesis. Much of the work conducted to date has focussed on two highly carcinogenic PAHs, dimethylbenzanthrene and 3-methylcholanthrene. While these two PAHs occur only at very low concentrations in environmental samples, as a family of compounds PAHs are likely candidates for hormonal disruption. A number of investigators (Payne et al. 1987; Hall and Oris 1991; van Brummelen 1998) have suggested the potential for interference of hormone function by PAHs. Hormonal effects of PAHs may be induced by PAH metabolites which have structural features similar to some steroid hormones (Jordan 1994; Müller et al. 1995). PAHs may also have indirect endocrine effects through induction of the MFO enzyme system, which is involved in the activation and deactivation of steroid hormones. While there is potential for PAHs to have direct or indirect hormonal effects, endocrine disruption due to environmental PAH exposure has yet to be definitively demonstrated (van Brummelen 1998).

Immunotoxicity, similar to hormonal effects, can be induced by exposure to PAHs. Exposure to subacute levels of PAHs has resulted in immunosupression of human T cells (Davila et al. 1997). There are several proposed mechanisms by which PAHs may induce immunosupression. PAH immunotoxicity may be induced by binding of PAHs to an aryl hydrocarbon (Ah) receptor in the organism, with subsequent induction of regulatory and possibly stress proteins. PAH metabolites may also induce autoimmune or hypersensitivity responses, via protein adduct formation (Griem et al. 1998). As with endocrine effects, it is difficult to relate impacts at the cellular level to impacts at the ecosystem level. While investigation of immunotoxic effects using model ecosystems has not shown that PAH exposure impairs immune response, it has been shown that PAHs can modulate innate immune responses at the cellular level (Karrow 1998).

1.4.4 Photosensitization

The toxicity of polycyclic aromatic hydrocarbons (PAHs) to aquatic organisms such as microbes, fish, and plants has been shown to greatly increase upon exposure to light, especially ultraviolet radiation. This is known to proceed via photosensitization and/or photooxidation of the compounds to more toxic species radiation (Huang et al. 1993; Bowling et al. 1983; Oris and Giesy 1986; Newsted and Giesy 1987; Schoeny et al. 1988; Gala and Giesy 1992; Ankley et al. 1994; Ren et al. 1994).

Photosensitization is a well studied mechanism of photoinduced toxicity. A schematic representation of a photosensitization reaction is shown in Figure 1.2. A PAH molecule absorbs a photon, then undergoes an intersystem crossing event to form a metastable triplet state. The triplet state PAH transfers its energy to ground state triplet oxygen, resulting in ground state singlet PAH and singlet oxygen. Singlet oxygen is a highly reactive oxygen species and can cause significant damage to biomolecules such as lipid bilayers, proteins, and DNA (Landrum et al. 1986; Krylov et al. 1997). As the PAH returns to ground state intact, it can repeat the process and many molecules of singlet oxygen can be produced by a single PAH molecule.

PAH mediated photosensitization is dependent upon several physiochemical and physiological factors (Krylov et al. 1997): the ability of the PAH to absorb incidental solar radiation, the efficiency of intersystem crossing to produce the triplet state PAH, the lifetime of the triplet state, and the efficacy of energy transfer to molecular oxygen. The physiological factors affecting the susceptibility of an organism to photosensitization are the uptake rate of PAH, the rate of PAH depuration, the degree of light penetration into sensitive tissues, and the ability of the organism to protect itself against free radical damage. These factors all have an influence and can be integrated to give the expected amount of singlet state oxygen reaching a target site within the organism. Photosensitization is a likely dominant mode of action, but only if the following conditions are met: the organism has light incident on sensitive organs, it is exposed to a high level of light, and there is sufficient PAH accumulated at the site of action.

15

Photosensitization has been implicated in the phototoxicity of PAHs to *Daphnia magna* (Newsted and Giesy 1987; Holst and Giesy 1989), the algae *Selenastrum capricornutum* (Cody et al. 1984; Gala and Giesy 1992), and the fish species *Lepomis macrochirus* (Oris and Giesy 1985; Oris and Giesy 1986). The degree to which PAHs are photosensitizers varies widely. Some PAHs such as fluoranthene and pyrene are potent photosensitizers, while others generate little or no singlet oxygen when exposed to light at wavelengths present in sunlight.

1.4.5 Toxicity of PAH Photoproducts

Another means by which PAHs can be toxic is by the creation of toxic photoproducts on exposure to light (Ren et al. 1994; Huang et al. 1995; Huang et al. 1997; McConkey et al. 1997). This means of phototoxicity is more complex than photosensitization, and has been less well studied. PAHs are photoreactive in the atmosphere (Zafiriou 1977), and the upper parts of the water column (Zepp and Schlotzhauer 1979), so there is little doubt that photoproducts are formed in the environment. It is likely that PAH photoproduct toxicity would impact organisms under different situations than photosensitization, as the expected conditions under which toxicity occurs are different. For photoproducts to form and accumulate in environmental compartments, the parent PAHs must be photochemically reactive, and the rate of degradation of photoproduct cannot be much faster than the rate of parent PAH degradation. The organisms exposed to the photoproducts do not need to be transparent for toxic effects to appear (unless the products are themselves photosensitizers), nor is co-exposure to light a requirement for toxic effects to be observed. To elicit a toxic effect, the photoproducts need to accumulate within the organism, so some degree of hydrophobicity of the products is a likely requirement for toxic effects. As these chemical species have a higher water solubility than the parent PAHs, organisms could be exposed to higher concentrations of PAH photoproducts as compared to the parent PAHs. This can present a greater toxic risk, especially since oxidised PAHs are known to be more reactive and biologically damaging than the parent compounds in some circumstances (Nikolaou et al. 1984; Arey et al. 1992; Huang et al. 1993; Ren et al. 1996; Kosian et al. 1998). It has been found that the

16

photoproducts of PAH oxidation are still hydrophobic enough to be readily assimilated into lipid tissues (Duxbury et al. 1997). The pathways of PAH degradation and the toxicity of specific PAH degradation products are not currently well characterised, and this question has been addressed in this thesis.

1.5 PAHs and mixture toxicity assessment

Assessment of mixture interactions is being recognised as increasingly important in environmental assessment, where it may be necessary to determine the combined deleterious effect of many factors (Calabrese 1991; Feron et al. 1995; Fay and Feron 1996; Cassee et al. 1998). When organisms are exposed to a mixture of chemicals, the possible toxic interactions theoretically range along a continuum from less than additive action (antagonism), through strict additivity, to greater than additive effects (synergism). For any given mixture, the difficulty is to determine where on the continuum the interaction falls.

PAHs, and by association PAH photoproducts, occur in the environment almost exclusively as complex mixtures (Nikolaou et al. 1984). The composition of these mixtures can vary widely, so much so that the relative abundance of PAHs has been used to trace the source of contaminants (Neff 1985). Estimating the toxicity of a mixture of PAHs might be accomplished through the use of predictive models, preferably ones that are capable of addressing interactions as well as main effects. Sometimes the assumption is made that all interactions are negligible, and effects may be predicted by a strictly additive model. While an additive model may provide a conservative estimator of effect in many cases, it does not necessarily apply to PAHs and particularly mixtures of PAHs and PAH photoproducts. When the hypothesis of additivity is presumed, it must still be tested. For this reason it was necessary to investigate what methods were available to assess interactions within complex mixtures. Ideally, a consistent, reliable method with good sensitivity to interactions could be used to test interaction models. Unfortunately, most existing experimental designs for mixtures concentrate either on main factor assessment in multi-component mixtures, or numerous points in a mixture containing few

17

components. This shortfall in the literature led to the generation of fractional simplex designs, discussed in Chapter 6. These designs have application outside of the field of toxicology as well as having application to environmental mixture assessment.

Existing mixture designs, as well as the new designs presented in Chapter 6, have the general goal of accounting for the contributions made to observed responses by main factors and factors in combination. Main factor screening designs have been addressed previously (Snee and Marquardt 1976), but they are generally not designed to screen for interactions. The most commonly used experimental designs for assessing mixture interactions with three or more components are the simplex-lattice and simplex-centroid designs (Scheffé 1958; Scheffé 1963). A relatively uncomplicated design for estimating main and quadratic effects in a system containing q factors is a $\{q,2\}$ simplex-lattice, which consists of a design point for each pure component and for each binary combination, resulting in $q(q+1)/2$ design points. The more rigorous full simplex-centroid design has 2^q-1 design points. As the number of components within the design increases, the number of design points in both of the above systems quickly become too large for practical testing. For larger numbers of components, even the testing of all binary combinations becomes unfeasible from an economical or pragmatic perspective (Calabrese 1991; Cassee et al. 1998). Thus, an experimental design that could screen for the largest interactions present without testing all possible binary combinations was needed, and is introduced in this thesis.

1.6 Statement of research objectives

The research objectives of this thesis are to identify the most abundant products of PAH photooxidation under environmental conditions, and to address the toxicity of the identified products. Likely routes of degradation of general PAH structures are also presented. The relative rates of PAH product formation and the relevance of this to environmental toxicology will be discussed, as will the conditions in which PAH photoproducts may be environmentally important.

As PAHs occur most frequently as mixtures in environmental compartments and PAH oxidation results in complex mixtures, methods for assessing the toxicity of many component

mixtures are also addressed. This led to the generation of new experimental designs termed 'fractional simplex designs'. This method is a practical approach for testing for meaningful interactions within a large number of components, and with a minimum number of design points. The basis on which the design arrays were generated and their means of construction are presented. General models appropriate for use with mixture data sets are discussed, and illustrated with a sample PAH data.

The thesis has been divided into chapters by chemical for chapters 2 through 5. Chapter 2 discusses the photooxidation of napthalene, and chapter 3 discusses the photochemical reactions of the four ring PAHs. Chapters 4 and 5 discuss the rates of formation and toxicity the photoproducts of phenanthrene and benzo(a)pyrene respectively. Chapter 6 introduces the fractional simplex designs, and chapter 7 illustrates the application of the designs in chapter 6 to a mixture of PAHs and PAH photoproducts.

CHAPTER 2

PHOTOOXIDATION PRODUCTS OF NAPHTHALENE

2.1 INTRODUCTION

Naphthalene (NAP) is the simplest PAH, consisting of two fused benzene rings. It has industrial and commercial applications as the active ingredient in mothballs and in the manufacture of carbaryl pesticides. It is also a major component of the aromatic fractions of crude oils, gasolines, and creosote (Cook et al. 1983; Neff 1985). As the most volatile and most water soluble of the PAHs, its physiochemical behaviour is an exception amongst PAHs. In an aquatic system, intact naphthalene tends to partition into the atmosphere, instead of into sediments like most other PAHs. Thus, previous research into the environmental and health impacts of naphthalene has focussed more on atmospheric exposure, and in particular human exposure via automobile exhaust and smog.

Naphthalene and methylnaphthalenes are a major component of the aromatic portion of diesel exhaust (Siegl et al. 1999). The products of naphthalene oxidation will be less volatile and thus more prone to remain in aqueous phase, so consideration of the effects of naphthalene photoproducts should not be limited to atmospheric exposures. Interestingly, NAP has been found to be the only PAH, among sixteen tested, to elicit direct cytotoxicity at concentrations well below its water solubility limit (Schirmer et al. 1998).

The toxicity of NAP has been previously studied, and like many PAHs the negative impacts of NAP to mammalian systems are believed to be associated with products of metabolic activation and not intact naphthalene (Kawabata and White 1990; Wilson et al. 1996; Sasaki et al. 1997; Zheng et al. 1997; Bagchi et al. 1998a; Bagchi et al. 1998b; Hoeke and Zellerhoff 1998). The toxicity of NAP to plants has been found to increase on exposure to light (Ren et al. 1994). The products of metabolic activation of NAP include 1-napthol and 1,2- and 1,4-napthoquinones, which have been implicated in the indirect cytotoxicity of naphthalene (Tingle et al. 1993; Flowers-Geary et al. 1996; Wilson et al. 1996; Zheng et al. 1997; Bagchi et al. 1998a; Bagchi et al. 1998b).

20

A major goal of this thesis is to understand the photomodification reactions of PAHs. As the smallest and most soluble PAH, NAP provides a simple model with which to begin these studies. NAP is not as photoreactive as some of the larger PAHs (Malkin 1992), but does undergo photoreactions under ambient environmental conditions. Possible initial photoreactions are [2,2] and [2,4] cycloadditions of oxygen (Gilbert and Baggott 1991; Malkin 1992) to form endoperoxides, which quickly undergo further reactions. Under oxidizing conditions dimerization reactions will be less favoured than oxidation reactions (Gilbert and Baggott 1991) and the products of NAP photooxidation will therefore be at most two ring structures. These products are likely to be sufficiently volatile and thermally stable to allow analysis by GC/MS. In addition, the relatively uncomplicated structures are favourable for mass spectral analysis, as representative mass spectra have a higher probability of being in the reference library (Palisade Co. 1990), and the fragmentation patterns are more readily interpreted. In contrast, larger PAH photoproducts are unlikely to be thermally stable and sufficiently volatile to permit separation by gas chromatography, and even those meeting this requirement will be more difficult to interpret.

In this chapter some of the major aqueous photoproducts of naphthalene were identified. Additionally, this provides a basis for identification of the products of larger PAHs. The toxicity of identified photoproducts will be discussed.

2.2 MATERIALS AND METHODS

2.2.1. Naphthalene photooxidation

Naphthalene (NAP), >98% purity, was purchased from Sigma-Aldrich Chemical Co. (Oakville, ON). A stock solution of 20 mg NAP was prepared in 2 ml HPLC grade dichloromethane (Fisher Scientific Ltd., Mississauga, ON). Two ml of the NAP stock was added to a 200 ml pyrex glass beaker and the solvent evaporated to dryness. 200 ml of distilled water was added to the beaker, and the beaker covered with polyethylene film. The system was allowed to equilibrate for 18 hours prior to light exposure. The pyrex glass had a measured light transmittance limit of 300 nm, determined as 10% transmission using an Perkin-Elmer Lambda 3 UV/Visible spectrophotometer. This is comparable to

the shortest wavelength of light transmitted through the atmosphere, approximately 298 nm. The polyethylene film used had a measured UV cutoff of 285 nm, effectively transmitting all wavelengths of incident solar radiation. The experimental setup provided a system containing NAP in solution, plus an additional source of NAP (in solid phase adsorbed to the bottom of the beaker) to replace the NAP consumed in photoreactions. The beaker containing the NAP and water was exposed to natural sunlight for a total of 24 hours over a three-day period. A control sample was prepared and incubated in darkness. The photooxidized solution contained a mixture of products at sufficient concentration for separation and identification.

2.2.2 Preparation of sample for analysis

The 200 ml aqueous photoproduct mixture was acidified to pH 2.0 by addition of phosphoric acid, and a liquid-liquid extraction was used to transfer photoproducts into dichloromethane. The 200 ml of aqueous solution was transferred to a 500 ml glass separatory funnel, and extracted with two volumes of 50 ml dichloromethane. The dichloromethane extractions were combined, and evaporated to approximately 2 ml using a rotary evaporator. The 2 ml of dichloromethane was transferred to a 15 ml conical graduated cylinder. The sample was solvent exchanged into 2 ml methanol, by addition of 5 ml methanol then evaporation under a stream of nitrogen to a volume of approximately 0.5 ml. The volume was then adjusted to 2.0 ml by further addition of methanol.

2.2.3 HPLC separation

The concentrated mixture of photoproducts was separated by high pressure liquid chromatography (HPLC), using a Spectraphysics model 8100 liquid chromatograph with an SP8400 UV/Visible detector and an SP4270 integrator. The detector was set at 254 nm with a 4 nm bandwidth. The column used was a 25 cm x 4.6 mm I.D. Supelcosil LC-18 reverse phase column, with a 5 μm packing (Supelco Inc. Bellafonte, PA USA). Double distilled water, adjusted to pH 2.5 with phosphoric acid, and HPLC grade methanol (VWR/Canlab, Mississauga, ON) were used as the elution solvents. The injection volume of the concentrated extract was 1 ml. An extended gradient

time program was used to obtain maximum separation of the photoproducts during elution from the HPLC column. The gradient profile was as follows: 10 minutes isocratic at 100% water, then a linear gradient to 10% methanol from 10 to 40 minutes, followed by a linear gradient to 50% methanol from 40 to 90 minutes, and isocratic at 50% methanol for the remaining 10 minutes. Constituents appearing as major peaks on the HPLC trace were collected at the detector outlet. Fractions (approximately 0.5 ml in methanol/water) were evaporated to dryness under a stream of nitrogen and resuspended in cyclohexane.

2.2.4 GC/MS analysis

A Hewlett-Packard Model 5890 gas chomatograph equipped with a model 5970 mass selective detector was used for analysis of the HPLC fraction components. An HP-5, 95% methyl:5% phenyl column (length 30 m, internal diameter 0.2 mm, 0.33 μm film thickness) was used. The GC injector port and initial oven temperature was set at 250°C and 60°C respectively. The initial oven temperature was held constant for two minutes after injection, then linearly increased to 250°C at a rate of 8°C/min and held at the maximum temperature for 2 minutes. This general temperature gradient program was used with all fractions. The detector was used in scan mode from 40 to 400 atomic mass units (amu).

The Wiley registry of mass spectral data (Palisade Co. 1990) was used for identification of products where possible. When a good library match was not obtained, compounds were identified by assigning partial structures to the observed peaks in the fragmentation mass spectra, using standard MS identification techniques and comparison to similar products for which reference mass spectra existed (Palisade Co. 1990; Silverstein et al. 1991).

23

2.3 RESULTS

2.3.1 Detection of photoproducts

Naphthalene was treated for a total of 24 hours under natural sunlight to produce a mixture of NAP photoproducts. There were approximately 11 major constituents and more than 40 minor constituents observed in the final mixture analyzed by HPLC (Figure 2.1). This is consistent with the expected presence of free radical reactions, which can result in numerous products (Andino et al. 1996; Forstner et al. 1997). While detection of products at 254 nm absorbance will not detect all products with the same efficiency, one can be reasonably certain that all compounds retaining an intact aromatic ring will be detected (Silverstein et al. 1991). The control sample did not exhibit accumulation of photoproduct.

2.3.2 Identification of photoproducts

GC/MS facilitated the identification of several of the major constituents of the mixture. The large peak at a retention time of 84.5 minutes was NAP, based on comparison of the retention time with a NAP standard. Three of the remaining major peaks (#1, #3, and #6 in Figure 2.1) were identified by comparison with spectra in the mass spectral library (Wiley 1990), and three additional products were tentatively identified based on their ion fragmentation patterns.

The identification of 1-naphthol (Figure 2.2) is consistent with an initial [2,2] photocycloaddition of oxygen at the 1,2 position of naphthalene, followed by dissociation of the endoperoxide and formation of a more chemically stable species. 1-naphthol is known to be photoactive, and acts as a photoinitiator, abstracting hydrogen atoms following light activation and causing the formation of peroxide and other radicals (Klein and Pilpel 1974; Payne and Phillips 1985). The generation of free radicals is a likely contributor to further photoreactions of NAP and NAP products.

Another expected product of an oxidative attack at the 1,2 positions of NAP is 1,2-naphthoquinone, which was not observed as one of the major products in this experiment. 1,2-naphthoquinone is likely not stable enough to survive the analytical methods. In addition, it would be

24
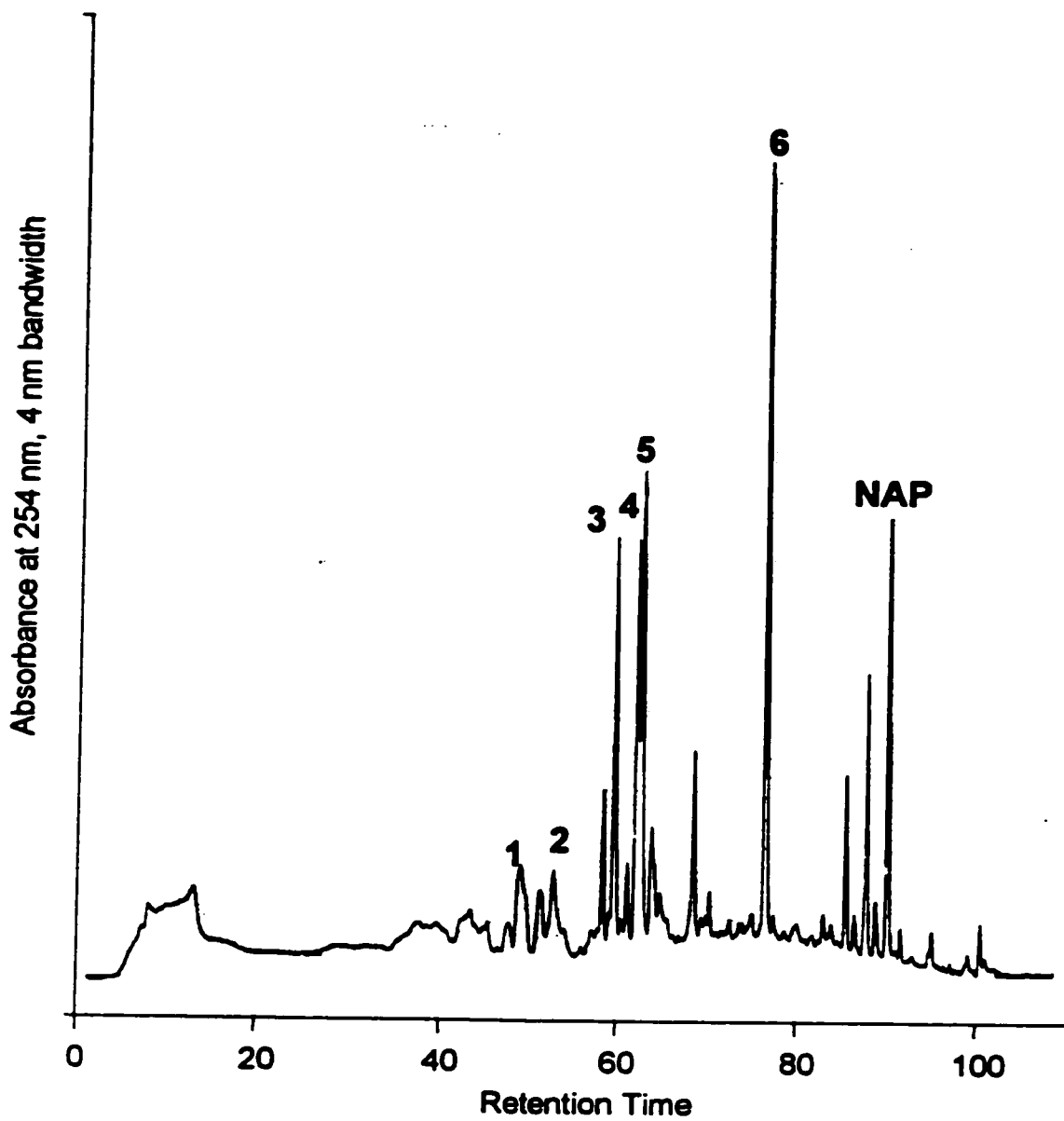
Figure 2.1. HPLC trace of photooxidised naphthalene (NAP), after 24 hours of sunlight exposure. Individual peaks were isolated from this sample; Peaks 1 to 6 were putatively identified by GC/MS.
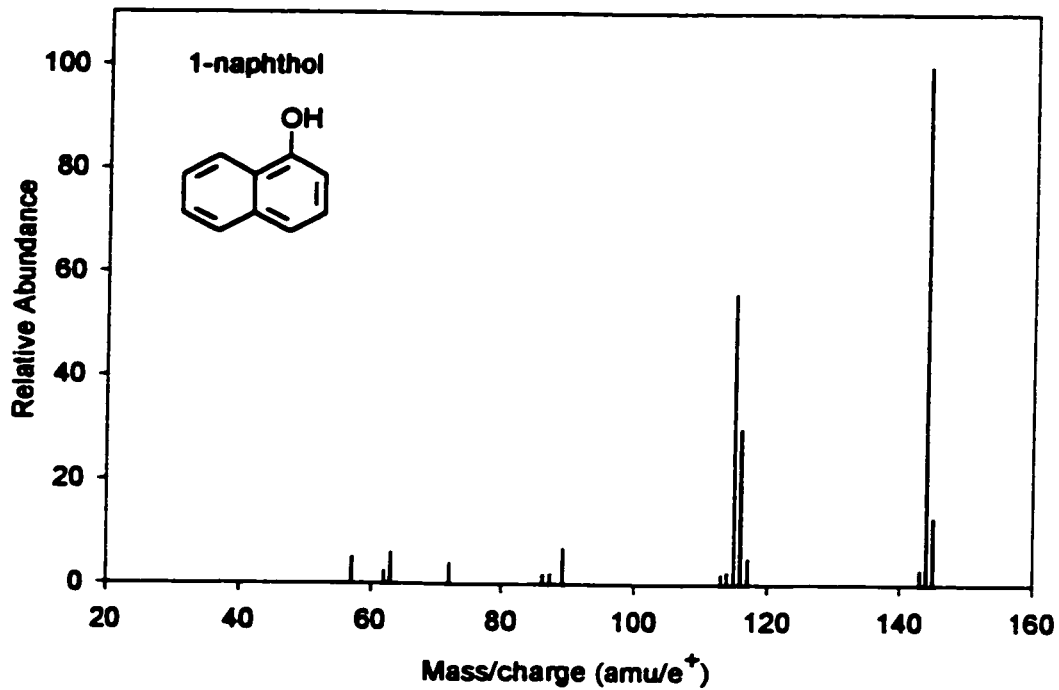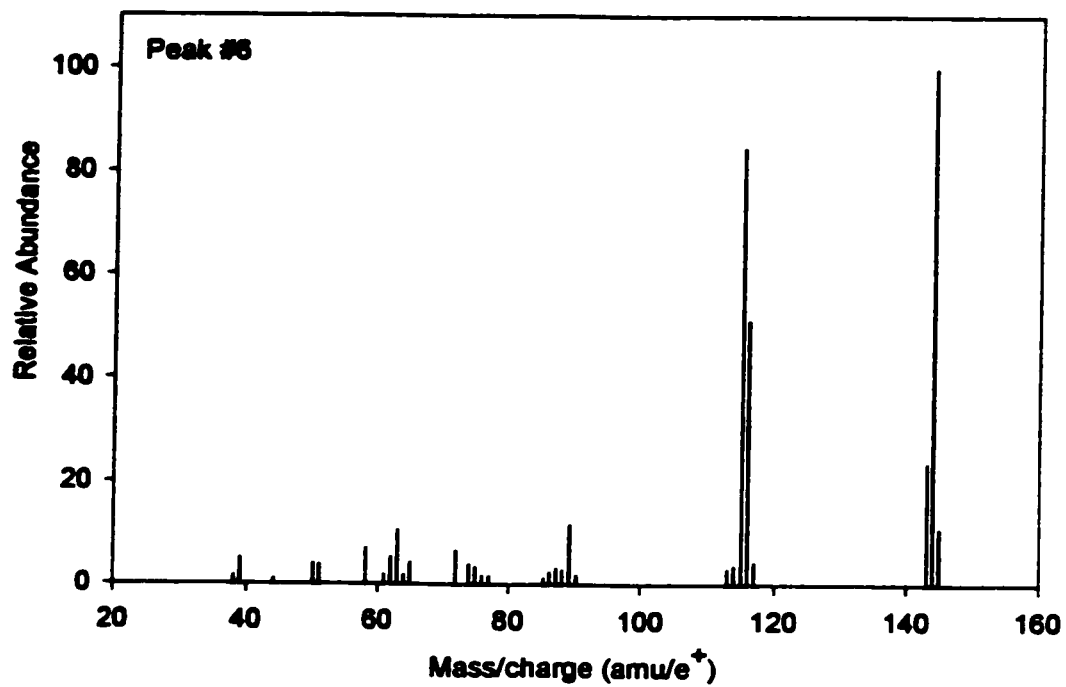
Figure 2.2. (Top) Mass spectra of peak #6 from Figure 2.1. The peak was identified as 1-naphthol, based on a library match (Bottom) from the Wiley mass spectral registry.

expected to undergo further rapid photochemical and oxidative transformations in the exposed solution. This contention is supported by the presence of products that have the 1,2-quinone as an intermediate.

A [2,4] photocycloaddition of oxygen at the 1,4 position of naphthalene is a possible product in the presence of photosensitizers (Saito and Matsuura 1979), proceeding via reaction of singlet oxygen with ground state NAP. The product of the reaction is a 1,4-endoperoxide. On exposure of the endoperoxide to light of the appropriate wavelength, the peroxide bond dissociates, forming a diradical which can then form 1,4-napthoquinone. If both oxygen radicals bond to the carbon at position 1, isobenzofuranone can result on rearrangement, with a concurrent loss of an acetylene molecule. Isobenzofuranone was one of the observed photoproducts and was identified by comparison with library spectra (Figure 2.3). Coumarin, the product identified in Figure 2.4, is likely the result of 1,2-napthoquinone reacting with molecular oxygen at the electron deficient 1 and 2 carbons, resulting in a loss of carbon dioxide and formation of the observed product.

The double bond at the 2,3 position in 1,4-napthoquinone can also undergo oxidative attack, by either singlet oxygen or the hydroxy radical (generated via 1-naphthol) resulting in a radical that can subsequently abstract a hydrogen atom from water. Hydrogen abstraction from water is the proposed mechanism by which free radical mediated reductions occur in atmospheric photoreactions (Andino et al. 1996; Forstner et al. 1997). The 2-hydroxy-2,3-dihydro-1,4-naphthoquinone is the molecule putatively identified to result from this reaction (Figure 2.5). This compound does not appear in the mass spectra library, so the identification was based on analysis of the fragmentation pattern. The peak at m/z = 176 is assigned as the molecular ion peak, consistent with a molecular formula of $C_{10}H_8O_3$. The peaks at m/z ratios of 51, 77, and 105 are indicative of a carbonyl group alpha to an unsubstituted benzene ring (Silverstein et al. 1991). On comparison with the library mass spectra in Figure 2.3 and the spectra of 1,4-napthoquinone, substitution at the 2' position of the benzene ring does not appear to significantly alter this fragmentation pattern. The peak at m/z = 133 suggests that an additional carbonyl group is present in the structure. Working back from the molecular ion, the peak at m/z 148 indicates a loss of a carbonyl group. A general occurrence in the

27
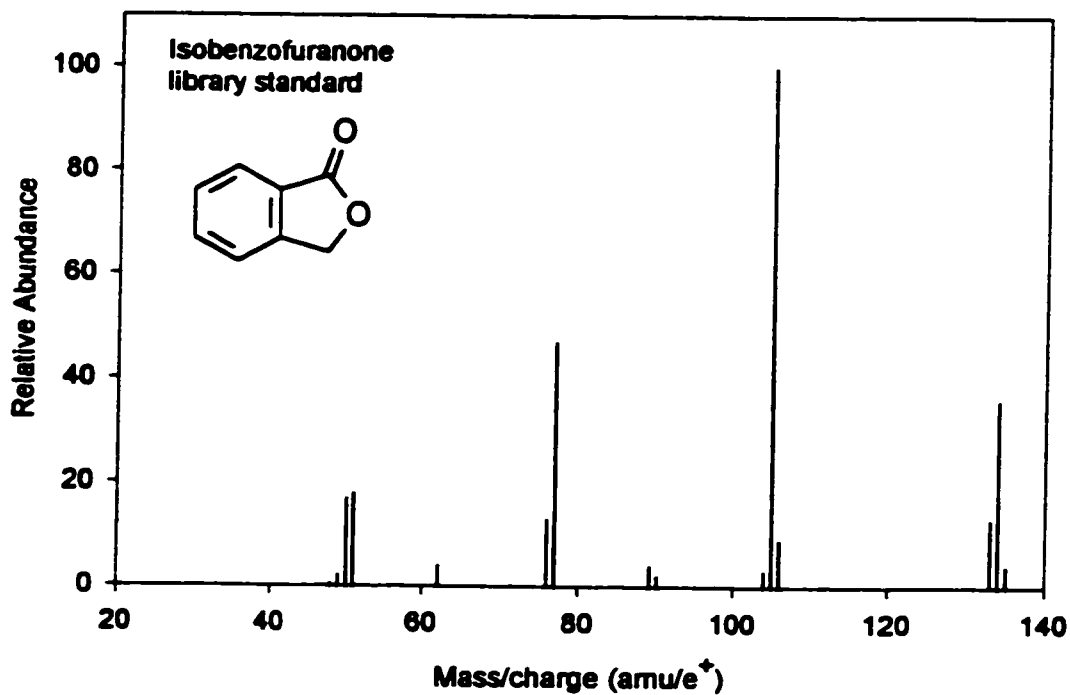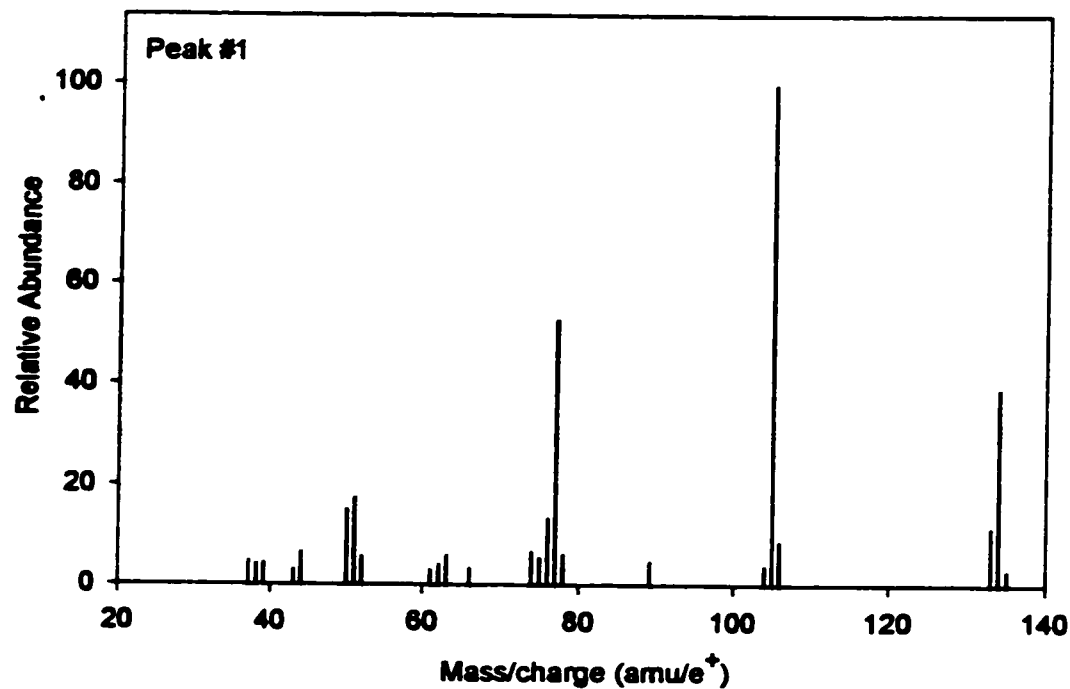
Figure 2.3. (Top) Mass spectra of peak #1 from Figure 2.1. The peak was identified as isobenzofuranone, based on a library match (Bottom) from the Wiley mass spectral registry.
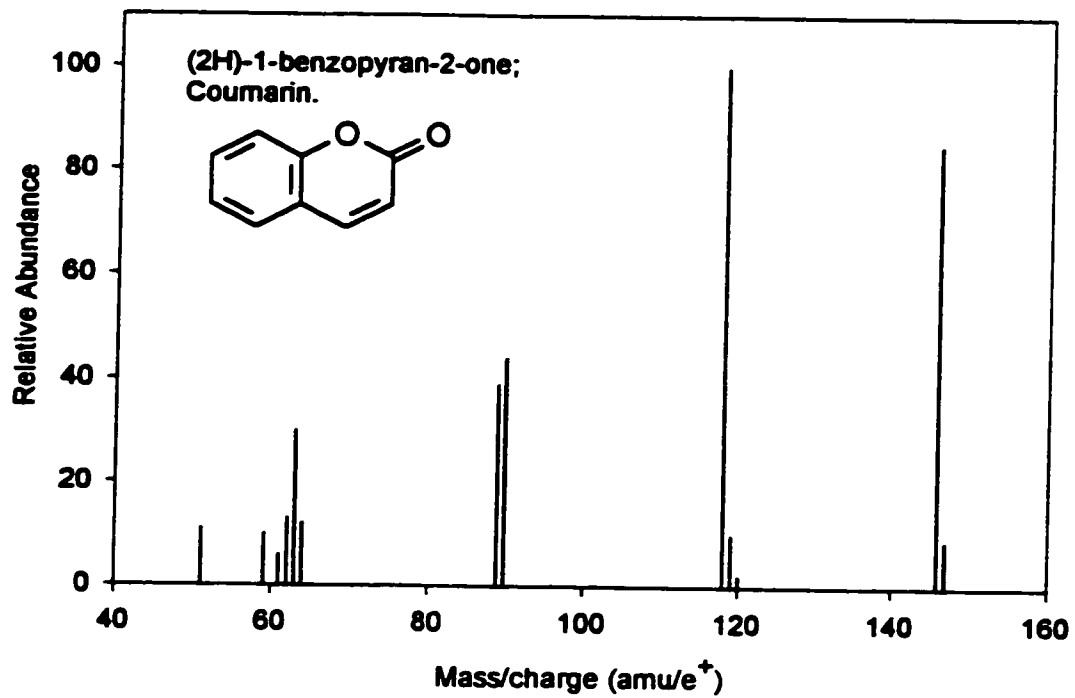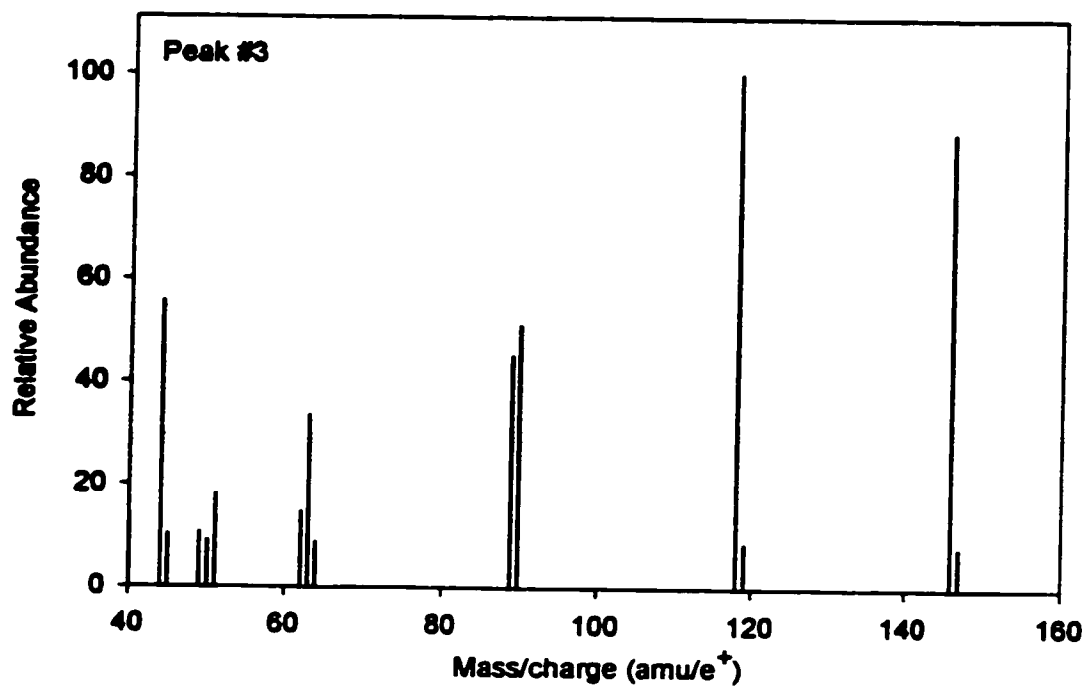
Figure 2.4. (Top) Mass spectra of peak #3 from Figure 2.1. The peak was identified as coumarin, based on a library match (Bottom) from the Wiley mass spectral registry.

Peak #2

Relative Abundance

100

80

60

40

20

0

20 40 60 80 100 120 140 160 180 200

Mass/charge (amu/e⁺)

Assignments:

2-hydroxy-2,3-dihydro-
1,4-naphthalenedione
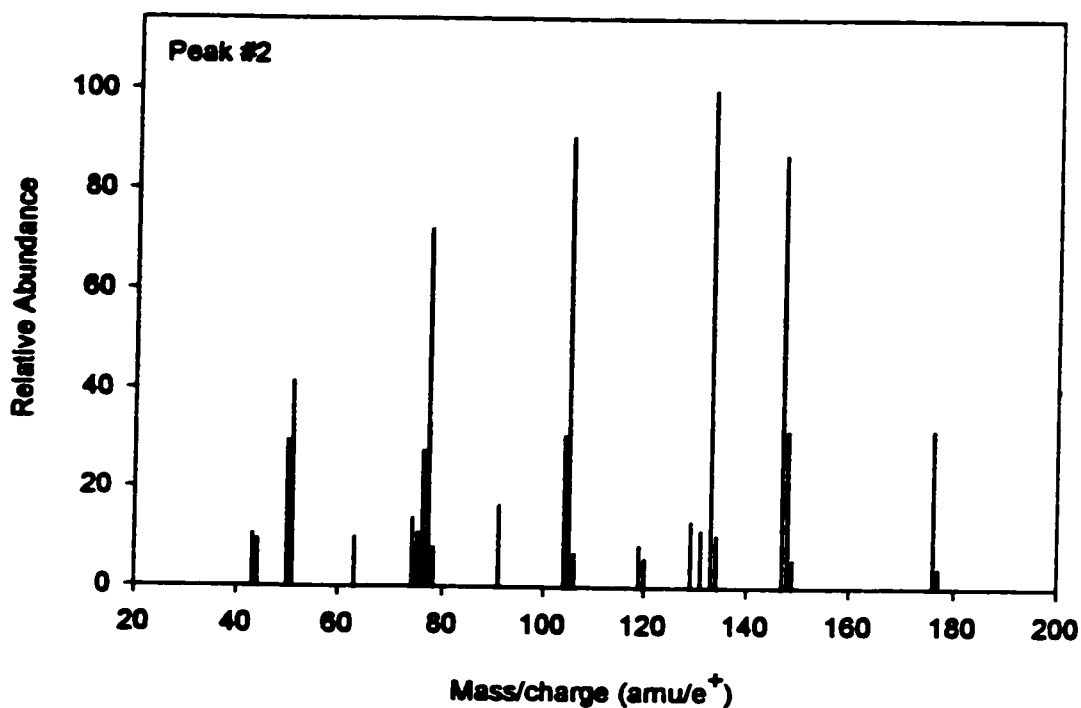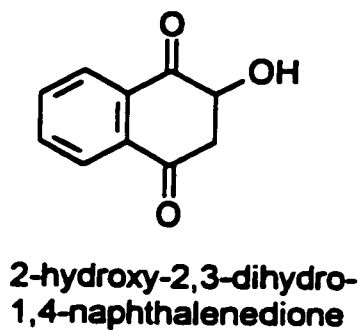
M.W.	Fragment
176	M⁺
148	[M - C=O]⁺
147	[M - CHO]⁺
133	[M - CH₂=CH–O]⁺
120	[M - 2 x C=O]+
119	[M - C=O - CHO]+
105	[C₆H₅–C=O]⁺
77	C₆H₅⁺
51	C₄H₃⁺

Figure 2.5. (Top) Mass spectra of Peak #2 from Figure 2.1. The peak was putatively identified as 2-hydroxy-2,3-dihydro-1,4-naphthalenedione, based on analysis of the ion fragmentation pattern. Molecular weight assignments for main fragments are shown (Bottom).

fragmentation of alcohols is dissociation of the C-C bond adjacent to the oxygen atom, which here

leads to loss of CHO (m/z 147) or CH$_2$=CHO (m/z 133). The lack of a strong peak at M$^+$ - 56

indicates that the two carbonyl groups are unlikely to be adjacent. This analysis provided sufficient

evidence to putatively identify the compound in Figure 2.5.

The product in Figure 2.6, *cis*-3-phenyl-2-propenal, was a very close match to the library

spectra for *trans*-3-phenyl-2-propenal. The primary difference between the library best match and the

observed spectra was the relative intensities of the molecular ion peak. For the trans compound, the

M$^+$ peak and M$^+$ - 1 peak are of comparable intensities, and the M$^+$ - 1 peak is due to loss of the

hydrogen adjacent to the carbonyl group. The observed spectra had a much stronger M$^+$ - 1 peak,

which was attributed both to loss of the hydrogen adjacent to the carbonyl and to the loss of a

hydrogen from the benzyl group, resulting in the stabilised ion with MW 131, shown in Figure 2.6.

The last product was provisionally identified as 8-hydroxy-1,2-napthoquinone. The

hydroxylated derivative would be expected to have greater stability than 1,2-naphthoquinone, as the

hydroxy group would stabilise the quinone due to intermolecular hydrogen bonding between the

hydroxy group and the oxygen on carbon 1. The mass spectra (Figure 2.7) had a strong molecular ion

peak at m/z 174, suggesting a bicyclic structure with molecular formula C$_{10}$H$_6$O$_3$, and also showed

strong peaks at m/z 146 and 118, corresponding to the loss of one and two carbonyl groups

respectively. The relatively strong peak at m/z 118 suggests that the carbonyls are adjacent. The peak

at m/z 92, assigned to C$_6$H$_4$O, and the lack of peaks at 77 and 105 indicate that the hydroxy group is

on a different ring than the carbonyls. It is thought that this product is a result of oxidation of 1-

naphthol or 1,2-naphthoquinone.

The reaction scheme shown in Figure 2.8 summarises the proposed pathways by which each

of these products were formed. Structures highlighted in boxes were putatively identified.
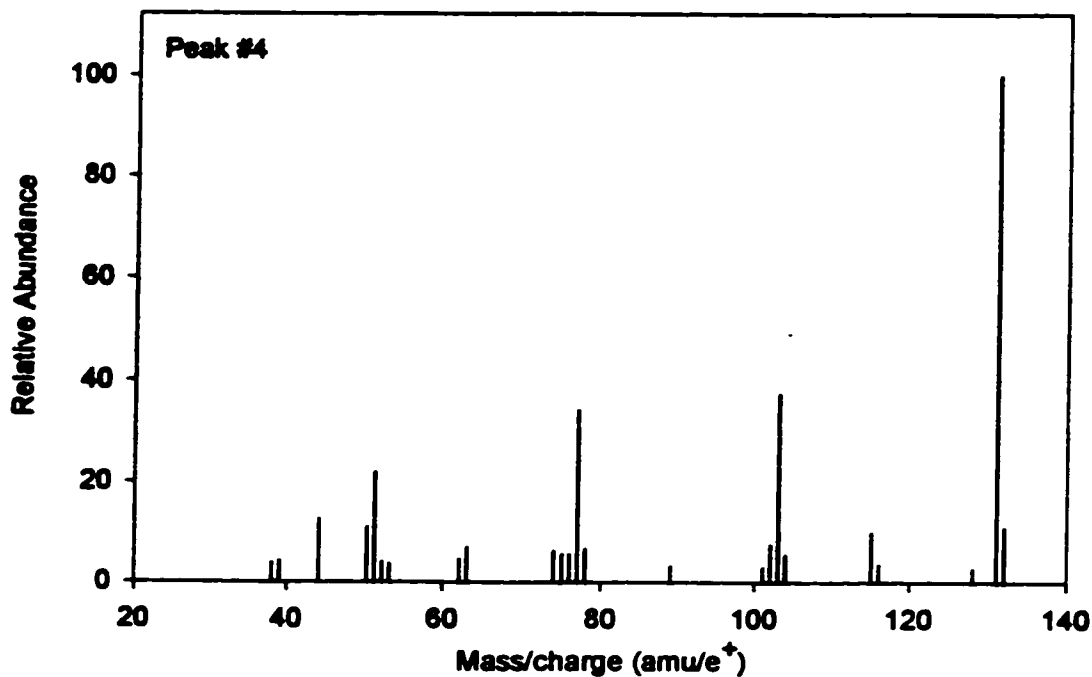
Peak #X, MW 132
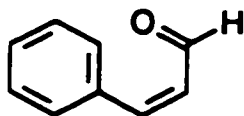
M.W.	Fragment
132	M$^+$
131	[M - H]$^+$
115	[M - OH]$^+$
103	[C$_6$H$_5$-CH=CH]$^+$, [M - CHO]$^+$
89	[C$_6$H$_5$-CH$_2$]$^+$
77	C$_6$H$_5$$^+$
51	C$_4$H$_3$$^+$
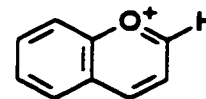
cis-3-phenyl-2-propenal

Figure 2.6. (Top) Mass spectra of Peak #4 from Figure 2.1. The peak was putatively identified as cis-3-phenyl-2-propenal, based on analysis of the ion fragmentation pattern. Molecular weight assignments for main fragments are shown (Bottom).

Peak #X, MW 174

M.W.	Fragment
174	M⁺
146	[M - CO]⁺
120	[M - CO-CH=CH]⁺
118	[M - 2 x CO]⁺
92	[C₆H₄O]⁺
89	C₇H₅⁺
63	C₅H₃⁺

8-hydroxy-1,2-naphthalenedione
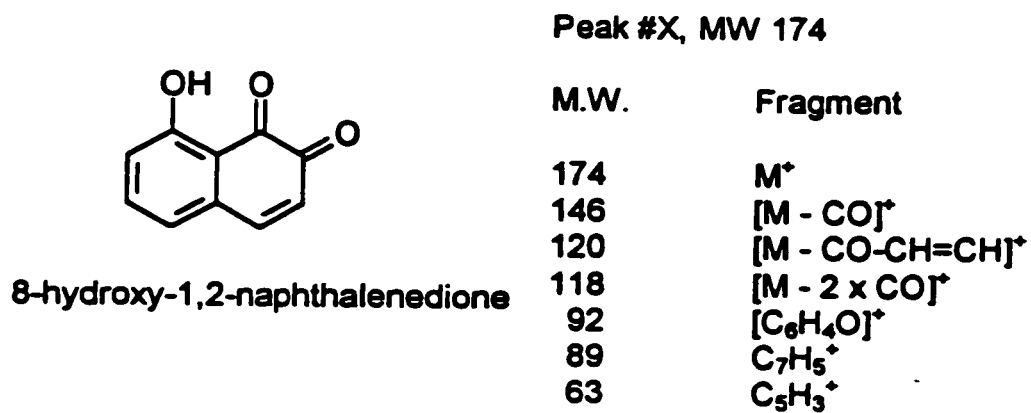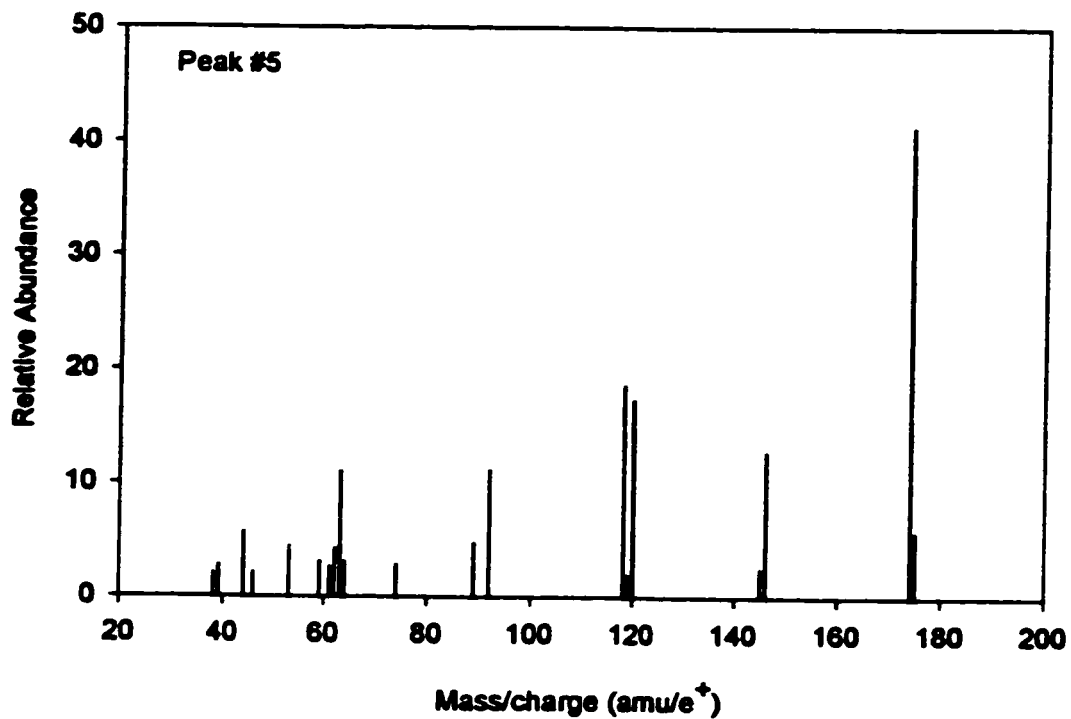
Figure 2.7. (Top) Mass spectra of Peak #5 from Figure 2.1. The peak was putatively identified as 8-hydroxy-1,2-naphthalenedione, based on analysis of the ion fragmentation pattern. Molecular weight assignments for main fragments are shown (Bottom).
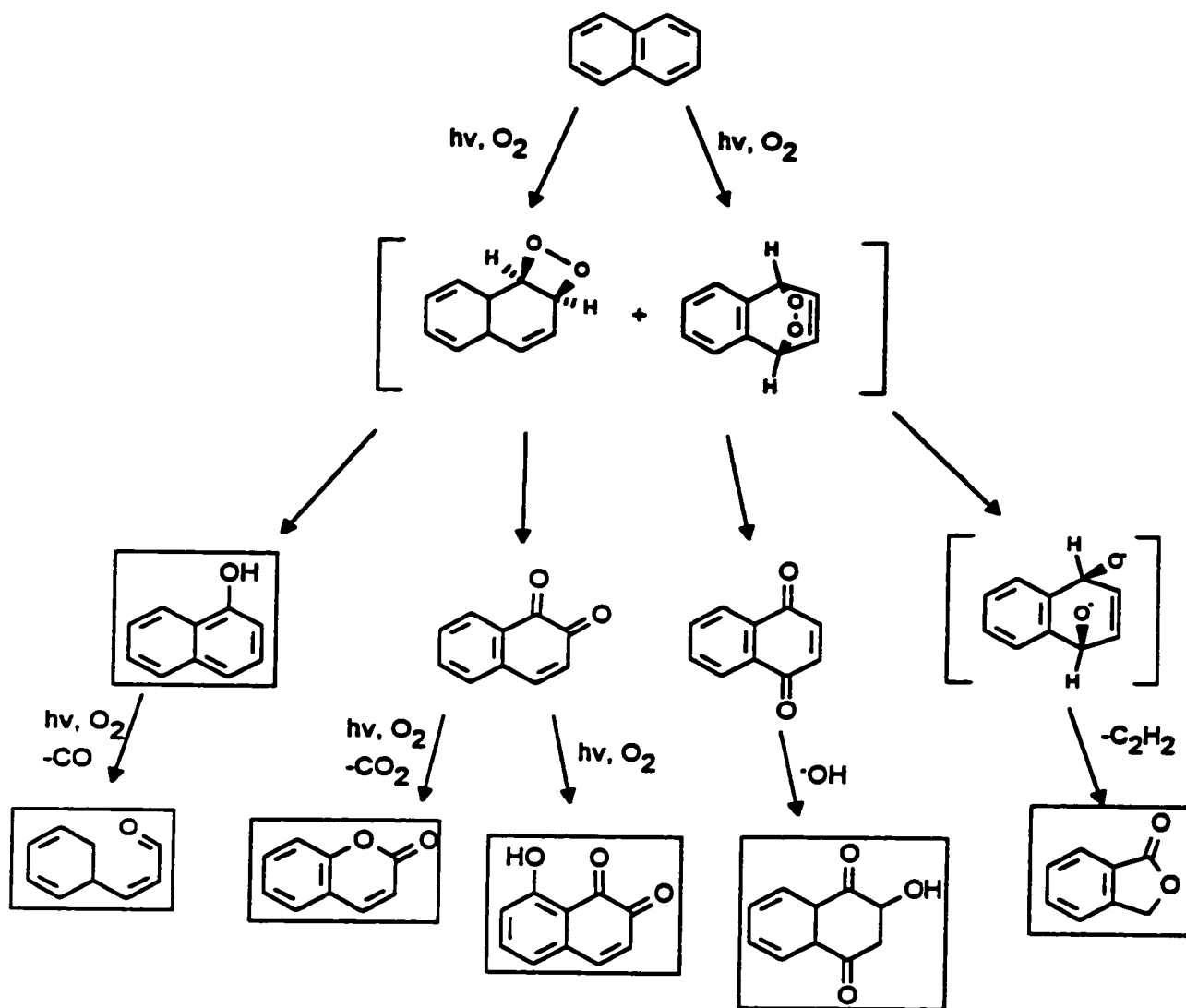
Figure 2.8. Proposed reaction scheme for photodegradation of naphthalene, leading to the observed products. Products in brackets are short lived intermediates. Products in boxes were putatively identified by comparison with library spectra or by analysis of the GC/MS ion fragmentation pattern.

2.4 DISCUSSION

The air oxidation of NAP has been previously investigated using silica or alumina as a solid substrate (Barbas et al. 1993). In the study by Barbas et al, 1993, only one primary photoproduct, phthalic acid, was identified as 49% of the reacted naphthalene. The aqueous oxidation of NAP from solid phase studied here produced quite a different result, with numerous products observed. The products from aqueous photooxidation were more akin to the products resulting from NAP metabolism by mammalian P450 enzymes (Tingle et al. 1993; Wilson et al. 1996; England et al. 1998) than from bound phase air oxidation. The difference in the oxidation pattern may be due to the presence of abstractable hydrogens from water.

The products of NAP metabolism have been implicated as the causative agents of NAP toxicity in mammalian systems (Kawabata and White 1990; Tingle et al. 1993; Wilson et al. 1996; Bagchi et al. 1998). Exposure to naphthalene causes increased production of oxygen free radicals, resulting in lipid peroxidation and DNA damage (Bagchi et al. 1998a, Bagchi et al. 1998b), and this is attributed to the products of metabolism and not intact NAP (Kawabata and White 1990; Tingle et al. 1993; Wilson et al. 1996; Bagchi et al. 1998).

Some of the identified products of photochemical oxidation of NAP have also been previously identified as the toxic products of NAP. In particular, 1-naphthol and 1,2- and 1,4-naphthoquinones are known to be toxic, and can be formed by metabolism. The measured toxicity of each of these three products was 2.5 times that of NAP, and the toxicity of NAP was attributed to the production of 1-naphthol (Wilson et al. 1996).

The exposure of an aqueous solution of naphthalene to light resulted in the generation of least three chemical species with known toxic effects. The chemistry of 1-naphthol in aqueous systems is particularly interesting; it is a photoinitiator, capable of abstracting hydrogens from alkanes and other hydrocarbons in the presence of light (Saito and Matsuura 1979; Payne and Phillips 1985). It would be expected to have the same effects in aquatic invertebrates, plants, or fish-gill epithelial tissues exposed to light. In addition, 1-naphthol is not dependent on light to elicit toxic effects; it is known to

35

be toxic via production of oxygen radicals and can be further metabolised to quinones capable of forming covalent products with proteins (Doherty et al. 1984).

Coumarin, another of the observed photoproducts, is a naturally occurring toxin produced by clover and acts as an anticoagulant if present in sufficient concentration. Coumarin has been tested as an environmental contaminant using the amphibian FETAX assay, and was found to be developmentally toxic (Fort et al. 1998). The toxicity of coumarin was increased on metabolic activation, suggesting formation of reactive intermediates. Coumarin may also act as a sensitizer (Hausen and Schmieder 1986). While it is uncertain that the oxidation of naphthalene will result in sufficient environmental concentrations of coumarin to elicit significant effects, it illustrates the difference in the modes of action of PAHs and their photoproducts.

Other identified products were (3H)-2-hydroxy-1,4-naphthoquinone, 1(3H)-isobenzofuranone, cis-3-phenyl-2-propenal (cis-cinnamaldehyde) and 8-hydroxy-1,2-napthoquinone. Cinnamaldehyde is an aromatic used in perfumes, and is not particularly toxic. The hydroxylated quinones may undergo futile redox cycling similar to their unhydroxylated counterparts, leading to free radical species and oxidative stress. Little information exists on the toxicity of isobenzofuranone.

1,2-naphthoquinone and 1,4-naphthoquinone were almost certainly present within the mixture of photooxidized products; they are expected are a result of epoxide degradation, and are also intermediates to some of the observed products. The concentration of quinones present however was less than that of the major products identified. Orthoquinones including 1,2-naphthoquinone are known to undergo redox cycling producing superoxide anion radical (O_2^-) and semiquinone alternant radicals, reducing cell viability and survival (Flowers-Geary et al. 1996). Orthoquinones are direct acting mutagens, as the quinones can intercalate and covalently bind to DNA (Flowers-Geary et al. 1996). They are reactive towards proteins as well, capable of direct arylation of protein sulfhydryl groups (Smith 1985). In particular, 1,2-naphthoquinone can bind to cysteine residues (Zheng et al. 1997).

The photooxidation of naphthalene provides a good illustration of the potential toxicity associated with oxidation products of PAHs. Naphthalene is not considered one of the more toxic

PAHs, and it does not act as a photosensitizer like other PAHs such as anthracene or fluoranthene. However, on exposure to light, photochemical reactions result in the formation of compounds with diverse modes of action and a toxicity greater than the baseline toxicity associated with non-polar narcosis (Ren et al. 1994). The photosensitizing capacity of 1-naphthol is of particular interest, as naphthol is the most abundant photoproduct of NAP and it shares a mode of action associated with PAHs. Thus, it can contribute to the phototoxicity of a mixture of PAHs occurring in an environmental system.

The photochemical reactions of PAHs can be quite varied. Naphthalene, the simplest PAH, has been shown to undergo initial reactions with oxygen in the form of [2,2] and [2,4] photocycloadditions. Subsequent reactions include loss of hydrogens to form quinones, rearrangements to form hydroxy compounds, formation of heterocyclic compounds incorporating oxygen in the ring structure, and hydrogen abstraction resulting in locally reduced carbons. These reactions are all likely to occur to varying degrees with the more complex PAHs as well, and will be illustrated in later chapters.

GC/MS proved quite useful for the identification of products form NAP oxidation, as it was possible to interpret the spectra obtained based on fundamental analytical principles. For the photoproducts originating from oxidation of the larger PAHs, the difficulty of interpretation of the mass spectra of products will increase. Additionally, the oxidation products of larger PAHs will generally be of higher molecular weight, and with increasing molecular weight, the photoproducts will be less thermally stable and less volatile. Both of these effects will decrease the probability of obtaining reliable mass spectra. Thus, the utility of GC/MS observed with the photooxidation of NAP may not be readily extrapolated to the identification of PAH structures. There are however other means of interpretation, such as HPLC/diode array, that can provide accurate information for the identification and quantification of products of PAH photooxidation, and these methods will be relied upon more heavily for the larger PAHs.

The parallel of photochemical oxidation of naphthalene to biochemical activation should be stressed. The capacity of PAHs as pro-carcinogens is widely recognised, and the pathway by which

selected PAHs (notably benzo(a)pyrene) undergo biochemical activation to active carcinogens is well understood. That active carcinogens can be formed by photochemical action alone is less well accepted, but is quite likely to occur due to the similarity of biochemical and aqueous photochemical oxidation of PAHs, exemplified here by naphthalene oxidation.

.

CHAPTER 3

REACTION RATES AND SITES OF OXIDATION OF FOUR RING PAHS

3.1 INTRODUCTION

The environmental fate of PAHs has in general not yet been fully characterised in aquatic systems, and in particular there is a need to investigate the identity and stability of PAH degradation products. Some PAH degradation products have significant toxic or mutagenic impacts (Smith 1985; Lesko et al. 1986; Huang et al. 1997; McConkey et al. 1997). Previously, modelling of the toxicity of PAHs to plants has resulted in the classification of PAHs into two groups, those acting predominantly by photosensitisation (production of $^1O_2$), and those acting predominantly by photomodification (e.g. oxidation reactions). Of sixteen PAHs tested, seven were classed as photosensitisers, and nine exhibited toxicity predominantly by photomodification of the PAHs (Krylov et al. 1997).

In the previous chapter, the photooxidation of naphthalene was examined as a model study of PAH oxidation in aqueous phase. For this chapter, the oxidation reactions of the more complex four ring PAHs will be discussed. The set of four-ring polycyclic aromatic hydrocarbons (PAHs) include six possible structures comprised of 6-carbon rings, plus five structures incorporating a non-terminal 5-membered ring. Of this set of 11 PAHs, four are commonly quantified in environmental samples: fluoranthene, pyrene, chrysene, and benzo(a)anthracene (Environment Canada 1994; van Brummelen 1995). These four, plus benzo(b)anthracene, will be discussed in this chapter. Chemical structure and nomenclature for these PAHs is shown in Figure 3.1.

Four-ring PAHs absorb UV and visible light with high efficiency, resulting in electronically excited state PAHs. Two possible chemical means of dissipating this energy are to transfer it to oxygen, resulting in biologically damaging oxygen species, or to undergo photochemical reactions forming new products. The most frequent products in atmospheric or aquatic systems are oxygenated PAHs, which in many cases are themselves toxic, phototoxic, or mutagenic (Huang et al. 1995; Legzdins et al. 1995; McConkey et al. 1997; Kosian et al. 1998).

39
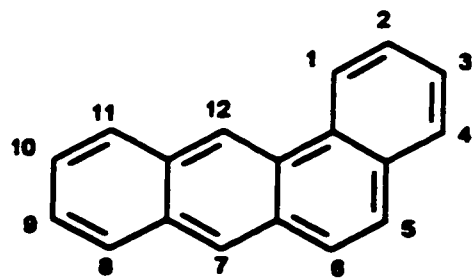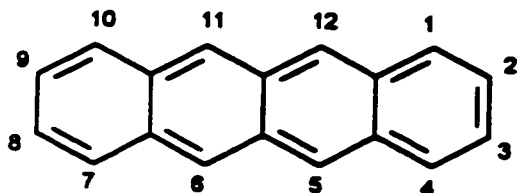
Benzo(a)anthracene
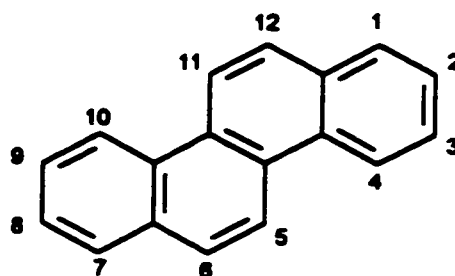
Benzo(b)anthracene
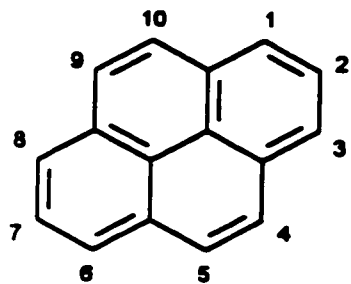
Chrysene

Pyrene
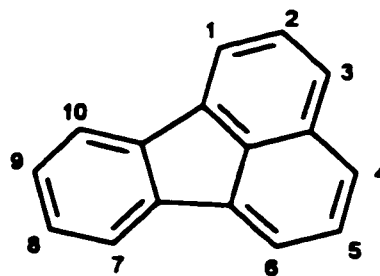
Fluoranthene

Figure 3.1: Chemical structures and nomenclature of four ring PAHs.

Benzo(b)anthracene, benzo(a)anthracene, and chrysene are structurally related, as each are linearly annealated four-ring PAHs, with zero, one and two obtuse angles respectively between aromatic ring centres. Based on energetic considerations alone, it was expected that the reactivity of these PAHs would decrease with an increasing number of obtuse angles between centres (Wiberg 1997), and this would have a large influence on the oxidation rates. Fluoranthene and pyrene are condensed PAH structures, each containing two ternary carbons (carbons bonded to three other carbons) which should impart an increased stability towards oxidative attack. The reaction rates of fluoranthene and pyrene are compared to that of the linearly annealated PAHs. The photochemical reaction rates and a means to determine the most energetically favoured sites of PAH oxidation are presented in this chapter. The influence of delocalisation energies and production of singlet oxygen on reaction rates and subsequent product formation will be discussed. Several products of PAH oxidation were also isolated and identified. The relative rates of photooxidation of PAHs and photoproducts are addressed, as it has implications for the environmental persistence and accumulation of PAHs and photoproducts found in environmental compartments.

3.2 MATERIALS AND METHODS

3.2.1 Preparation of PAH solutions

Benzo(a)anthracene, chrysene, fluoranthene, pyrene, and benzo(b)anthracene, each of greater than 97% purity, were obtained from Sigma Chemical Co. (St. Louis, MO, USA). The purity of the compounds was confirmed using high pressure liquid chromatography. The water used in all experiments was HPLC grade water, obtained from a Barnstead E-pure ultrafiltration system (VWR/Canlab, Mississauga, ON). PAHs were delivered to aqueous phase (HPLC grade water) using dimethylsulfoxide (DMSO) (BDH Inc., Toronto, ON) as a carrier solvent. Stock solutions of a given PAH in DMSO were prepared at a nominal concentration of 2.0 mg/ml, except for benzo(b)anthracene, which was prepared at a concentration of 1.0 mg/ml due to its lesser solubility in DMSO and water. Two hundred μl of the stock solution was added to 200 ml of rapidly stirred water in 250 ml pyrex beakers, creating an extremely fine suspension of emulsified PAH in aqueous phase.

41

The resultant nominal concentration of PAH was 2.0 mg/L (1.0 mg/L for benzo(b)anthracene) in an aqueous solution with 0.1% DMSO. The pyrex beaker was covered with a polyethylene film, transparent to UV-B, UV-A and visible light. The glass beaker had a measured UV transmittance cutoff of 300 nm, closely corresponding to the minimum wavelength present in sunlight at ground level.

3.2.2 Light exposure of solutions

Samples were exposed to sunlight in June at 43°N latitude, between 10 and 4 p.m. on days with less than 10% estimated cloud cover, providing a reasonably constant source of high intensity light. The solar spectrum (Figure 3.2) was measured using a spectroradiometer (Model 77400, Oriel Corporation, Stratford, CT USA). The proportion of light energy absorbed by each PAH was estimated from published absorbance curves (Karcher et al. 1985; Karcher 1988) and the measured solar spectrum. The absorbance curves and solar spectra were quantified in 2 nm increments, and the total absorption was calculated as $ABS = \Sigma \, \varepsilon_\lambda I_\lambda \, d\lambda$. ABS is the absorbance of the PAH, ε_λ is the extinction coefficient of the PAH at a given 2 nm increment, I_λ is the measured solar irradiance at wavelength λ, and $d\lambda$ is the step size of 2 nm. ABS was calculated from 295 to 500 nm, the range in which $I_\lambda > 0$ and $\varepsilon_\lambda > 0$. Absorbance curves obtained from the literature were measured in organic solvents, but this is not expected to have a significant impact on the relative total absorbance of each PAH.

3.2.3 Chemical analysis of PAHs and photoproducts

Water samples of 1 ml were periodically removed from the beakers for chemical analysis once solar exposure began. Chromatographic analysis was performed with a Shimadzu HPLC system comprised of an SCL-10A system controller, two LC-10AD dual pumps, an SCL-10A diode array detector, and an SIL-10A autoinjector (Shimadzu Scientific Instruments Inc., Columbia, MD, USA). The HPLC column used for chemical analyses was a 25 cm x 4.6 mm I.D. Supelcosil C_{18} reverse-phase column with a 5 μm packing (Supelco Inc., Bellefonte, PA, USA). HPLC grade water (adjusted to pH 3 with phosphoric acid)
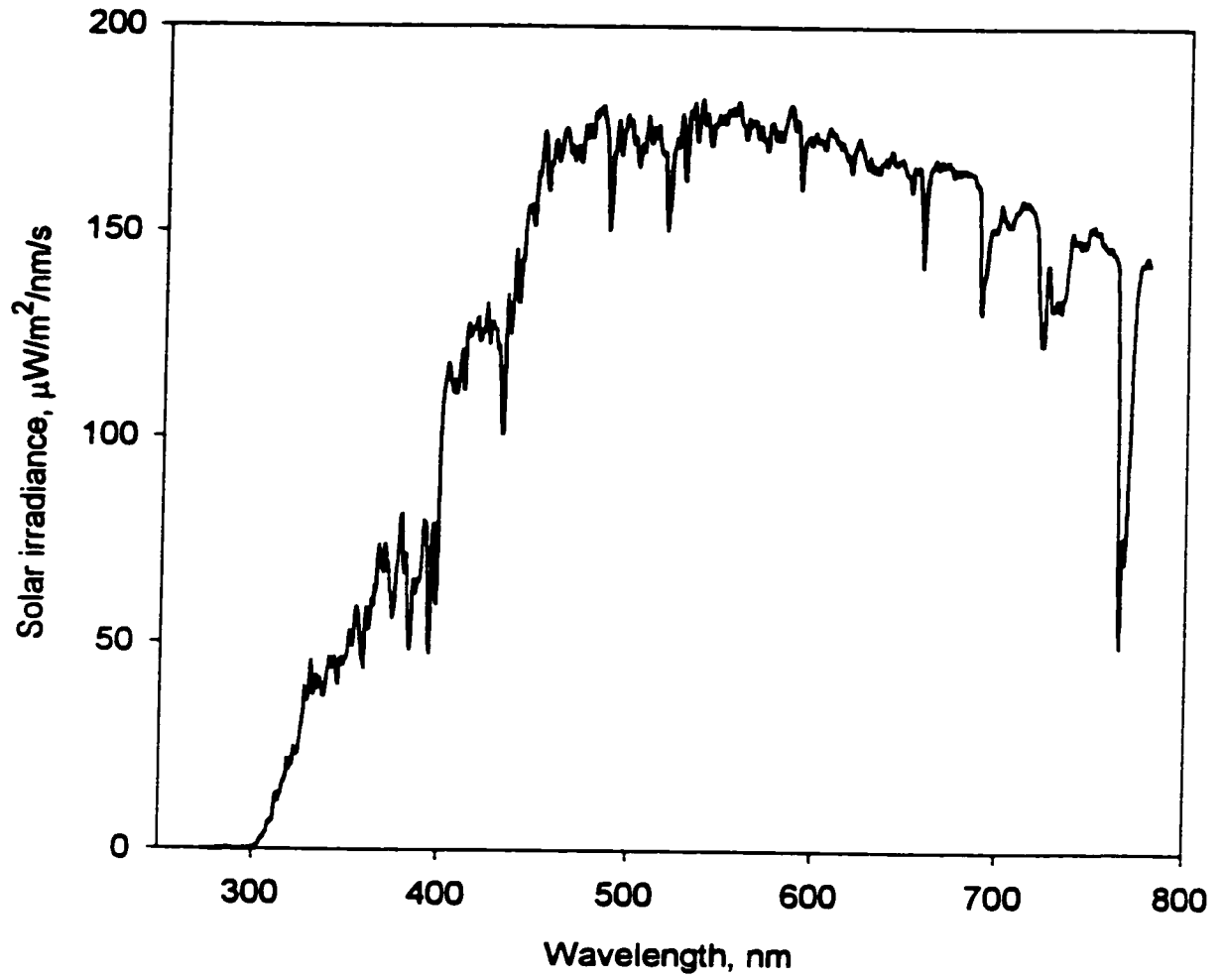
Figure 3.2. Sample solar spectra, June, 43°N lattitude.

and acetonitrile, both degassed with helium, were used as elution solvents at a constant flow rate of 1 ml/min. The gradient used was 95:5 water:actonitrile (v/v) for 5 minutes, then a linear gradient to 5:95 water:acetonitrile over 30 minutes, and held at 95% acetonitrile for 5 minutes. An injection volume of 200 ul was used for the aqueous samples.

Where possible, authentic standards were used to identify photoproducts. Standards of benzo(a)anthracene-7,12-dione and benzo(b)anthracene-5,12-dione were purchased from Sigma Chemical Co., St. Louis, MO. Where standards were not available, products were putatively identified based on absorbance spectra and theoretical considerations, such as reactive sites on the parent PAH and observed chemical properties such as hydrophobicity (e.g. HPLC column retention). The concentrations of PAHs and PAH photoproducts were fitted to specified kinetic models, using Systat 8.0 (Wilkinson 1998). All errors are expressed as ± one standard deviation.

3.3 RESULTS

3.3.1 Degradation kinetics

PAH photooxidation reactions are dependent on the presence of light, oxygen, and the concentration of PAH. In an aqueous solution exposed to air, the concentration of dissolved oxygen is high, at approximately 0.25 mM (Robinson and Cooper 1970), and reactions of almost all PAHs with oxygen will be diffusion limited (Krylov et al. 1997). Thus the reaction rate of PAHs in aqueous solution with a constant light source will be a function of PAH concentration alone, and the rate of degradation can be described by a first order model. The kinetic models discussed here assume an initial amount of PAH exposed to a light source, with PAH degradation occurring solely due to photoreactions and no additional input of PAH over time. Assuming a constant level of both light and oxygen, the kinetics of PAH photooxidation may be approximated by a first order rate equation:

$$d[PAH]/dt = -k_1[PAH] \qquad (3.1)$$

Solving for the concentration of PAH,

$$[PAH] = [PAH]_0 e^{-k_1 t}. \qquad (3.2)$$

$[PAH]_0$ is the initial concentration of PAH, t is exposure time in hours, and k_1 is the rate constant with

44

units of hours^{-1}. If a photoproduct (PP) is formed in proportion to the loss of parent PAH, and is itself degraded according to a first order model, the rate of change of photoproduct will be

d[PP]/dt = rate of formation of product – rate of loss of product,

$$d[PP]/dt = \Phi_{12}k_1[PAH] - k_2[PP]. \tag{3.3}$$

where [PP] is the amount of photoproduct, Φ_{12} is the efficiency of product formation (i.e. the fraction of product formed per unit PAH lost), and k_2 is the rate constant for product degradation. For a system dosed with an initial quantity of PAH, the amount of PAH follows (3.2) and the change in product concentration is

$$d[PP]/dt = \Phi_{12} k_1[PAH]_0 e^{-k_1 t} - k_2[PP]. \tag{3.4}$$

Equation (3.4) may be rearranged and solved as a linear first order differential equation (Spiegel 1981) with the solution

$$[PP] = \{\Phi_{12} [PAH]_0 k_1/(k_2-k_1)\}(e^{-k_1 t} - e^{-k_2 t}). \tag{3.5}$$

To provide a basis for comparison, we are interested in the relative amounts of PAH and photoproduct. If a one-to-one conversion ($\Phi_{12} = 1$) of PAH to a stable photoproduct is assumed, then the maximum quantity of photoproduct on a molar basis is [PAH]$_0$. If both the PAH and photoproduct have approximately the same rate of degradation, $k_1 \approx k_2$, then the maximum concentration of product over time may be shown to be $1/e = 0.368$. If $k_2 >> k_1$, the product is itself quickly degraded and only low levels of product will be observed. The kinetic models of photoproduct amounts will be applied to acquired data in section 3.3.3.

The first order model of PAH degradation could approximate a situation of a single dose occurring in an environmental system, such as a spill event. In many cases, a model incorporating a constant input term is a more realistic environmental model. Thus, a steady state model is a better model for environmental systems assuming a constant rate of PAH input. This simplifies equation (3.3) as the concentration of both PAH and photoproduct will be constant at steady state, and d[PP]/dt = d[PAH]/dt = 0. The resulting ratio of photoproduct to PAH is

$$[PP]/[PAH] = \Phi_{12}k_1/k_2. \tag{3.6}$$

Thus, the ratio of photoproduct to PAH is proportional to the relative rates of loss of the PAH versus photoproduct in a steady state system, assuming equal light exposure of both PAH and photoproduct. In a steady state system, if the conversion efficiency Φ_{12} is approximately unity and the PAH and photoproduct have comparable rates of loss, the concentration of photoproduct will be comparable to the amount of PAH. One implication of this is that the low concentrations of photoproducts observed in a closed system, such as the experimental setup used here to determine the rate of PAH loss, will underestimate potential environmental concentrations.

3.3.2 Photooxidation rates

Solutions of PAH were exposed to sunlight and the rate of loss of PAH from solution was monitored (Figure 3.3). The rate of loss was fit to a first order kinetic model (3.2) using the GLM (General Linear Model) module of SYSTAT 8.0 (Wilkinson 1998). The estimated rate constants for photooxidation are shown in Table 3.1. Reaction of the PAHs with oxygen is most likely to occur from the triplet state. Thus, the rate of PAH oxidation will be dependent on the amount of light absorbed by the PAH, the PAH triplet state yield, and the yield for photooxidation from the triplet state. The amount of light absorbed (ABS) by each PAH and the triplet quantum yields are shown in Table 3.1. The yield for photooxidation is a function partially dependent upon the triplet state energy (E_T) of the PAH. Triplet state energies may be compared to the energy of the lowest singlet state of oxygen, 92 kJ/mol (Gilbert and Baggott 1991) above ground state. Two possible outcomes of the reaction of triplet state PAH with oxygen are production of $^1O_2$, or oxidation of the PAH to form a new chemical species. It will be assumed that a key factor in PAH oxidation from triplet state is the ability of the PAH to transfer energy to oxygen, as an initial reaction step. Given this assumption, both types of reaction with oxygen are a function of the PAHs' ability to generate singlet oxygen. Which mechanism is favoured is then a function of the energy barrier of reaction, and the ground state energy of the reaction product.

46
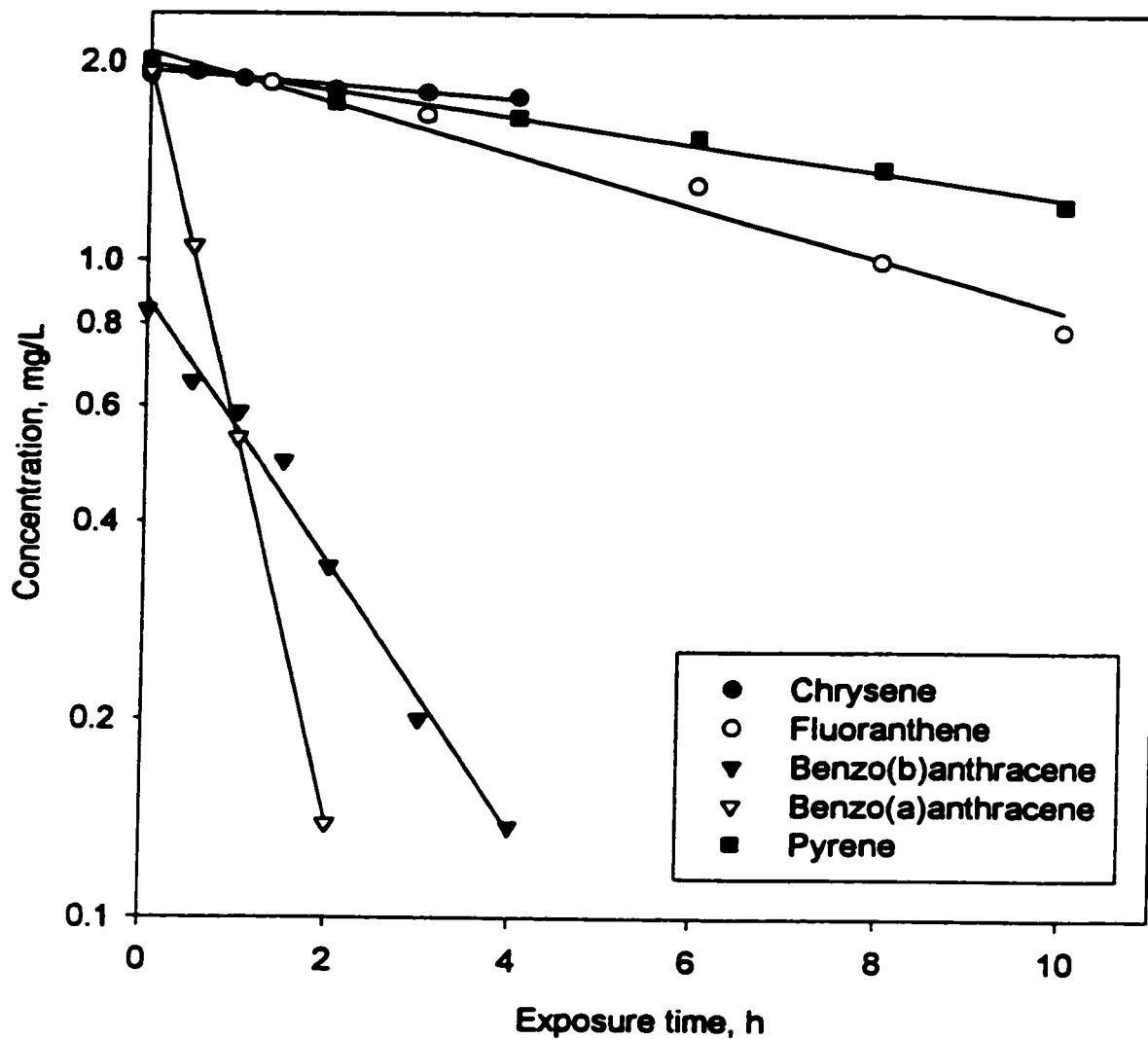
Figure 3.3. Measured oxidation rates of four-ring PAHs in sunlight. Nominal initial concentrations were 2.0 mg/L, except for benzo(b)anthracene which had a nominal concentration of 1.0 mg/L. All experiments were performed in aqueous solution with 0.1% dimethyl sulfoxide as a solvent carrier.

Table 3.1: Rates of photooxidation, relative light absorbance, and estimated photochemical reactivity of PAHs. Triplet state energies and triplet state half-lives also shown.

Chemical	k_{obs} Sunlight, h^{-1}	ABS	Triplet energy[1], E_T, kJ/mol	Triplet state yield[2], φ
Benzo(a)anthracene	1.33 ± 0.03	0.53	197	0.80
Chrysene	0.025 ± 0.003	0.14	239	0.67
Fluoranthene	0.090 ± 0.008	0.63	221	0.60
Benzo(b)anthracene	0.462 ± 0.031	1.90	123	0.65
Pyrene	0.046 ± 0.003	1.00	203	0.27

[1] from Morgan et al. 1977
[2] from Krylov et al. 1997

A primary determinant of the ground state energy of PAH photoproducts is the change in delocalisation energy (E_D), on loss of a portion of the aromatic structure of the PAH when the PAH is oxidised. The change in delocalisation energy was used as a factor in modeling the reaction rates of PAHs, as well as to determine the most likely sites of oxidation on the PAH carbon skeleton (Section 3.3.3).

The delocalisation energies of PAHs and compounds used as a basis set for calculations were obtained from published values, which were estimated using molecular modelling software (Wiberg 1997). The PAH and basis set delocalisation energies are shown in Table 3.2. The delocalization energy of benzo(a)anthracene was estimated as the average of benzo(b)anthracene and chrysene, as the changes in delocalisation energy are expected to be proportional to the number of obtuse angles between aromatic centres (Wiberg 1997). As fluoranthene is a non-alternant PAH composed of a benzyl and naphthenyl domain in the ground state, its delocalisation energy could be estimated as the sum of delocalisation energies of benzene, naphthalene, and two bonds similar to the 1,1' bond of biphenyl. The delocalisation energies of products were calculated as the sum of separate aromatic domains within the product on oxidation of the parent PAH. This assumes that the initial oxidation product results in a local loss of conjugated aromatic structure, as would be the case with epoxide

Table 3.2: Delocalization energies and sites of oxidation. Delocalisation energies were obtained from Wiberg, 1997 except where noted. All energies are in kJ/mol. See text for method of ψ_{1O2} estimation.

Chemical	Oxidation reaction	Delocalisation energy, E_D	ΔE_D on oxidation	Estimated Efficiency of $^1O_2$ production, ψ_{1O2}
E_D Basis set				
Butadiene		12		
Benzene		151		
Styrene		151 + 8		
Naphthalene		251		
Biphenyl		2 x 151 + 8		
Anthracene		335		
Phenanthrene		356		
Chrysene		456		0.75
	1,2 addition		92	
	5,6 addition		54	
Benzo(b)anthracene		414		1.02
	1,2 addition		71	
	5,12 addition		12	
Benzo(a)anthracene		435[1]		3.24
	1,2 addition		92	
	5,6 addition		33	
	7,12 addition		33	
	8,9 addition		71	
Fluoranthene		418[2]		1.49
	2,3 addition		108	
	7,10 addition		151	
Pyrene				2.76

[1] estimated as [E_D(benzo(b)anthracene) + E_D(chrysene)]/2

[2] estimated as E_D(benzene) + E_D(naphthalene) + $2E_D$(1,1' bond of biphenyl)

additions. The changes in delocalisation energies on oxidation of each PAH at specific carbons are shown in Table 3.2. The delocalisation energy of pyrene was not available in the published literature, but it would be expected to be at least as large as that of fluoranthene, due to its highly condensed, symmetrical structure.

In addition to the change in energy on oxidation, the other suspected main factor in PAH oxidation was the ability to transfer energy to oxygen, producing $^1O_2$. Experimentally determined rates of singlet oxygen production by individual PAHs in aqueous media were not found in the literature. However, short term acute phototoxicity data of PAHs was available (Newsted and Giesy 1987). Here, the photoinduced toxicity of PAHs to *Daphnia magna* was measured as time to lethality (between 0.8 and 24 hours). Due to the short exposure times used, the toxicity could be attributed predominantly to photosensitisation reactions, i.e. production of $^1O_2$. Thus it was possible to use this data to estimate the efficiency of energy transfer from ^{3}PAH to $^3O_2$. The toxicity data was highly dependent upon the PAH triplet state energies, and the adjusted time to lethality (ALT50) could be expressed as a function of triplet state energy (Newsted and Giesy 1987):

$$ALT50 = 1.53 \times 10^{-20}(E_T)^{9.64} + 6.52 \times 10^{12}(E_T)^{-4.70} \tag{3.7}$$

The time to lethality is expected to be inversely proportional to the rate of singlet oxygen production. Using (3.7), an term proportional to the efficiency of $^1O_2$ production, ψ_{1O2}, could be defined:

$$\psi_{1O2} = 1000 \times [1.53 \times 10^{-20}(E_T)^{9.64} + 6.52 \times 10^{12}(E_T)^{-4.70}]^{-1} \tag{3.8}$$

While this term is only an estimate, it is useful in determining whether the rate of $^1O_2$ production has an influence on the oxidation rates of PAHs. The estimate of $^1O_2$ production efficiency, ψ_{1O2}, is shown in Table 3.2.

The specific dependency of the reaction rate on each of these terms is unknown. However, the reaction rate may be approximated as a product of two factors:

$$R_{ox} = F(\text{triplet state formation}) \ast F(\text{reaction of } ^3PAH \text{ with } ^3O_2).$$

Expressed as a linear function of quantified parameters,

$$R_{ox} \propto ABS \ast \phi_T \ast (1/\Delta E_D) \ast \psi_{1O2}. \tag{3.9}$$

50

To determine if the change in delocalisation energy and ψ_{1O_2} were in fact correlated to the observed reaction rates, the observed reaction rates were plotted against $[ABS * \varphi_T * (1/\Delta E_D)]$ and $[ABS * \varphi_T * (1/\Delta E_D) * \psi_{1O_2}]$ (figures not shown). The goodness of fit determined as R^2 values, were $R^2 = 0.53$ and $R^2 = 0.81$ respectively. Thus, the delocalisation energy and the production of singlet oxygen both influence the reaction rates.

3.3.3 Products of PAH oxidation

While the delocalisation energies are related to rates of oxidation, they have greater utility in predicting the oxidation sites on the PAH carbon skeleton. It is expected that the products of PAH photo-oxidation will favour those with a minimal loss of delocalisation energy. Additionally, if singlet oxygen is generated, a 1,4 addition across a ring will be favoured over the 1,2 addition to adjacent carbons (Gilbert and Baggott 1991). Using the four-ring PAHs as an example, favoured sites of oxidation on the carbon skeleton were predicted. In addition, expected reaction products were confirmed where standards were available, and the relative photochemical stability of products and parent PAH were compared.

Pyrene, as a highly symmetrical, highly conjugated PAH, was expected to degrade slowly relative to the other PAHs. The observed reaction rate was in accordance with this hypothesis, with a half-life of 15 hours in full sunlight (Figure 3.3), amoung longest of any of the PAHs tested. Reactions of pyrene are most likely to be initiated at the 1-carbon position, resulting in an intermediate radical species containing a phenalenyl radical. The phenalenyl radical consists of three aromatic rings sharing a common carbon and is a comparatively stable radical. Oxidation initiated at either of the other two possible sites, the 2 or 4 carbons, results in intermediates with a restricted number of resonance states. As intermediate species resulting from oxidation at the 1-carbon position have more resonance states, it is expected that they will have lower transition energy and hence will be favoured. After the initial oxidation step, it is expected that a second oxidation of the resultant radical will favour the formation of a symmetrical product, as a symmetrical product will have a greater delocalisation energy (Malkin 1992). Thus, expected products after an initial oxidation at the

51

1-carbon are 1,6- and 1,8-pyrene-diones. This is analogous to the oxidation products observed with benzo(a)pyrene (Chapter 5). Two products with appropriate HPLC retention times and absorbance spectra were observed to increase over the course of the experiment, suggesting that the products are relatively stable. Based on retention times, absorbance spectra, and comparison with those of the benzo(a)pyrenediones (Chapter 5), the two products were tentatively identified as 1,6- and 1,8-pyrenediones and are indicated as P1 and P2 respectively in Figure 3.4.

Benzo(a)anthracene was the most rapidly oxidised PAH of the five tested. The expected site of initial oxidation is across the 7,12 position resulting in an endoperoxide, which is likely to dissociate in sunlight, producing benzo(a)anthracene-7,12-dione (BAAQ). HPLC analysis of photo-oxidised BAA showed two primary products, one of which was identified as BAAQ (Figure 3.4). Anthraquinone was also identified as a minor product of BAA photooxidation.

The concentration of BAA and BAAQ were determined over the course of the experiment (Figure 3.5). The maximum amount of BAAQ over time was 10% of the initial PAH concentration. To determine the relative stability of the product versus the parent PAH, a solution of benzo(a)-anthracene-7,12-quinone was exposed to solar radiation, and the rate of decomposition monitored (Figure 3.5). BAAQ had an observed half-life of 0.19 ± 0.04 hours, as compared to the half-life of BAA, 0.52 ± 0.01 hours. Thus, the product is less stable than the parent PAH, partially explaining why little accumulated over the course of the experiment. It is expected that BAAQ degradation would proceed via fission of the bonds alpha to the carbonyl groups, as this retains the aromatic domains and is also a favoured photochemical reaction of the carbonyl moiety (Gilbert and Baggott 1991). The first order degradation models (2) and (5) were fitted to the concentrations of BAA and BAAQ, and the efficiency of formation was estimated as $\Phi_{BAA \rightarrow BAAQ} = 0.33$. Interestingly, further oxidation of BAA and BAAQ will result in similar products as those formed on photooxidation of anthracene (Mallakin et al. 1999), which are known to have a toxic impact greater than intact anthracene.
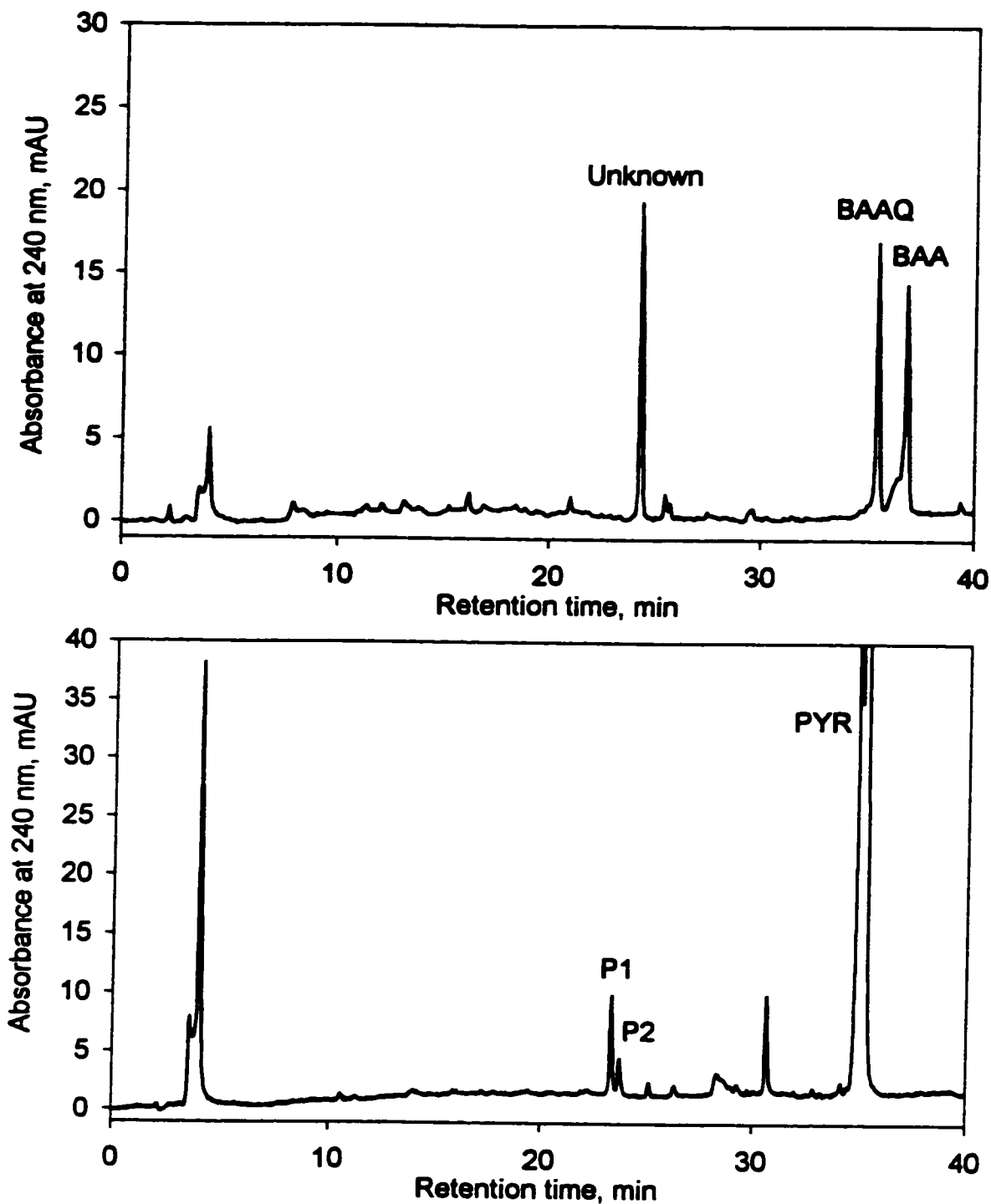
Figure 3.4. HPLC traces of PAH photooxidation products. Top: Benzo(a)anthracene (BAA) photooxidation, 3 hours sunlight. One product, benzo(a)anthracene-7,12-quinone (BAAQ), was identified by comparison versus a purchased standard. A second unknown product was also detected. Bottom: Pyrene (PYR), 4 hours sunlight. Two photooxidation products, labelled P1 and P2, were tentatively identified as 1,6- and 1,8-pyrenequinone respectively.

53
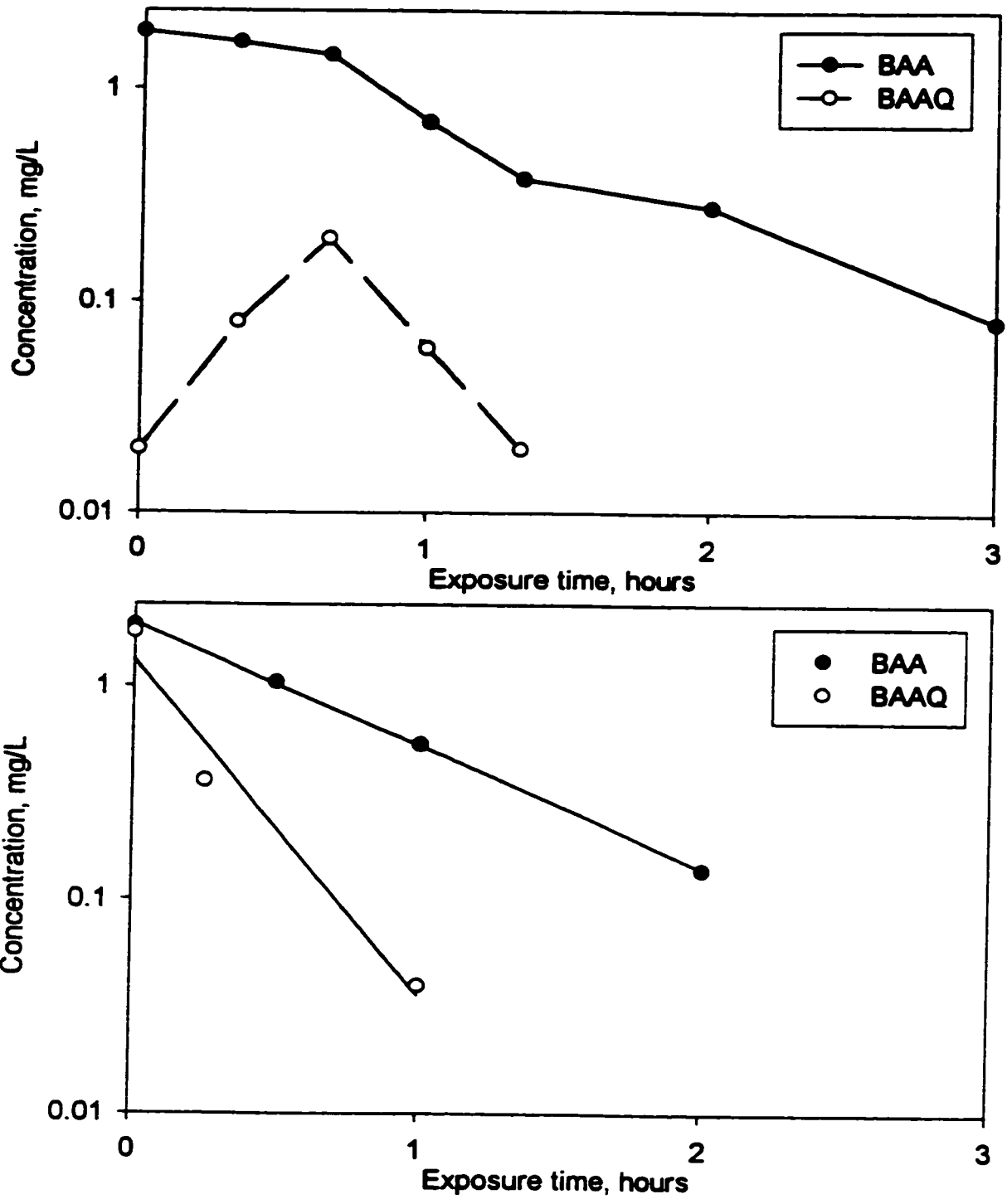
Figure 3.5. Photooxidation of Benzo(a)anthracene. Top: degradation of BAA and formation of BAAQ. Maximum concentration of BAAQ was 11% of initial PAH concentration. Bottom: the relative rates of photooxidation of BAA and BAAQ, in separate experiments. The degradation rate of BAAQ was 7x faster than that of BAA.

Due to the small change in delocalisation energy (12 kJ/mol), the expected site of oxidation of benzo(b)anthracene (BBA) is at the 5,12 position. One product from this reaction, benzo(b)-anthracene-5,12-dione (BBAQ), was observed albeit at a low concentration. The concentrations of BBA and BBAQ in solution over time are shown in Figure 3.6. A solution of BBAQ was separately prepared at a nominal concentration of 1.0 mg/L, and exposed to solar radiation to determine the relative half-lives of BBAQ and BBA (Figure 3.6). The half-life of BBAQ in sunlight was determined as 20.8 ± 3.2 hours and the half-life of BBA was 1.5 ± 0.1 hours. Based on the relative rates of oxidation the efficiency of formation of BBAQ from BBA was estimated as $\Phi = 0.043$ using a non-linear curve fit (Equation 3.5). BBA and BBAQ will also degrade further, forming a spectrum of products similar to BAA.

Several small peaks resulted from the oxidation of chrysene and fluoranthene, but either occurred in very small amounts or had a low efficiency of UV absorption. Both these PAHs have a very stable aromatic structure, and were oxidised comparatively slowly. Chrysene was particularly recalcitrant, due both to its low absorption of light and the resistance to oxidation imparted by its high delocalisation energy. The most abundant product of fluoranthene eluted as a small broad peak at 23 minutes retention time. One possibility for this peak is 2,3-fluoranthene-dione. This product will degrade further and may result in 1-hydroxyfluorene, among other products. The identification of the product is speculative, in the absence of a standard of fluoranthene-2,3-dione to make a definitive identification. No peaks of significant absorbance were detected during the course of the chrysene oxidation experiment. One possible product that is energetically favoured is chrysene-5,6-dione.

3.4 DISCUSSION

Summary reaction schemes for the photooxidation of the PAHs in this study are shown in Figure 3.7. Two products, BAAQ and BBAQ, were identified by comparison with standards, and another two were tentatively identified on the HPLC traces as 1,6- and 1,8- pyrenediones, based on absorbance spectra, retention time, and the energetically favoured sites of reaction. Other products shown are
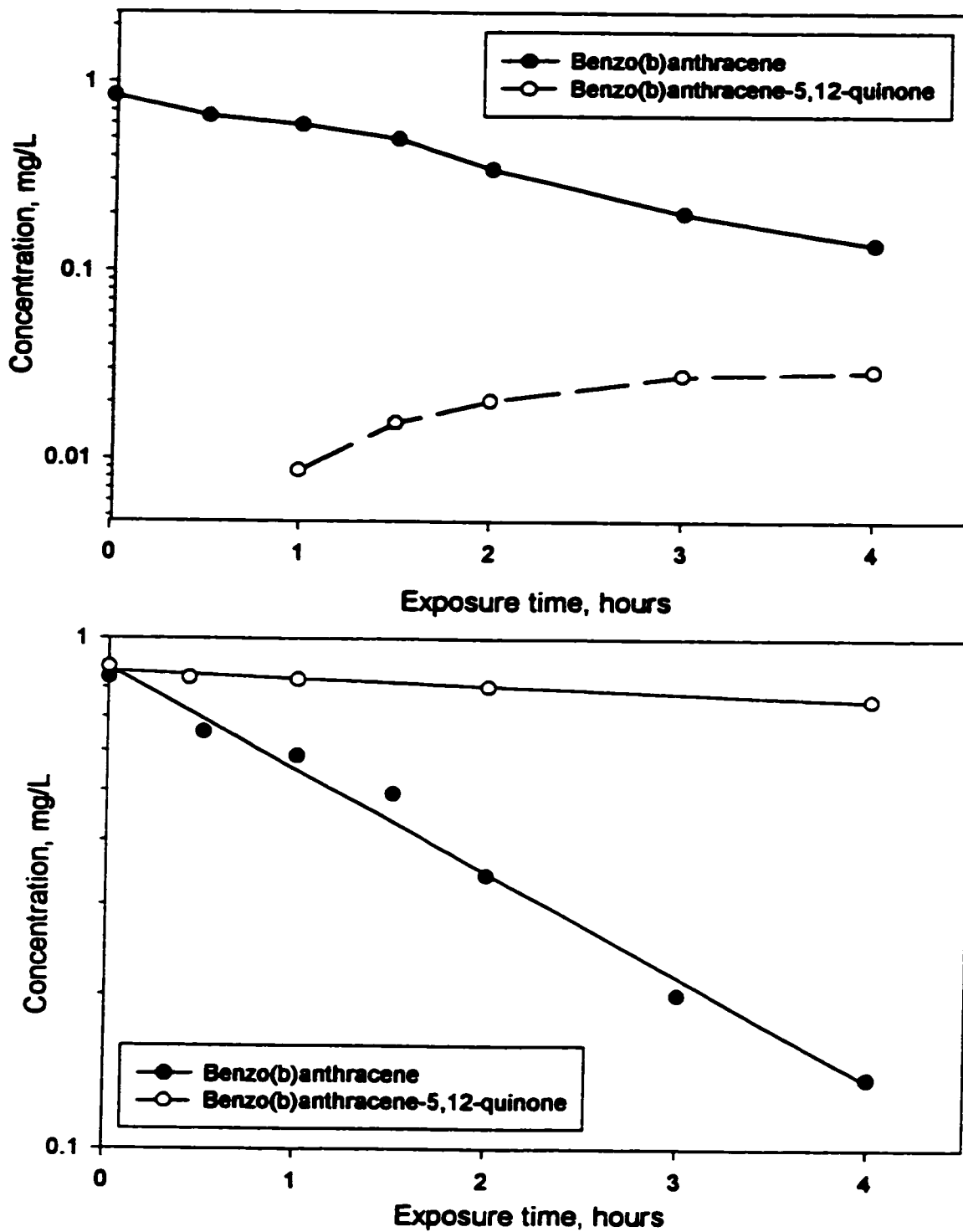
Figure 3.6. Photooxidation of benzo(b)anthracene (BBA). Top: degradation of BBA and formation of BBAQ. Maximum concentration of BBAQ was 3.4% of initial PAH concentration. Bottom: the relative rates of photooxidation of BBA and BBAQ, in separate experiments. The degradation rate of BBAQ was 14x slower than that of BBA.

56
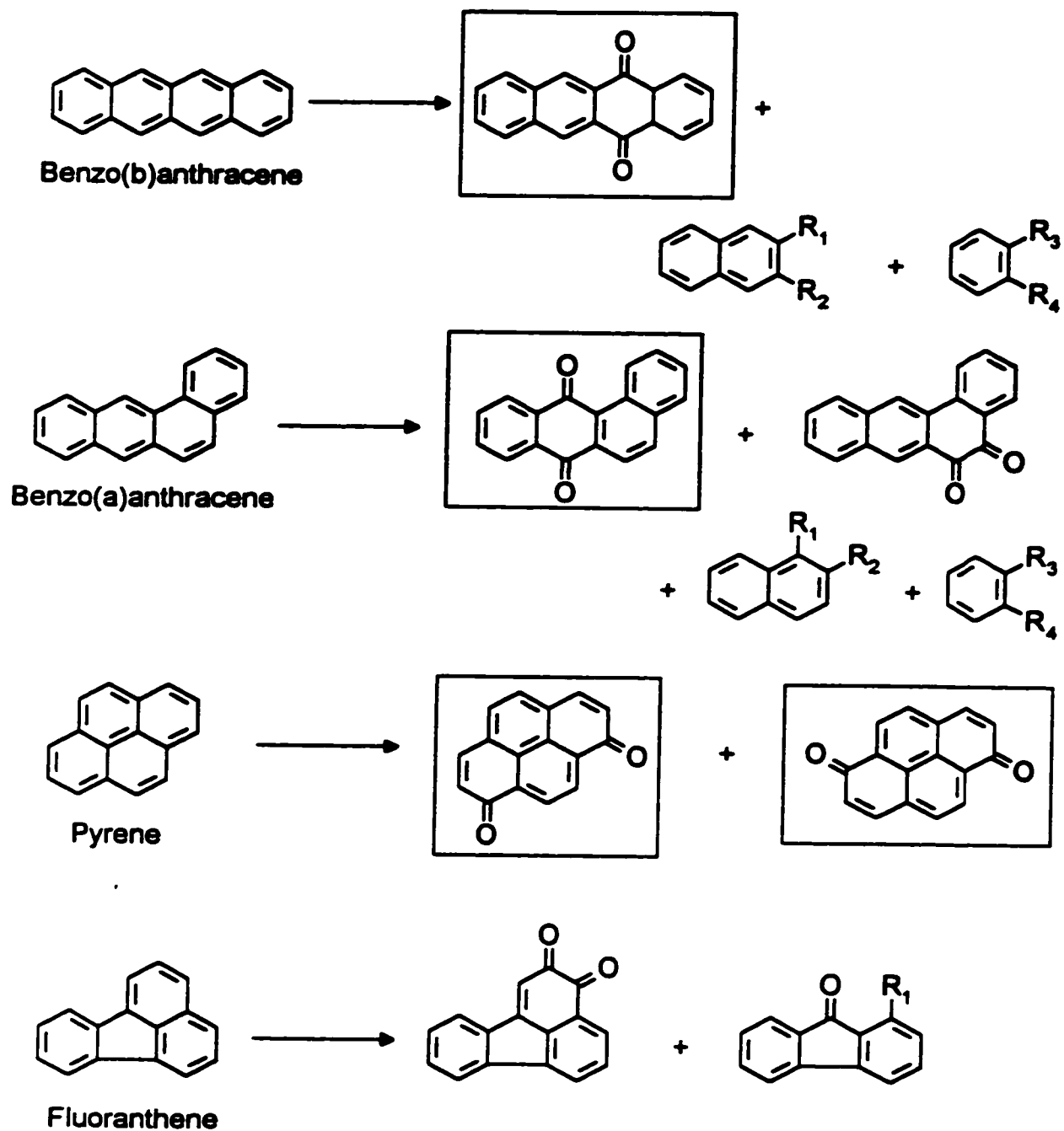
Figure 3.7. Proposed reaction schemes for benzo(b)anthracene, benzo(a)anthracene, pyrene, and fluoranthene. Products in boxes were either confirmed against reference standards or putatively identified.

57

expected products of PAH oxidation, based on the most reactive sites on the PAH carbon skeleton. These products were not confirmed as reaction products.

The products of oxidation will occur at lower concentrations than the initial amount of PAH, unless there is only one product formed. Additionally, the products contain oxygen, which causes a broadening of peaks in the absorbance spectra relative to intact PAHs. This results in products having a higher threshold of detection than the parent PAHs. As some of the initial products retain a highly conjugated aromatic structure, they can undergo further photoreactions. The secondary reactions can occur at a greater or lesser rate than the initial oxidation of the PAH, as exemplified by the relative rates of oxidation of BAA vs. BAAQ, and BBA vs. BBAQ (Figures 3.5 and 3.6). In general, the rate of photooxidation is dependent upon the amount of light absorbed by the chemical, and its photochemical stability (including propensity to react with $^1O_2$, or dissociate alpha to a carbonyl group), and changes in delocalisation energy. Because some oxidation products absorb well into the visible region of the spectrum, further degradation of these products is also quite likely. Aromatic products containing a carbonyl moiety may or may not be stable, depending on the relative energies of the molecules' excited states. The rate of fission of the carbon-carbon sigma bond alpha to the carbonyl group is dependent upon whether the lowest excited state has the carbonyl portion in an (n,π^*) state or a (π,π^*) state. The (n,π^*) state can undergo a facile dissociation alpha to the carboxy bond (Gilbert and Baggott 1991), whereas the (π,π^*) state is more resistant to decomposition. For example, anthraquinone and benzophenone have very similar structures, differing only by one additional carbonyl group, but anthraquinone is an order of magnitude more stable (Malkin 1992). Here, the (π,π^*) state is lower than the (n,π^*) state and thus preferred, giving a more photostable compound. A similar situation may exist with 7,12-benzo(b)anthracenedione and 5,12-benzo(a)anthracenedione; although very similar in structure, the BAA dione is much more reactive, and may undergo a facile fission at the C-C bond alpha to the carbonyl group. This would explain the observed reaction rates shown in Figure 3.5 and 3.6.

If the photooxidation rates were ranked *a priori* based on loss of delocalisation energy on oxidation, it would be expected that the rates of the linearly annealed would be benzo(b)anthracene > benzo(a)anthracene > chrysene. The observed reaction rates did not follow this pattern exactly, as benzo(a)anthracene oxidised faster than benzo(b)anthracene. This was attributed to a greater efficiency of $^1O_2$ generation by benzo(a)anthracene. Assuming that this hypothesis is accurate, it then follows that the rapid oxidation of BAA is due to reaction with singlet oxygen, or equivalently as a concerted reaction involving energy transfer between BAA and oxygen as the initial step. The oxidation of benzo(b)anthracene may be initiated differently, via the reaction of the excited state PAH directly with ground state oxygen, and not via the intermediate singlet state. The relatively small fraction of benzo(b)anthracene forming the 5,12-quinone is partial evidence for this - if the reaction was mediated by singlet oxygen, a 1,4-addition across a ring would be the most likely reaction and would result in significant amounts of quinone formation, similar to benzo(a)anthracene oxidation. That chrysene was the most stable is consistent with both delocalisation energy and $^1O_2$ generation, as chrysene has a greater loss in delocalisation energy on oxidation and does not form $^1O_2$ efficiently.

Fluoranthene and pyrene are both efficient at $^1O_2$ production. However, they are also more thermochemically stable than the linearly annealed PAHs. Thus the singlet oxygen produced will react with the PAH inefficiently, and the excitation energy of $^1O_2$ is more likely to be quenched via other interactions or dissipated as heat. Due to the combination of stability and $^1O_2$ production, it is not surprising that these two compounds have been identified as major contributors of the toxicity due to PAH photosensitisation (Newsted and Giesy 1987; Ankley et al. 1994; Boxall and Maltby 1997; Krylov et al. 1997). The oxidation of fluoranthene and pyrene that does occur is likely to proceed by addition of singlet oxygen to the PAHs. In the case of fluoranthene, oxidation of the benzylic ring is not favoured energetically, and there are no other available sites for a 1,4 addition. A 1,2 addition of oxygen can occur, albeit at a slower rate. Similarly, pyrene does not have any sites available for a 1,4 addition, so the oxidation of pyrene will likely occur in a two step oxidation mechanism, and will involve oxidation sites on different rings.

The products identified here may in some situations have greater biological impacts than the parent PAHs. It has been found that some PAH photoproducts are more toxic than the parent compounds (Huang et al. 1997; McConkey et al. 1997; Mallakin et al. 1999). In particular, the identification of the pyrene diones is an important result, as pyrene itself is not a potent nor direct acting mutagen, but the 1,6- and 1,8- pyrene quinones have been identified as direct acting mutagens (Sakai et al. 1985). These products are also likely to be redox cycling agents similar to other PAH quinones, with an associated increase in toxicity (Smith 1985; Lesko et al. 1986; Hartman and Goldstein 1989; Hasspieler and Di Giulio 1994; Flowers-Geary et al. 1996). Thus, metabolic activation is not required for the formation of direct acting mutagenic species from PAHs, as photoreactions occur which result in similar products.

CHAPTER 4

COMPARATIVE TOXICITY OF PHENANTHRENE AND ITS PRIMARY PHOTOPRODUCT, PHENANTHRENEQUINONE*

*Based on the journal article
McConkey, B.J., C.L. Duxbury, D.G. Dixon and B.M. Greenberg (1997) "Toxicity of a PAH Photooxidation Product to the Bacteria *Photobacterium phosphoreum* and the Duckweed *Lemna gibba*: Effects of Phenanthrene and its Primary Photoproduct, Phenanthrenequinone."
Environ. Toxicol. Chem. 16(5): 892-899

4.1 INTRODUCTION

The toxicity of polycyclic aromatic hydrocarbons (PAHs) to aquatic organisms such as microbes, fish, and plants has been shown to greatly increase upon exposure to light, especially ultraviolet radiation (Bowling et al. 1983; Oris and Giesy 1985; Huang et al. 1993; Ankley et al. 1994; Newsted and Giesy 1987; Schoeny et al. 1988; Gala and Giesy 1992; Ren et al. 1994). This is known to proceed via two processes: photosensitization reactions (e.g. production of singlet oxygen) and photooxidation of the compounds to more toxic species (Bowling et al. 1983; Oris and Giesy 1985; Newsted and Giesy 1987; Schoeny et al. 1988; Gala and Giesy 1992; Huang et al. 1993; Ankley et al. 1994; Ren et al. 1994). The primary photooxidation pathway of PAHs proceeds via unstable endoperoxide and/or peroxide intermediates leading to diols and quinones (Katz et al. 1979; Zepp and Schlotzhauer 1979; Nikolaou et al. 1984; David and Boule 1993). These products may be more or less stable than the parent PAH. If the product is more stable, it is possible that significant amounts may accrue in environmental compartments. As these chemical species are more water soluble than the parent PAHs, organisms could be exposed to higher concentrations of PAH photoproducts than the parent PAHs. This can present a greater toxic risk, as some oxidized PAHs are known to be more reactive and biologically damaging than the parent compounds (Nikolaou et al. 1984; Arey et al. 1992; Huang et al. 1993; Ren et al. 1994; Flowers-Geary et al. 1996).

61

Toxicity assessments with the higher aquatic plant *Lemna gibba* (duckweed) and the terrestrial plant *Brassica napus* (canola) have shown that the complex mixtures of unidentified photoproducts generated by treatment of PAHs with actinic radiation are more toxic than the parent compounds alone (Greenberg et al. 1993; Huang et al. 1993; Ren et al. 1994; Huang et al. 1995; Ren et al. 1996). This increase in toxicity can be quite dramatic, with $EC_{50}s$ decreasing more than an order of magnitude in some instances (Huang et al. 1993; Ren et al. 1994; Huang et al. 1995; Ren et al. 1996). While it is known that complex mixtures of photooxidized PAHs are more toxic than their parent PAHs, the relative toxicity of specific photooxidation products to the parent compounds have yet not been characterised.

Phenanthrene (PHE), one of the most prevalent PAHs in the environment (Basu and Saxena 1978; Cook et al. 1983; Edwards 1983; Eadie 1984; Jacobs et al. 1993), undergoes an increase in toxicity to plants when exposed to actinic radiation (Greenberg et al. 1993; Huang et al. 1993). After sufficient exposure of PHE to a light source such as simulated or natural solar radiation, one predominant photoproduct of PHE, 9,10-phenanthrenequinone (PHEQ), is formed, along with other photoproducts in minor quantities (David and Boule 1993; McConkey et al. 1993). Based on the delocalisation energy methodology presented in chapter 3, the expected site of oxidation of PHE is at the 9,10 positions, which is consistent with the observed primary reaction. PHEQ is a known environmental contaminant and has been demonstrated to undergo redox cycling leading to oxidative stress (Chesis et al. 1984; Hasspieler and Di Giulio 1994). Since both PHE and PHEQ are commercially available in 99% purity, it was possible to compare the toxicity of PHE, PHEQ, and mixtures of PHE and PHEQ to the mixture of compounds resulting from PHE photooxidation.

4.1.1 Organisms used for toxicity testing

In initiating this study on phenanthrene photooxidation and toxicity, it was decided to use two different species for toxicity testing, as it would help assess if the effects were of a general nature (Menzer et al. 1994). For instance, if the mechanism of toxicity is specific to a given metabolic pathway, there can be large interspecies differences in toxicity. Two organisms that have been widely used in ecotoxicology

are the luminescent marine bacteria, *Photobacterium phosphoreum*, and the higher plant *Lemna gibba*. Since luminescence of *P. phosphoreum* is directly linked to respiratory activity, it provides a good indicator of metabolic activity, and therefore of the general cytotoxicity of a given compound (Bulich 1986; Environment Canada 1993). Additionally, *P. phosphoreum* is an important marine picoplankton with sensitivity to organic compounds qualitatively comparable to lethality endpoints for cyprinids, salmonids and daphnids (Munkittrick and Power 1989). Additionally, because the *P. phosphoreum* toxicity assay is rapid (<30 min), and independent of light or dark exposure, it is ideal for testing photoactive contaminants. *L. gibba* also has significant advantages for toxicity testing, including preliminary evaluation of contaminant impacts on primary productivity (Greenberg et al. 1992). *L. gibba* assays were conducted by Dr. Cheryl Duxbury, and are included here to corroborate the observed toxicity of PHE and PHEQ assessed using the bacterial assay.

To compare the toxicity of PHE and its primary photoproduct PHEQ, *P. phosphoreum* and *L. gibba* were exposed to the pure chemicals, to a photomodified PHE solution containing known amounts of PHE and PHEQ, and to a prepared PHE and PHEQ mixture. Impacts were assessed as diminished luminescence from *P. phosphoreum* and inhibited growth of *L. gibba*. For both species, PHEQ was the dominant toxicant and the toxicity of this compound was not photoinduced.

4.2 MATERIALS AND METHODS

4.2.1 Chemical analysis of PHE and photoproducts

PHE and PHEQ (99% purity) were purchased from Sigma Chemical Co. (St. Louis, MO, USA). The compounds were used as purchased after confirming purity by HPLC. Chromatographic analysis was performed with a dual pump chromatography system equipped with a diode array detector (Shimadzu Scientific Instruments Inc., Columbia, MD, USA) and a Supelcosil C_{18} reverse-phase column, 25 cm x 4.6 mm I.D., 5 µm packing (Supelco Inc., Bellefonte, PA, USA). Analytical sample volumes of 200 µl were applied to the column with an autosampler. HPLC grade water (adjusted to pH 3 with phosphoric acid) and acetonitrile, both degassed with helium, were used as elution solvents at a flow rate of 1 ml/min. The elution profile was 1% acetonitrile for 2 minutes, followed by a linear gradient to 90% acetonitrile over 30 minutes.

PHE (retention time: 27.4 min) and PHEQ (retention time: 21.0 min) were readily identified in treated samples by diode array detection, based on their absorbance spectra and comparison to authentic samples (Figure 4.1). Appropriate standard curves were used to determine concentrations.

4.2.2 Light exposure of PHE

To provide a solid substrate from which PHE could both dissolve and undergo photoreactions, PHE was adsorbed to acid washed fine sand (Sigma Chemical Co.). Ten mg of PHE in 5 ml of HPLC grade dichloromethane (Fisher Scientific Ltd., Mississauga, ON, Canada) was combined with 5 g of sand in a 1 L glass beaker. The dichloromethane was quantitatively removed by evaporation in darkness, and 1 L of HPLC grade water was added to the beaker. The beaker was sealed with polyethylene film, a material transparent to UV-B, UV-A and visible light. Beakers containing the sand/water/PHE composite were exposed to either 100 μmol m^{-2}s^{-1} of simulated solar radiation (SSR, visible:UV-A:UV-B ratio of 100:10:1 which parallels that of sunlight) (Huang et al. 1993; Greenberg et al. 1995) or to natural sunlight. To determine the dissolution rate of PHE and if non-photochemical degradation occurred, a duplicate sand/water/PHE composite was incubated in darkness for 96 hours. Samples of 1 ml were removed from the aqueous phase exposed to SSR or darkness at various time points from 1 to 96 hours, and HPLC analysis was used to determine the concentrations of PHE and PHEQ in solution (Figure 4.1). Approximately 500 ml of the PHE solution treated for 96 hours in SSR (pmPHE) was used for toxicity testing.

For toxicity testing of PHE or PHEQ individually, DMSO was used for direct delivery of the chemicals to the appropriate aqueous media by 1000-fold dilution. This was required for full dose-response toxicity profiles. Using DMSO, supersaturated solutions of PAH can be generated, allowing for testing of concentrations of chemical above the aqueous solubility limit. A 0.1% (v/v) DMSO solution was used for the control experiments; this concentration exerted no toxic effects on either *P. phosphoreum* or *L. gibba* (Greenberg et al. 1992; Environment Canada 1993).
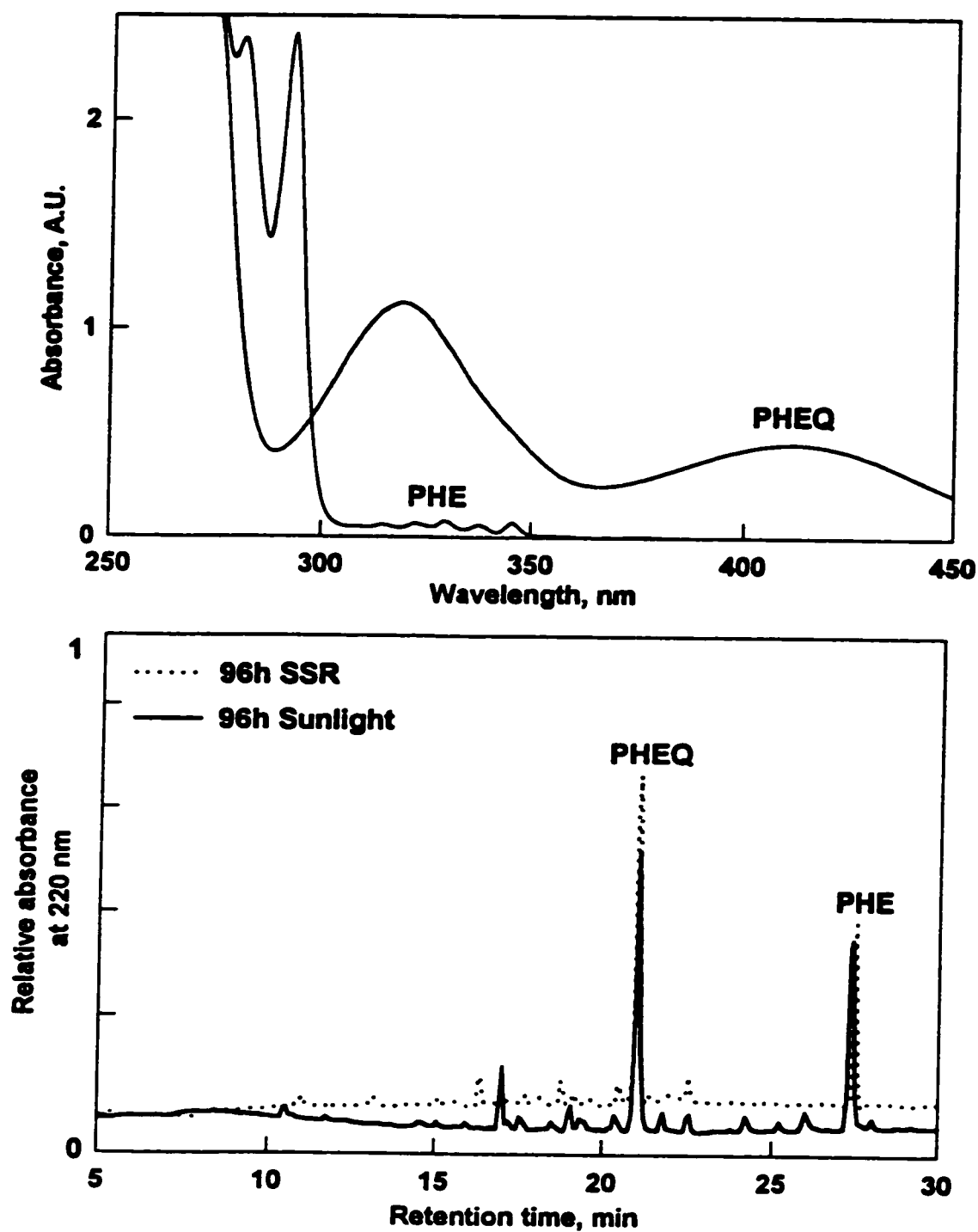
Figure 4.1. UV/Visible absorbance spectra of PHE and PHEQ, and HPLC analysis of photooxidised PHE. A: Absorbance spectra of 50 mg mL^{-1} PHE and 50 mg mL^{-1} PHEQ, in methanol. B: HPLC chromatogram of photomodified PHE. 5 mg of PHE was adsorbed to 5 g of sand and incubated with 1 L of water, exposed to SSR or sunlight for 96 hours. The primary photoproduct is PHEQ.

Concentrations of PHE and PHEQ in the media were measured by HPLC. To confirm the accuracy of the toxicity estimates, the chemicals were dissolved directly in medium without a carrier solvent to concentrations corresponding to the lower end of the dose-response curves. These concentrations were also determined by HPLC. Indistinguishable levels of toxicity were observed regardless of route of delivery.

An additional mixture of PHE and PHEQ was generated and assessed for toxicity (PHE+PHEQ). This mixture was designed to mimic the concentrations of PHE and PHEQ in the light exposed PHE solution, pmPHE. Crystalline PHE and PHEQ were added individually to HPLC grade water and agitated in darkness for 24 h. Excess crystals were removed by filtration through a 0.45 μm nylon membrane filter (Supelco Inc.). The concentrations of PHE and PHEQ in this solution were determined by HPLC as 0.29 mg L^{-1} and 0.54 mg L^{-1}, respectively.

Three routes were used for delivering the chemical to aqueous media, depending on the experiment to be performed; incubation of sand-adsorbed PHE with water, delivery of PHE or PHEQ in a carrier solvent (DMSO, Aldrich Chemical Co., Milwaukee, WI), and direct dissolution of crystalline PHE and PHEQ in water.

4.2.3 P. phosphoreum *toxicity testing*

The luminescent bacteria P. phosphoreum (strain NRRL B-11177) were obtained from the Midwest Area National Centre for Agricultural Utilisation Research, Peoria, IL. Prior to toxicity testing, cultures of P. phosphoreum were grown in darkness at 15°C in liquid medium, composed of 2.5 g L^{-1} KH$_2$PO$_4$, 30 g L^{-1} NaCl, 5 g L^{-1} glycerol, 1 g L^{-1} yeast extract, 12.5 g L^{-1} Tryptone, and 2.5 g L^{-1} Bactopeptamin, pH adjusted to 7.1 with NaOH. Yeast extract and Tryptone were obtained from BDH Inc., Toronto, ON, and Bactopeptamin was obtained from Difco Laboratories, Detroit, MI. Cultures were harvested when they reached an absorbance of 0.3 at 600 nm, as measured using a spectrophotometer (Shimadzu Scientific Instruments Inc., Columbia, MD, USA). Fifteen ml of the culture was centrifuged at 5000g for 5 min and the pellet resuspended in 15 ml of a 2% (w/v) saline solution immediately prior to toxicity testing. Twenty-four 500 μl aliquots of cells were added to a 48-well tissue culture plate (Falcon Safety Products, VWR

Scientific Ltd, Toronto, ON, Canada). The bacteria in saline were kept at 15°C at all times to allow comparison of our endpoint with published Microtox™ data (Bulich 1986; Munkittrick and Power 1989; Environment Canada 1993; Jacobs et al. 1993). After 5 minutes acclimatisation in the 48-well culture plates, the luminescence of the cells was measured. Cells were then dosed with the chemical (see below) and incubated in darkness or SSR for 15 min, after which bacterial luminescence was remeasured. Luminescence was measured at 460 nm (40 nm bandwidth) using a Cytofluor 2350 fluorescence measurement system (Millipore Ltd., Mississauga, ON, Canada). The excitation lamp of the detector was turned off to eliminate any background fluorescence.

Toxicity was measured as percent inhibition of light emission from a treated aliquot, corrected for loss of light in the control as:

$$\% \text{ Inhibition} = 100\left(1 - \frac{L_f \cdot C_i}{L_i \cdot C_f}\right)$$

(1)

where L_i is the initial luminescence of the bacteria prior to toxicant exposure, L_f is the luminescence of the bacteria following a 15 min chemical exposure, and C_i and C_f are the initial and final luminescence of the control bacteria.

Calculation of $EC_{50}s$ (the estimated toxicant concentration causing a 50% reduction in light output) was based on a logit function for continuous response data (Sanathanan et al. 1987). The data for % inhibition vs. chemical concentration can be fit to the equation

$$\% \text{ Inhibition} = \left(\frac{100}{1 + e^{\beta(x-\mu)}}\right)$$

(2)

where x is the logarithm of the concentration, μ is the logarithm of the EC50, and β is a measure of the slope of the concentration-response curve.

4.2.4 P. phosphoreum exposure

After the initial measurement of bacterial luminescence discussed above, the bacteria were dosed with chemical(s). 500 µl aliquots of resuspended cell culture were combined with equal volumes of

chemical(s) in 2% saline at 2 times the concentrations required for toxicity testing. A dilution series of each chemical or solution of chemicals, plus controls, were added to the wells in triplicate providing 3 replicates of each concentration per individual assay. For toxicity testing of PHE and PHEQ, stock solutions of each chemical (5 mg ml^{-1} of PHE and 1 mg ml^{-1} of PHEQ) were prepared in DMSO and diluted with 2% saline to give the desired concentrations. Seven concentrations in a geometric series were used for testing with each chemical. The concentration of DMSO was ≤0.1% in each of the final mixtures. For toxicity testing of the pmPHE solution (described above), the salinity of this solution was adjusted to 2% by addition of solid NaCl, and a series of dilutions were made with a 2% saline solution (w/v). This series was further diluted by half after addition to the bacterial aliquot, resulting in the following exposures: 50%, 25%, 12.5%, 6.25%, 3.13%, 1.56%, 0.78%, and 0% as a control (i.e. the 50% pmPHE treatment contained 0.13 mg L^{-1} PHE and 0.29 mg L^{-1} PHEQ). The prepared PHE+PHEQ mixture was combined with the bacterial suspension using the same dilution profile as used for the pmPHE solution. Concentrations reported in all toxicity assays were the amounts present at the start of the toxicity test, as determined by HPLC. After dosing, the cells were incubated in darkness or SSR at 15°C for 15 minutes, and the luminescence measured again.

4.2.5 L. gibba *toxicity testing*

The methods used for testing *L. gibba* are described in detail elsewhere (McConkey et al. 1997), and will only be summarised here. The irradiation source for plant growth during chemical treatment was SSR or visible light, each with a total visible light fluence rate of 100 μmol m^{-2} s^{-1}. Toxicity was assessed as inhibition of plant growth (Greenberg et al. 1992; Ren et al. 1994). For all toxicity assays two plants (total of 8 fronds) were exposed to concentrations of chemical(s) in a geometric series and incubated in visible light or SSR. The growth media and chemical(s) were renewed every 2 days. After 8 d the plants were removed and the leaves were counted to determine the growth rates as follows:

$$F_t = F_o 2^n \qquad (4)$$

where F_o and F_t are the number of fronds at time zero or at time t (in days), respectively. The number of times the plants have doubled (n) is solved by:

68

$$n = \frac{\log\left(\frac{F_t}{F_o}\right)}{\log 2} \qquad (5)$$

The growth rate is n/t (Greenberg et al. 1992; Ren et al. 1994). $EC_{50}s$, in this case measured as a 50% reduction in growth rate, were calculated in the same manner as $EC_{50}s$ for the *P. phosphoreum* assay.

4.2.6 Curve fitting and statistics

The measured responses used in both toxicity assays were continuous variables (a percent decrease in light production for *P. phosphoreum*, and a percent decrease in growth rate for *L. gibba*), and the variance was approximately uniform over the range of experimental concentrations. Accordingly, an iterative least squares method was chosen as the most suitable means of calculating EC_{50} values. Data analysis and curve fitting was done using SYSTAT™ (Wilkinson 1994.).

Two methods of data handling were used to calculate $EC_{50}s$ and confidence intervals. As all the wells on each plate in the *P. phosphoreum* assay contained organisms from the same batch culture, it could be argued that the wells are not true replicates. However, within plate variation was still a source of error, as well as between replicate plates from different batch cultures. Thus two methods of variance estimation were used, and the more conservative estimate of the confidence interval was chosen in each case. In the first method, an EC_{50} value for each replicate assay was calculated, and then an overall EC_{50} was calculated by averaging the $EC_{50}s$ obtained from each replicate. Confidence intervals on the resulting mean EC_{50} were calculated using established methods (Kuehl 1994). In the second method, $EC_{50}s$ and confidence intervals were calculated from a set of data pooled from experimental replicates. The EC_{50} was estimated as e^μ from the parameter μ in equation (2) after fitting the equation to the pooled data set using the NONLIN module of SYSTAT™. The corresponding confidence intervals were calculated from the confidence intervals of μ predicted by the NONLIN module of SYSTAT™ (Wilkinson 1994.). Analysis of variance calculations were conducted as a 2 x 2 factorial design (chemical x light) utilizing the MGLH module of SYSTAT™. Statistical significance was tested at a level of $\alpha=0.05$ for all experiments.

69

4.3 RESULTS

4.3.1 Solubility and Degradation of PHE

To analyze the photooxidation of PHE, the chemical was adsorbed onto sand, covered with water, and incubated in SSR, natural sunlight or darkness. During the exposure, the release from bound phase monitored. When the composite was incubated in darkness there was rapid release of PHE to the aqueous phase to an equilibrium concentration of 0.40 mg L^{-1}, with no observed degradation of PHE (Figure 4.2). In SSR, the initial rate of release of PHE from the bound phase was nearly the same as in darkness (Figure 4.2). A maximum concentration of 0.43 mg L^{-1} PHE in solution was attained at 18 h, after which the concentration decreased to 0.26 mg L^{-1} by 96 hours. In SSR, PHE was photooxidised to one primary photoproduct, PHEQ (Figures 4.1 and 4.2), which was present at 0.58 mg L^{-1} after 96 h. HPLC analysis revealed the formation of only small amounts of secondary photoproducts (Figure 4.1). This product profile due to exposure of PHE to SSR is strikingly similar to the profile obtained from exposure to natural sunlight (Figure 4.1), indicating that PHEQ will be a key photooxidation product in the environment.

4.3.2 Toxicity of PHE and PHEQ to P. phosphoreum

P. phosphoreum was incubated in SSR with either PHE or PHEQ to determine the relative toxic potency of each chemical (Figure 4.3). The calculated EC50 of PHE was 0.53 mg L^{-1}, which agrees well with published EC$_{50}$s obtained using the Microtox™ assay (Jacobs et al. 1993). The EC$_{50}$ of PHE is above the concentration of PHE obtained by release of PHE from sand (Figure 4.2, Table 4.1) but is less than the published solubility of 1.1 mg L^{-1} (Billington et al. 1988). The calculated EC$_{50}$ of PHEQ was 0.102 mg L^{-1} in darkness, 5 times more toxic than PHE, and well within experimental solubility limits (Figure 4.2). The short exposure time to SSR in experiments with *P. phosphoreum* (15 min) precluded any measurable photooxidation of PHE to PHEQ, ensuring that the observed toxicity could be attributed solely to PHE or PHEQ, and not to any photooxidation products that might form during the course of the assay.
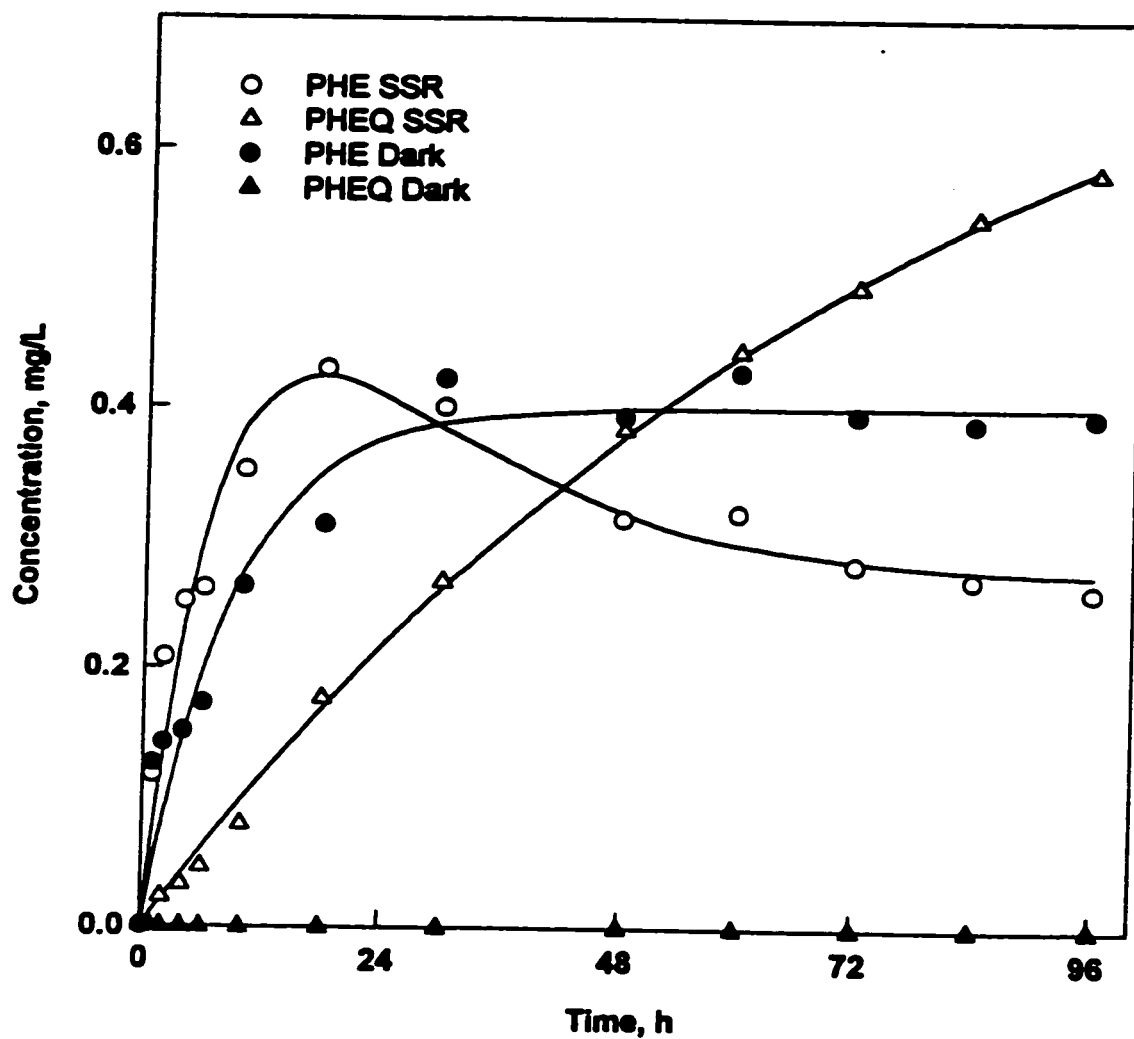
Figure 4.2. Kinetics of release and photooxidation of PHE from sand. Incubation of a sand/PHE/water composite was carried out in darkness or SSR (100 $\mu mol\ m^{-1}\ s^{-1}$), as described in Methods. In SSR, one primary photoproduct (PHEQ) was observed. No degradation products of PHE were observed in the dark incubated sample. Concentrations of PHE and PHEQ were determined by HPLC.

71
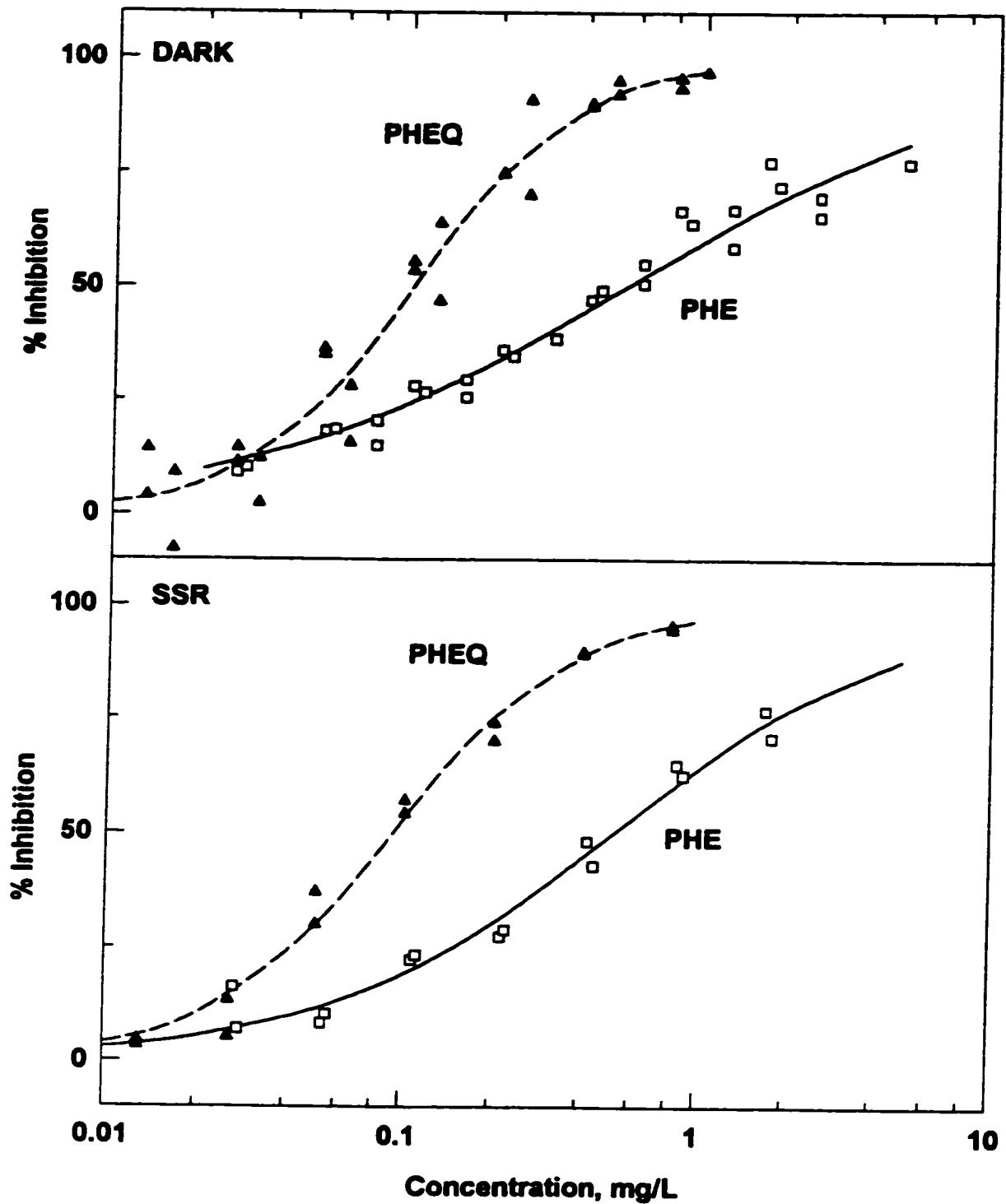
Figure 4.3: Dose-response of *P. phosphoreum* to PHE and PHEQ. *P. phosphoreum* was exposed to a concentration series of PHE and PHEQ for 15 min in the dark or in SSR. Bacterial response was measured as percent inhibition of luminescence and plotted versus chemical concentration. Each data point represents an average of three replicates of a given concentration from one experiment.

Table 4.1: Calculated $EC_{50}s$ for toxicity of PHE and PHEQ to *P. phosphoreum* and *L. gibba*, under different lighting conditions. Data are presented as $EC_{50}s$ (lower 95% confidence interval, upper 95% confidence interval, number of replicates) in mg L^{-1}.

Organism	Toxicant	EC$_{50}$	
		DARK	SSR
P. phosphoreum	PHE	0.53 (0.38, 0.68, 4)	0.53 (0.32, 0.74, 2)
	PHEQ	0.102 (0.079, 0.125, 4)	0.093 (0.061, 0.125, 2)
		Visible	SSR
L. gibba	PHE	>5.0[a]	3.48 (3.18, 3.80, 3)[b]
	PHEQ	0.53 (0.49, 0.57, 3)	0.57 (0.53, 0.61, 3)

[a] a maximum inhibition of 44% was observed at a concentration of 5 mg L^{-1}, the highest concentration used in the assay.

[b] confidence intervals calculated from pooled data set.

To determine if the toxicity of PHE or PHEQ observed in SSR could be attributed to photosensitization reactions (e.g. production of singlet oxygen) initiated by either compound, *P. phosphoreum* was incubated in the dark with the chemicals (Figure 4.3). The calculated $EC_{50}s$ for each chemical in SSR or darkness were not statistically different (Table 4.1), indicating that photoactivation of PHE or PHEQ was not a factor in these short-term toxicity assays. In both SSR and darkness, PHEQ was more toxic than PHE.

To further examine the toxicity of PHE and PHEQ, *P. phosphoreum* was incubated with 2 different mixtures of the chemicals. The first mixture of PHE and PHEQ was generated by incubating PHE in SSR for 96 h (pmPHE). The final concentrations of the mixture were 0.26 mg L^{-1} PHE and 0.58 mg L^{-1} PHEQ. The pmPHE solution also contained several minor photoproducts that were not characterized (Figure 4.1). The second mixture of PHE and PHEQ, PHE+PHEQ, was prepared from stock solutions to approximate the concentrations of these 2 chemicals in the pmPHE mixture. This

resulted in a solution containing 0.29 mg L^{-1} PHE and 0.54 mg L^{-1} PHEQ. Dilutions were made of both mixtures as a percent of the original solution, and tested with *P. phosphoreum* in SSR and darkness (Figure 4.4).

The EC$_{50}$ for the pmPHE mixture in darkness corresponded to a 11.5% solution (Table 4.2), or concentrations of 0.030 mg L^{-1} PHE and 0.067 mg L^{-1} PHEQ. Comparable results were obtained in SSR for the pmPHE mixture (Table 4.2). For the PHE+PHEQ mixture the EC50 in darkness was 11% (or 0.032 mg L^{-1} PHE and 0.060 mg L^{-1} PHEQ). For both the pmPHE and PHE+PHEQ mixtures there was no significant increase in toxicity in SSR, confirming that except for the photooxidation of PHE to PHEQ, light does not have an activating role in the toxicity of these chemicals to *P. phosphoreum* (Figure 4.4). Because both the pmPHE mixture and the PHE+PHEQ mixture gave rise to very similar EC$_{50}$s, and no additional toxicity could be attributed to the minor products in the pmPHE mixture. The concentration of PHE in the mixtures at EC$_{50}$ was 15-fold lower than the EC$_{50}$ for pure PHE. However, the concentration of PHEQ in the mixtures at EC$_{50}$ (0.060 to 0.067 mg L^{-1}) was close to the EC$_{50}$ for pure PHEQ (0.093 to 0.102 mg L^{-1}), further implying that PHEQ contributed the majority of the toxicity observed in the mixtures.

4.3.3 Toxicity of PHE and PHEQ to L. gibba

The toxicity of PHE and PHEQ to *L. gibba* was assessed by Dr. Cheryl Duxbury. This assay provided a means to determine if the increase in toxicity of PHE on photooxidation was similar between different species. While experiments with *L. gibba* cannot be performed in the dark, visible light and SSR can be used to determine if the presence of UV radiation had an activating role in toxicity. As PHE doesn't absorb visible light and PHEQ absorbs primarily in the UV region of the spectrum (Figure 4.1), UV radiation would be required for phototoxicity. *L. gibba* was incubated with either PHE or PHEQ in the presence of visible light or SSR for 8 days. The calculated EC$_{50}$ for PHE was 3.5 mg L^{-1} in SSR and >5.0 mg L^{-1} in visible light (Figure 4.5, Table 4.1). While these concentrations were above the solubility limits for PHE (Figure 4.2) (Billington et al. 1988), significant inhibition of growth was
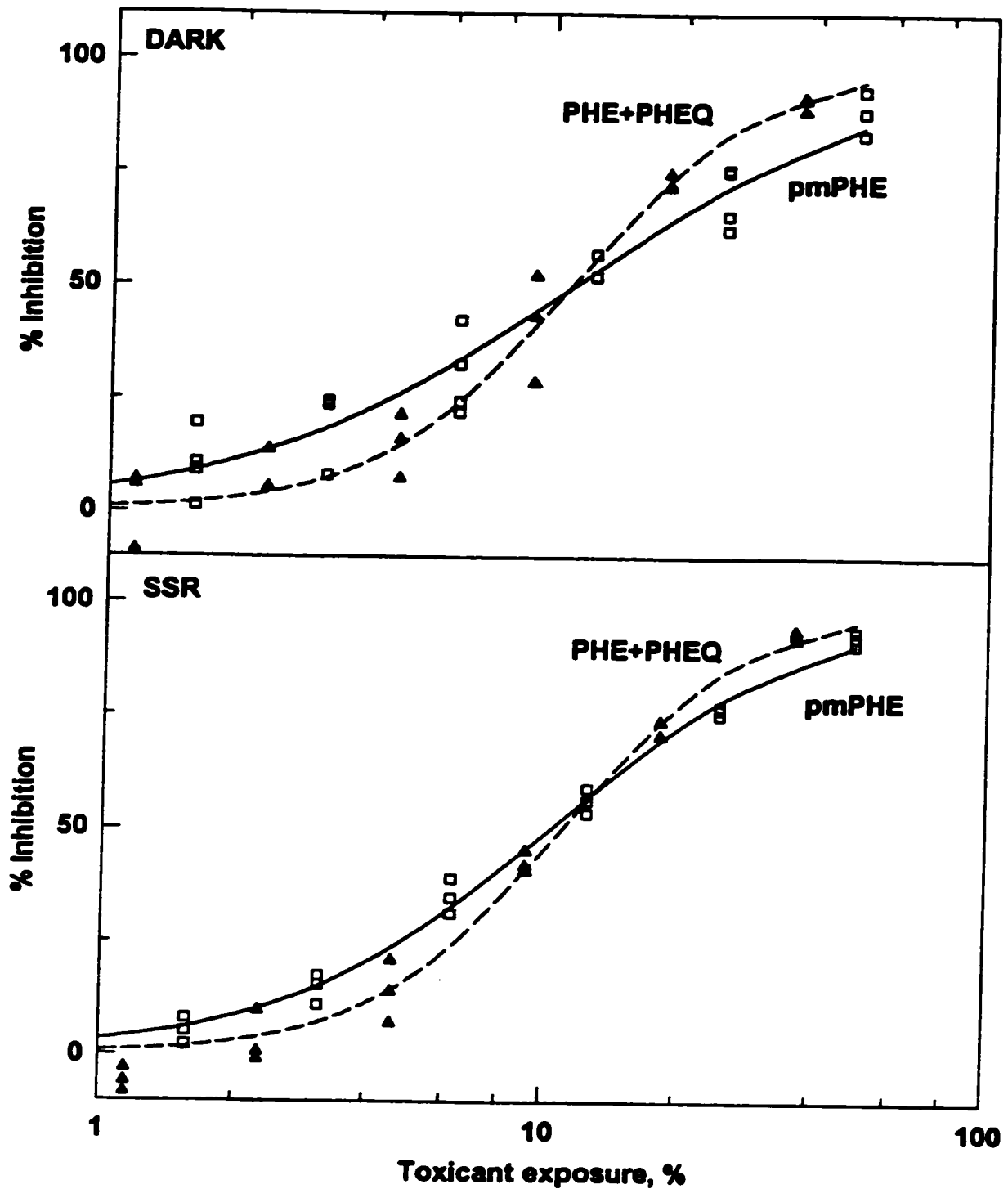
Figure 4.4. Dose-response of *P. phosphoreum* to photomodified PHE, and a mixture of PHE and PHEQ. Photomodified PHE (pmPHE) was prepared by exposure to SSR for 96 h. The resultant stock solution contained 0.26 mg L^{-1} PHE, 0.58 mg L^{-1} PHEQ, and minor photoproducts. A second mixture of PHE and PHEQ (PHE+PHEQ) was prepared using reagent grade chemicals to approximate the concentrations of PHE and PHEQ present in pmPHE. The stock solution contained 0.29 mg L^{-1} PHE and 0.54 mg L^{-1} PHEQ. Data points are the mean of 3 replicates from one experiment.

Table 4.2: Calculated EC$_{50}$s for the pmPHE mixture (stock solution concentrations: 0.26 mg L^{-1} PHE and 0.58 mg L^{-1} PHEQ) and PHE+PHEQ mixture (stock solution concentrations: 0.29 mg L^{-1} PHE and 0.54 mg L^{-1} PHEQ) to *P. phosphoreum* in darkness and SSR, and the pmPHE mixture to *L. gibba* in visible light and SSR. Data are presented as EC$_{50}$s (lower 95% confidence interval, upper 95% confidence interval, number of replicates), where the EC$_{50}$ is reported as a percentage of the stock solution. Concentrations of PHE and PHEQ in the mixtures at EC$_{50}$ are reported in mg L^{-1} below the percentage EC$_{50}$s.

Organism	Toxicant	EC$_{50}$	
		DARK	SSR
P. phosphoreum	pmPHE	11.5% (9.0%, 14.0%, 4)	10.3% (7.4%, 13.1%, 3)
	PHE, mg L^{-1}	0.030	0.027
	PHEQ, mg L^{-1}	0.067	0.060
P. phosphoreum	PHE+PHEQ	11.0% (9.8%,12.4%,3)[1]	11.0% (10.1%,12.0%,3)[1]
	PHE, mg L^{-1}	0.032	0.032
	PHEQ, mg L^{-1}	0.060	0.060
		Visible	SSR
L. gibba	pmPHE	72.0%(69.8%,74.2%,3)[1]	73.8% (71.2%,76.5%,3)[1]
	PHE, mg L^{-1}	0.19	0.19
	PHEQ, mg L^{-1}	0.42	0.43

[1]confidence intervals calculated from pooled data set.

observed at concentrations within the solubility range (<1.1 mg L^{-1}) (Figure 4.5). Similar to *P. phosphoreum*, the toxicity of PHEQ was much greater than that of PHE, and the toxicity of PHEQ was essentially the same in visible and SSR (Table 4.1). We note that for *L. gibba*, PHE toxicity is greatly enhanced by UV radiation; however, with an 8 day toxicity test based on a 2 day static renewal cycle, there would be time for a considerable amount of the more toxic PHEQ to be formed in SSR.

L. gibba was also treated with the pmPHE mixture in the presence of visible light and SSR. In both SSR and visible light, the EC$_{50}$ was approximately a 73% solution (Figure 4.6, Table 4.2), which

corresponds to 0.19 mg L^{-1} PHE and 0.42 mg L^{-1} PHEQ. Once again the PHEQ concentration in the pmPHE mixture at the EC$_{50}$ correlated well with the EC$_{50}$ concentration of PHEQ when applied in pure form (Tables 4.1 and 4.2), indicating that PHEQ was the major contributor to the toxicity of the pmPHE mixture.

4.4 DISCUSSION

Based on our work with the bacteria *P. phosphoreum* and the aquatic plant *L. gibba*, the primary photomodification product of PHE, PHEQ, is the primary toxicant in PHE contaminated media that has been exposed to actinic radiation. The toxicity of PHEQ was not altered by darkness, visible light or SSR, indicating that its toxicity is independent of either photosensitization or further photooxidation. For each organism, the pmPHE mixture, PHE+PHEQ mixture and PHEQ had similar impacts based on PHEQ concentration, indicating that neither PHE nor the minor photoproducts of PHE contributed significantly to toxicity of the mixtures. Since solutions of PHEQ alone gave EC$_{50}$s comparable to the PHE+PHEQ and/or pmPHE solution with both organisms, it can be concluded that the dominant toxicant in the mixtures was PHEQ.

Previous work with PAHs has demonstrated that a photomodified solution of a PAH exhibits greater toxicity than a solution of the parent PAH (Huang et al. 1993; Ankley et al. 1994; Ren et al. 1994; Huang et al. 1995; Ren et al. 1996). In those studies the photomodification products were not identified, and so the relative contributions of individual photoproducts could not be assessed. PHE is a unique PAH as it produces only one major photoproduct after 96 h exposure to SSR. The photoproduct, PHEQ, accounts for over 90% of the total photoproducts formed. The remaining unidentified photoproducts are few and present in very small amounts. The commercial availability of pure PHEQ allowed for comparison studies of the pmPHE mixture containing additional minor photoproducts against solutions of PHE or PHEQ alone, and of a PHE and PHEQ mixture free of additional photoproducts. Based on the work presented here, PHEQ was clearly the major toxicant. If one assumes PHE and PHEQ toxicity are approximately additive, PHEQ would account for the majority of the toxicity of a PHE solution that had been exposed to simulated or natural sunlight.

77
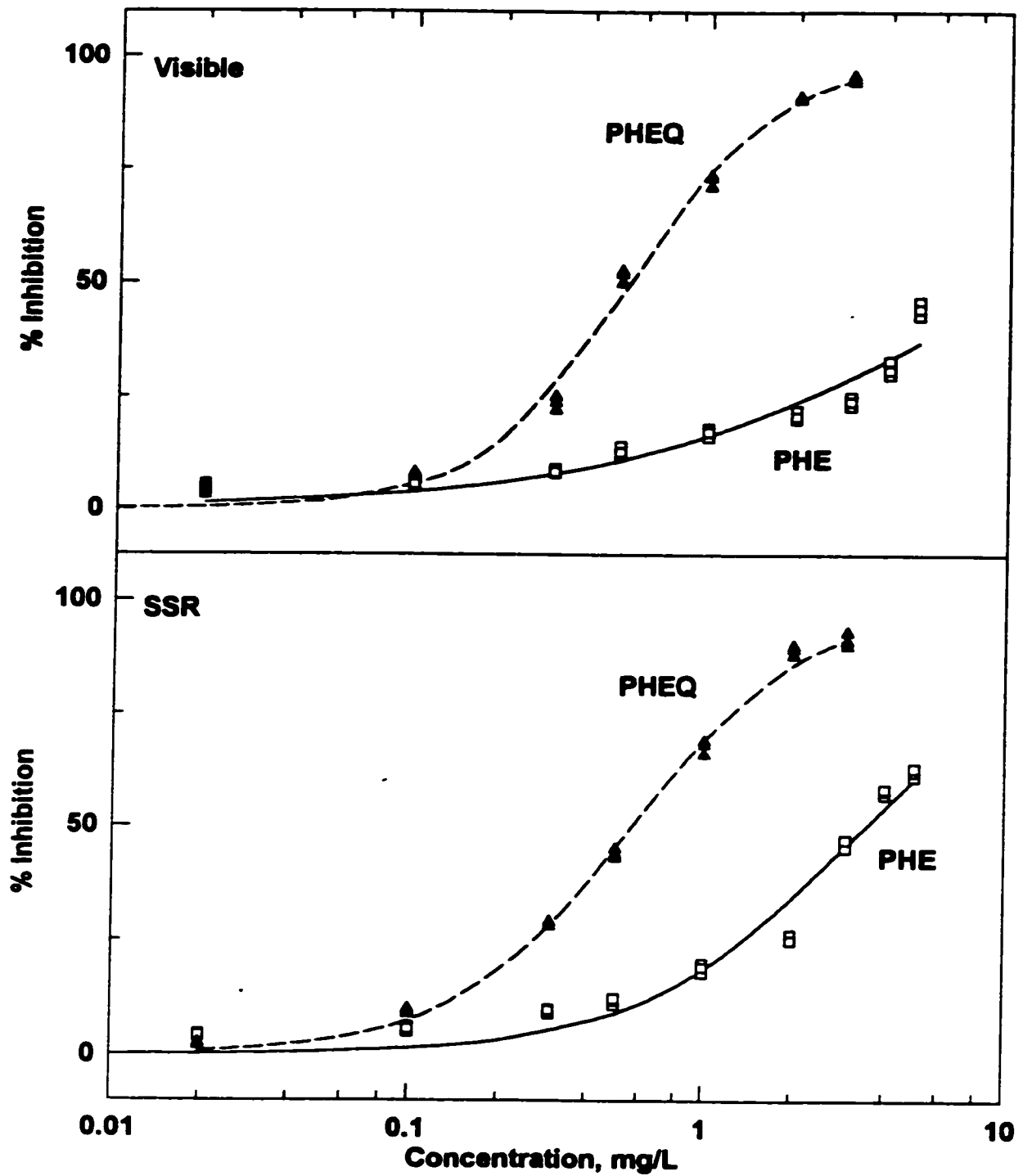
Figure 4.5. Dose-response of *L. gibba* to PHE and PHEQ in visible light and SSR. Plants were exposed to several concentrations of the two chemicals in a geometric series, and the response was measured as the doubling rate over an 8 day period. Data is reported as inhibition of growth. Data points are the mean of 3 replicates from one experiment.
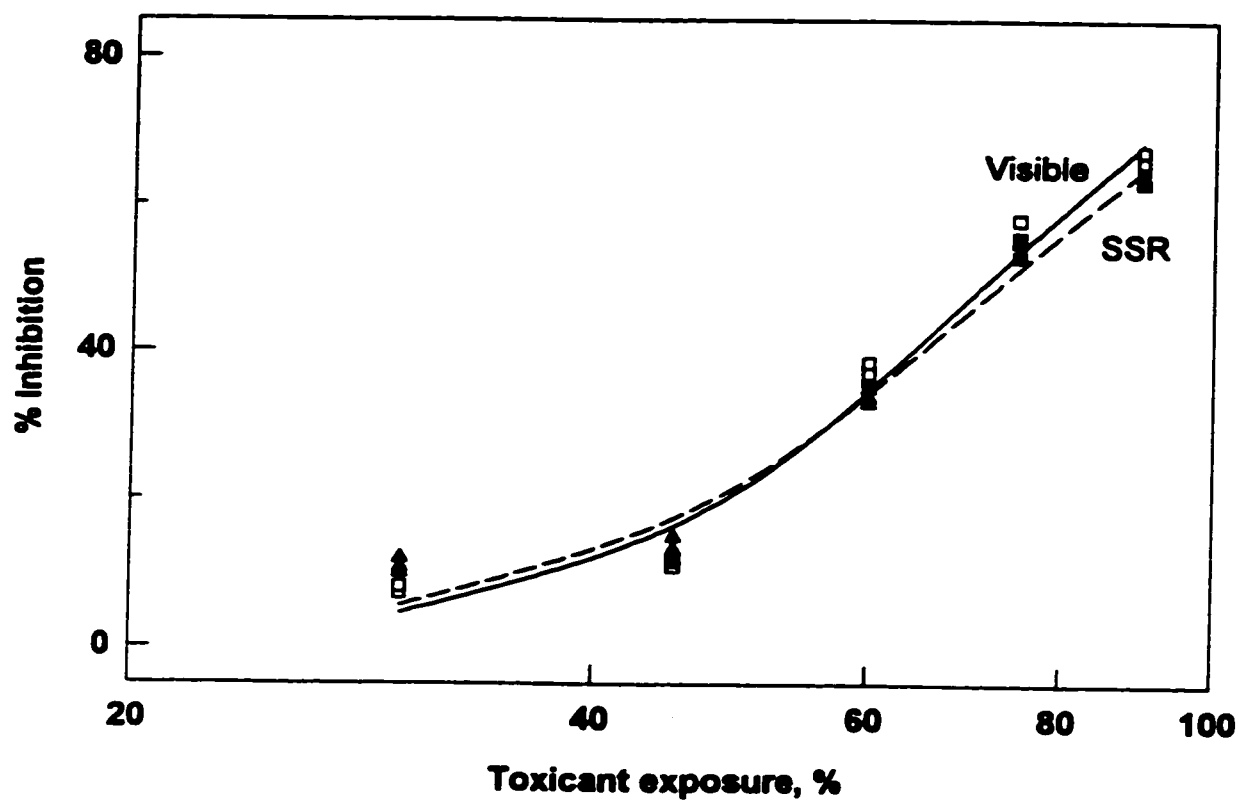
Figure 4.6. Dose-response of *L. gibba* to photomodified PHE in visible light and SSR. A dilution series of the pmPHE stock solution (0.26 mg/L PHE and 0.58 mg/L PHEQ), from 0 to 90% of the original concentration, were used as described in Methods. Data points represent percent inhibition of growth as described in Figure 5.

The bioavailability of PAHs is important when considering their toxic effects in the environment. As a result of the low water solubility of intact PAHs, they adsorb to sediments in aqueous environments resulting in low accessibility to aquatic plants and animals (Basu and Saxena 1978; Cook et al. 1983; Eadie 1984). Indeed, the calculated $EC_{50}s$ of PHE for *P. phosphoreum* and *L. gibba* are above levels found in contaminated waters (Basu and Saxena 1978; Cook et al. 1983; Eadie 1984). When PAHs are exposed to sunlight, however, they are rapidly photooxidized to products which are generally more water soluble and therefore more accessible to aquatic organisms. The calculated $EC_{50}s$ of PHEQ are well below its solubility limit and considerably less the estimated $EC_{50}s$ of PHE. Given the short half-life of PHE (approximately 48 h in SSR), relatively high PHEQ concentrations could be formed in environmental compartments exposed to sunlight. The continuous release of sediment-bound PHE to the water column and subsequent light mediated conversion to PHEQ would significantly increase the environmental risk associated with the original PHE. Unfortunately, consideration of PHEQ, as well as the photomodification products of the other PAHs, are currently not included in most environmental risk assessments.

The two organisms used for toxicity testing were both sensitive to the compounds tested, although $EC_{50}s$ for *P. phosphoreum* were an order of magnitude lower than those for *L. gibba*. This difference in toxicity can be attributed to the nature of the organisms. As a bacteria, almost all cellular functions of *P. phosphoreum* are immediately and directly exposed to the toxicant once the cellular membranes are breached. In contrast, *L. gibba* is protected by the structural compartmentalization associated with plants. The plant cell wall is an additional barrier to toxicant uptake. Nonetheless, each organism responded to the toxicants in a similar relative manner, with PHEQ more toxic than PHE.

In the PHE toxicity experiments with *P. phosphoreum*, the short exposure time to SSR precluded significant photooxidation. Because the toxicity of PHE to *P. phosphoreum* was the same in darkness and in light, photosensitization was not important to the mechanism of toxicity for PHE. In the experiments with *L. gibba*, however, PHE toxicity was photoinduced, with toxicity in SSR much greater than toxicity in visible light. If one assumes that photosensitization was not a factor in the mechanism of toxicity of PHE, as was the case with *P. phosphoreum*, then it can be concluded that the

increased toxicity of PHE to *L. gibba* in SSR was due to photooxidation. In the two day static renewal method used with *L. gibba* photooxidation of PHE would occur. However, since the half-life of PHE in SSR is 48 h, not all the PHE would photooxidize. Accordingly, it is not surprising that PHEQ was more toxic than PHE in SSR. PHEQ toxicity was also not photoactivated; the level of toxicity was the same in both visible light and SSR. That UV radiation does not alter the toxicity of PHEQ indicates that it is not a good photosensitizer and is resistant to photooxidation.

Although many PAHs are toxic or give rise to photomodification products that exhibit increased solubility and toxicity over the parent chemical, not all PAHs will give rise to highly toxic photomodification products (Oris and Giesy 1985; Newsted and Giesy 1987; Huang et al. 1993; Ankley et al. 1994; Ren et al. 1994). To ascertain which PAHs can generate more toxic photoproducts, it is instructive to look at predictive models of toxicity. Quantitative Structure Activity Relationships (QSARs) have been developed to predict the toxicity of PAHs (Krylov et al. 1997; Huang et al. 1997; Newsted and Giesy 1987; Greenberg et al. 1993; Ankley et al. 1994). It is interesting to note that in models of the photosensitization activity of intact PAHs, PHE is predicted to have low activity (Newsted and Giesy 1987; Ankley et al. 1994). However, when the toxicity of photomodified PAHs is considered in QSAR modeling of photoinduced toxicity, PHE becomes a moderately toxic PAH (Greenberg et al. 1993). With the agreement between QSAR models and the enhanced toxicity of PHEQ relative to PHE, clearly identification and toxicity testing of other photooxidized PAHs should be of high priority. This will generate better information to assess which compounds in contaminated ecosystems are damaging. The photooxidation of PAHs may have significant impact in aquatic environments, as photooxidation increases the solubility of the chemicals thereby increasing bioavailability. Even when the PAHs are sequestered in sediment or in topsoil away from sunlight, mechanical disruptions can occur that will expose the parent PAHs to sunlight.

CHAPTER 5

BENZO(A)PYRENE PHOTOOXIDATION AND TOXICITY OF PHOTOPRODUCTS

5.1 INTRODUCTION

Benzo(a)pyrene has been identified as one of the most potent PAH procarcinogens, and is one of the better studied PAHs (Varanasi 1989). Benzo(a)pyrene (BAP) is not a carcinogen itself, but requires enzymatic activation by cytochrome P450 to have carcinogenic effects. The cytochrome P450 monooxygenase system produces a variety of oxidised, hydroxylated and epoxide forms, and many of these are further metabolised to harmless water soluble metabolites. Activation of BAP to its most carcinogenic form requires two sequential oxidations, resulting in BAP-7,8-diol-9,10-epoxide. This metabolite forms covalent bonds to the guanosine moiety of DNA, which results in point mutations and can eventually lead to events such as oncogene activation and tumour formation (Marshall et al. 1984; Meehan et al. 1997).

Procarcinogen activation of BAP and other PAHs has been documented in fish as well as in rats (Thornton et al. 1982; Buhler and Williams 1989), and DNA damage has been shown to be due to other BAP metabolites as well as the 7,8-diol-9,10-epoxide (Lesko and Lorentzen 1985). Benzo(a)pyrene quinones in particular have been shown to elicit toxic effects (Lorentzen et al. 1979; Smolarek et al. 1987), and both benzo(a)pyrene quinones and the structurally related pyrene quinones have been shown to have mutagenic activity (Sakai et al. 1985; Flowers-Geary et al. 1996). In addition to the demostrated toxicity, carcinogenicity, and mutagenicity of BAP and metabolites, it is also phototoxic (Cody et al. 1984) and increases in toxicity on photooxidation (Huang et al. 1993; Krylov et al. 1997).

The environmental fate of benzo(a)pyrene in aquatic systems has not yet been fully characterized. The metabolic activation of BAP to deleterious metabolites is well known, but the activation of BAP by means other than metabolic (such as light activation) has not been as well studied. It is likely that the photooxidation products of BAP are structurally similar to some of the metabolic products, particularly quinones; the activation of BAP to deleterious chemical species is

therefore possible in the absence of metabolism.

Benzo(a)pyrene undergoes photooxidation reactions similar to other PAHs, and this is likely the major route of decomposition of BAP in environmental systems. The photodegradation of BAP was investigated to identify the photoproducts, the kinetics of their formation, and the rate of degradation of photoproducts relative to the parent PAH. The system used to investigate BAP photooxidation used simulated solar radiation (SSR) for exposures, providing a light source with ratios of UV and visible light similar to those in natural aquatic systems (Huang et al. 1993; Greenberg et al. 1995; Huang et al. 1995). A carrier solvent was used to deliver BAP to the aqueous phase; the solvent carrier also acted as a sink for a fraction of the free radicals generated by photoreactions, as would humic acids and other components of natural systems. The toxicity of photoproducts was confirmed using the *Photobacterium phosphoreum* toxicity assay. Three primary photoproducts of BAP photodegradation were identified, and two more products were identified as a result of further degradation of the primary photoproducts.

5.2 MATERIALS AND METHODS

5.2.1 Preparation of benzo[a]pyrene solutions

Benzo[a]pyrene (BAP), >97% purity, was purchased from Sigma Chemical Co. (St. Louis, MO, USA). The purity of the compounds was confirmed using high pressure liquid chromatography (HPLC). The water used in all experiments was HPLC grade water, obtained from an Barnstead E-pure ultrafiltration system (VWR/Canlab, Mississauga, ON). Two means of delivery were used to investigate the photodegradation of BAP in an aqueous environment. The first was by direct suspension of BAP in the aqueous phase, accomplished using dimethylsulfoxide (DMSO) (BDH Inc., Toronto, ON) as a carrier solvent. A stock solution of BAP in DMSO was prepared at a nominal concentration of 2.0 mg/ml, a sufficiently high concentration to permit quantitative analysis of BAP and photoproducts. 200 μl of the stock solution was added to 200 ml of rapidly stirring water in 250 ml pyrex beakers. This created an extremely fine suspension of BAP in the aqueous phase, mimicking particulate bound BAP in a natural aquatic system. The resultant concentration of BAP was 2.0 mg/L

83

in an aqueous solution with 0.1% DMSO.

The second system used to monitor BAP photodegradation was the adsorption of chemical to acid-washed fine sand (Sigma Chemical Co.), providing a simple system to model BAP behaviour in sediments. Two milligrams of BAP was dissolved in 2 ml of HPLC grade dichloromethane (Fisher Scientific Ltd., Mississauga, ON) and combined with 5 g of sand in a 250 ml glass beaker. The dichloromethane was removed by evaporation for 2 hours in the absence of light to minimise incidental photoreactions, and the BAP-adsorbed sand was covered with 200 ml of HPLC grade water. The beaker was covered with polyethylene film, a material transparent to UV-B, UV-A and visible light.

5.2.2. Light exposure of solutions

Beakers containing either the BAP suspension in water or the sand/water/BAP composite were exposed to 180 μmol m^{-2} s^{-1} of simulated solar radiation (SSR, visible:UV-A:UV-B ratio of 100:10:1, similar to that of sunlight) (Huang et al. 1993; Greenberg et al. 1995). Control beakers were prepared at the same concentrations and incubated in the dark. Water samples of 1 ml were removed from control and treated BAP suspensions every 24 hours over a six day period, for subsequent chemical analysis. After six days exposure, approximately 190 ml of the BAP suspension was concentrated onto a 3 ml ENVI-18 solid phase extraction cartridge (Supelco Inc., Bellefonte, PA, USA) and eluted with 2 ml of 100% methanol. This provided a concentrated sample to confirm the identity of the photoproducts detected in the quantitative aliquots.

Two beakers of the BAP/sand/water composite, at two and four days exposure, were extracted using liquid-liquid extraction. The liquid-liquid extraction procedure was used instead of solid phase extraction, as it could better accommodate extraction of BAP from bound phase. The majority of the aqueous phase of the composite was removed and put into a 500 ml separatory funnel, and extracted twice with 100 ml HPLC grade dichloromethane. The remaining sand and BAP in bound phase was extracted three times with 20 ml dichloromethane. Each extract was filtered through a GF/C glass microfiber filter (VWR/Canlab, Mississauga, ON) and combined into a separatory

funnel, permitting the separation of the organic phase from the residual aqueous phase. The sand extract and the aqueous phase extract were combined and concentrated using a rotary evaporator to approximately 10 ml dichloromethane, then dried under a stream of nitrogen to approximately 0.5 ml. Sufficient methanol was added to the concentrated extracts to give 1.0 ml total volume.

5.2.3. Chemical analysis of benzo[a]pyrene and photoproducts

Chromatographic analysis was performed with a Shimadzu HPLC system comprised of an SCL-10A system controller, an SIL-10A autoinjector, two LC-10AD dual pumps, and an SCL-10A diode array detector (Shimadzu Scientific Instruments Inc., Columbia, MD, USA). The HPLC column used for chemical analyses was a 25 cm x 4.6 mm I.D. Supelcosil C_{18} reverse-phase column with a 5 μm packing (Supelco Inc., Bellefonte, PA, USA). HPLC grade water (adjusted to pH 3 with phosphoric acid) and acetonitrile, both degassed with helium, were used as elution solvents at a constant flow rate of 1 ml/min. The gradient used was water:actonitrile (95:5 v/v) for 5 minutes, then a linear gradient to water:acetonitrile (5:95 v/v) over 30 minutes, and held at 95% acetonitrile for 5 minutes. An injection volume of 200 µl was used for aqueous samples, and an injection volume of 100 µl was used for the concentrated extracts in dichloromethane:methanol. A second gradient was used for the separation of BAP and photoproducts for confirmation of product identifications and toxicity testing, as acetonitrile was not a suitable solvent to use with toxicity assays. The same experimental setup was used, with a methanol/water gradient used in place of the acetonitrile/water gradient. The initial conditions were methanol:water (65:35 v/v) at pH 3 and held constant for two minutes, followed by a linear gradient to 80% methanol over 20 minutes, then to 95% methanol over 3 minutes. The 95% methanol was held constant for an additional 10 minutes.

Where possible, purchased standards of likely photoproducts were used to identify the photoproducts of BAP. Standards of benzo(a)pyrenediones were obtained from the National Cancer Institute Chemical Carcinogen Repository, Midwest Research Institute, Kansas City, MO. Anthraquinone and benzanthrone standards were obtained from Sigma Chemical Co., St. Louis, MO.

5.2.4 Toxicity testing of photoproducts

The luminescent marine bacteria *Photobacterium phosphoreum* was used to screen the toxicity of isolated BAP photoproducts. The method used was presented in Chapter 4, and so will not be presented in detail here. Briefly, the assay used was a 15 minute acute toxicity assay, conducted at 15°C. The toxicity test was conducted on a 48-well tissue culture plate (Falcon Safety Products, VWR Scientific Ltd, Toronto, ON, Canada). Inhibition of luminescence was used as a measure of the toxicity of chemicals tested. Luminescence was measured at 460 nm (40 nm bandwidth) using a Cytofluor 2350 fluorescence measurement system (Millipore Ltd., Mississauga, ON, Canada). The excitation lamp of the detector was turned off to eliminate any background fluorescence.

Fractions for toxicity testing were isolated from a concentrated sample of BAP exposed to SSR for six days. Products were isolated at the detector outlet of the HPLC system. The concentration and purity of isolated products was estimated by comparison with standard curves using authentic photoproduct, where standards existed. The fractions were in 65% to 100% methanol, and were diluted 100-fold with 2% saline solution prior to toxicity testing.

Toxicity was quantified as percent inhibition of light emission, corrected for loss of light in the control. Calculation of $EC_{50}s$ (the toxicant concentration effective in causing a 50% reduction in light output) were based on a logit function for continuous response data (Sanathanan et al. 1987). The bacteria were exposed to a control plus seven concentrations of chemical in a geometric series, with successive halvings of the concentration at each step. An additional control was used to determine the effect of methanol on the test organism. The concentration of methanol used in the dilution series was a maximum of 1%, a concentration of methanol that elicited no response in a carrier solvent control.

5.3 RESULTS

5.3.1 Solubility and degradation of BAP

Aqueous suspensions of BAP were incubated under SSR and darkness, and the resulting rate of degradation was monitored (Figure 5.1). The dark incubated solution exhibited a very slow decrease
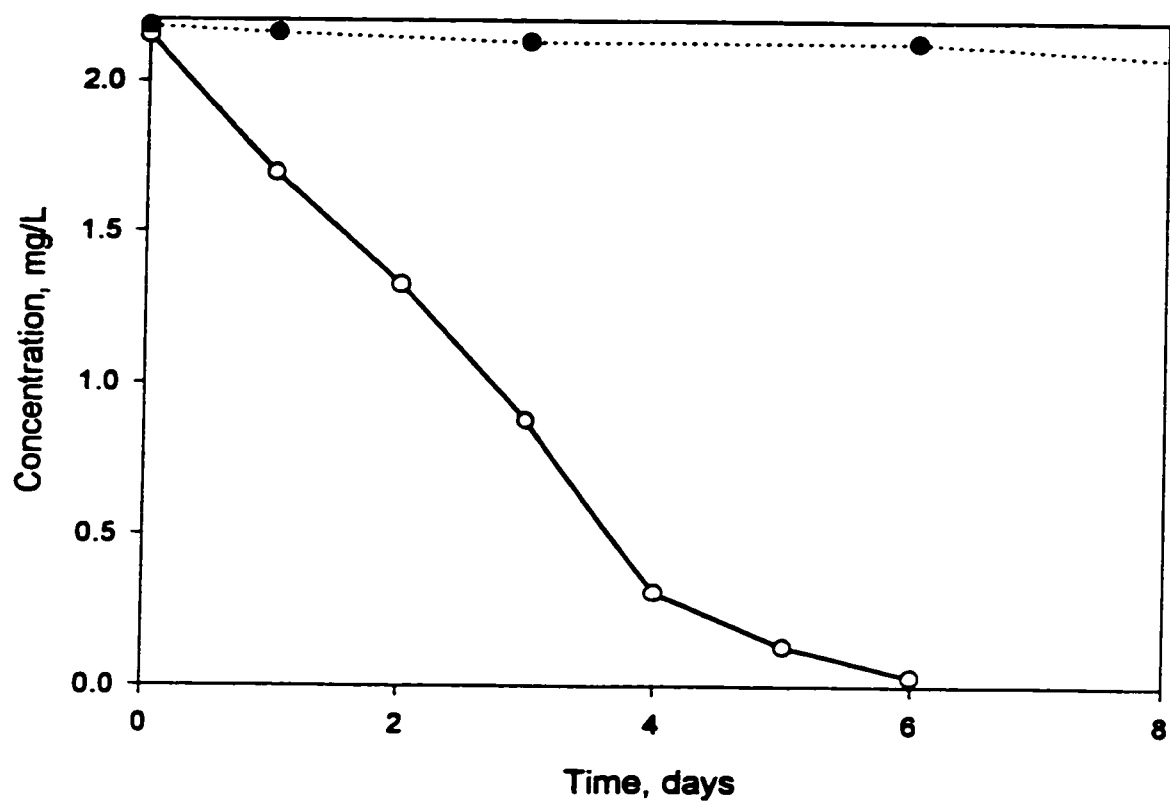
Figure 5.1. Light dependent degradation of benzo(a)pyrene. Initial conditions were 2 mg/L nominal BAP concentration in water with 0.1% DMSO. Concentrations were determined by HPLC/diode array, 240 nm absorbance with 10 nm bandwidth. Solid line is BAP in 180 mmol/m^2/s SSR, dotted line is BAP in dark.

in BAP concentration over the incubation period, with the concentration decreasing by less than 5% over six days. This indicated that loss of parent product due to evaporation, precipitation, or non-photochemical degradation was minimal over the course of the experiment. The light exposed sample exhibited a linear decrease in concentration of 0.449 mg L^{-1} d^{-1} over the first 4 days exposure, followed by an exponential-like decrease until the concentration of BAP was below the detection limit.

5.3.2 Detection of photoproducts

After six days exposure, >98% of the original BAP had been converted to photoproducts. The HPLC chromatogram of the 6-day exposed BAP suspension, determined using the methanol/water gradient, is shown in Figure 5.2. The remaining BAP eluted at a retention time of 33.0 minutes. Five photoproducts were detected at retention times between 13 and 23 minutes, plus an additional product which co-eluted with the solvent and injection spikes (between 2 and 4 minutes retention time).

5.3.3. Identification of products

To identify the products of BAP photooxidation, the 6-day exposed BAP suspension was extracted by C-18 solid phase extraction, providing a more concentrated sample and better resolution of the absorbance spectra on the diode array (Figure 5.2). A few additional products were detected between 3 and 10 minutes retention time in the concentrated sample. Comparing the analytical and concentrated samples shown in figure 5.2, the retention times and ratio of peak heights were preserved, indicating a quantitative recovery of the mixture components.

Where possible, individual components were identified by comparison of their observed absorbance spectra with that of authentic standards. The three peaks at retention times of 18.8, 19.7, and 22.4 (Figure 5.2) were identified as BAP quinones, on the basis of their absorbance spectra and similar column retention times to purchased standards. These three products were identified as BAP-1,6-dione, BAP-3,6-dione, and BAP-6,12-dione respectively (Figure 5.3). One of the additional peaks, a product of degradation of the BAP-quinones, was identified as 9,10-anthraquinone by
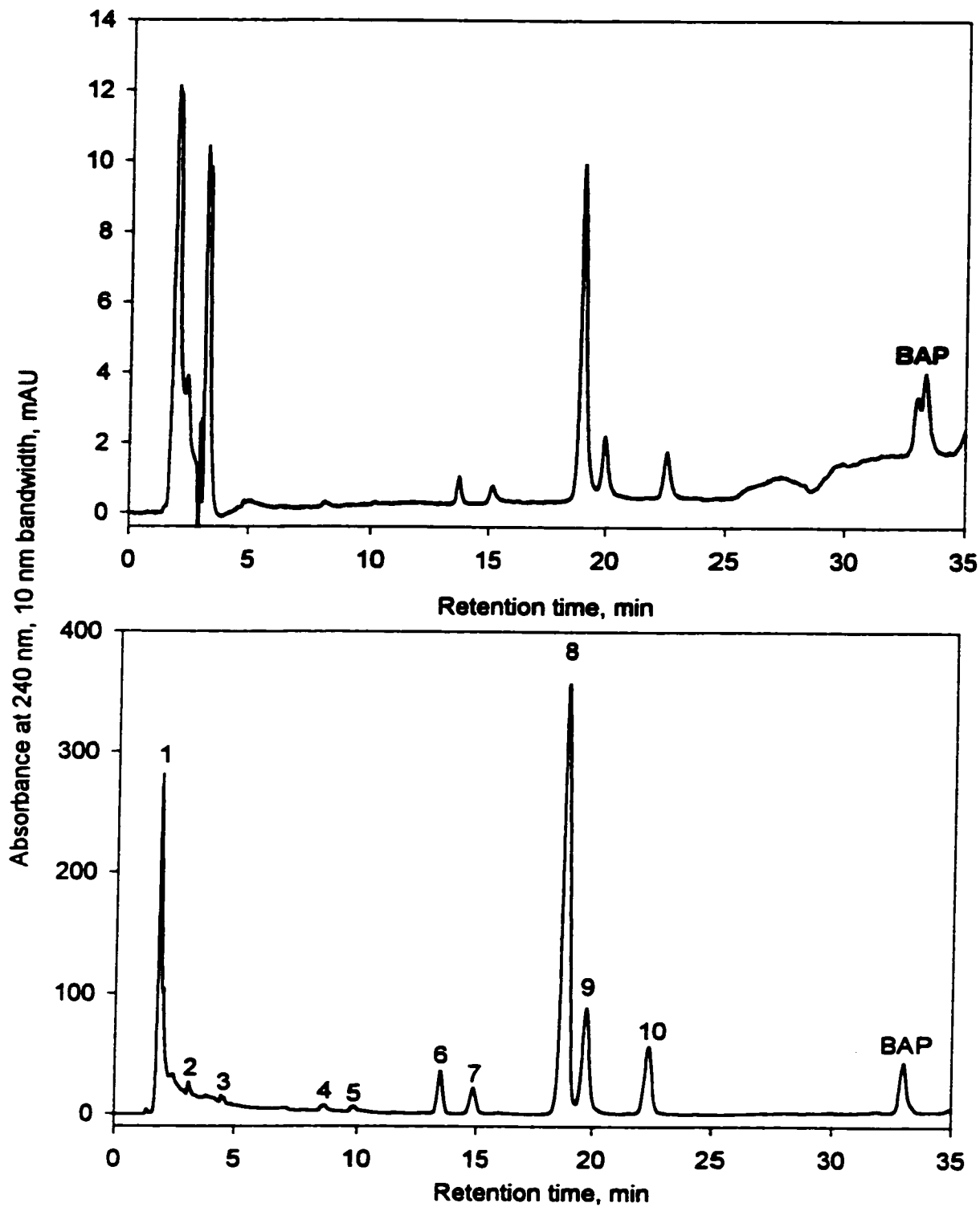
Figure 5.2: Photooxidation of benzo(a)pyrene. TOP: 2 mg/L benzo(a)pyrene, photooxidized in 180 mmol/m^2/s SSR for 6 days. A sample volume of 200 µl aqueous solution was analysed by HPLC. Bottom: Identical sample, concentrated 200x using SPE cartridge. Peaks in the concentrated sample were used for identification of mixture components.

comparison of absorbance spectra and retention time versus an authentic standard (Figure 5.3). All absorbance spectra in Figure 5.3 were normalised to 1.0 at 250 nm to facilitate comparison between products and standards. A degradation product for which no standard existed co-eluted with the injection and solvent spikes, at the beginning of the HPLC trace. This product had a similar absorbance spectra to minor photoproducts present in the mixture, eluting at retention times of 3.1, 8.6, and 14.8 minutes. These products were tentatively identified as substituted benzanthrones, based on their absorbance spectra and as compared to the absorbance spectra of a benzanthrone standard (Figure 5.4). The compound that co-eluted with the solvent/injection spike is suspected to be a 3,4-dicarboxybenzanthrone. The absorbance spectra is consistent with a four ring PAH, absorbing light into the visible portion of the spectrum, and as it eluted very early in the chromatogram it is suspected to have moderate to strong acidity. Additionally, the formation of substituted benzanthrones is consistent with the expected products of BAP quinone oxidation. A proposed pathway of BAP photooxidation is shown in Figure 5.5.

5.3.4. Kinetics of BAP degradation

The relative rates of BAP and photoproduct degradation can provide a measure of the amount of photoproduct expected in environmental systems, as the amount of photoproduct will be inversely related to its rate of degradation. (Section 3.3.3). However, the amount of photoproduct is not proportional to either the amount of PAH present, nor the degradation rate of the parent PAH (Section 3.3.3), so these may not readily be used as a basis of comparison in the experimental system or in environmental samples.

The degradation of BAP followed a zero order, concentration independent decay for the first 4 days of the exposure, followed by a decay from 4 to 6 days more closely resembling first order kinetics. At moderately low concentrations of PAH, it is expected that the rate of decay is concentration independent (Stevens et al. 1974; Zepp and Schlotzhauer 1979) and so a zero order model of reactivity is appropriate.
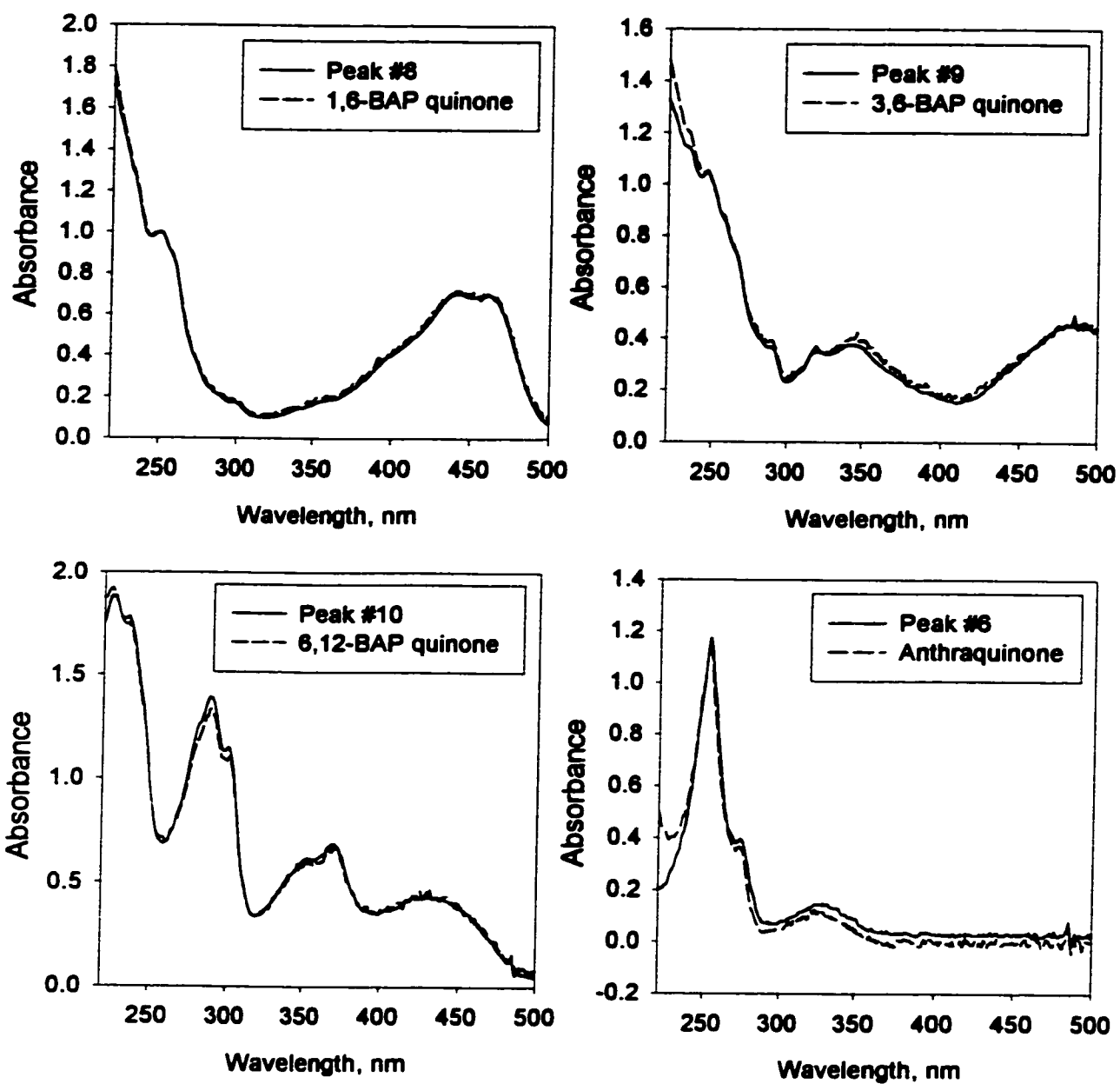
Figure 5.3: Absorbance spectra of quinones identified as benzo[a]pyrene photoproducts. Additional confirmation of identification was obtained by comparison of retention times of the unknown vs. purchased standard. Peak numbers correspond to those in figure 5.2.
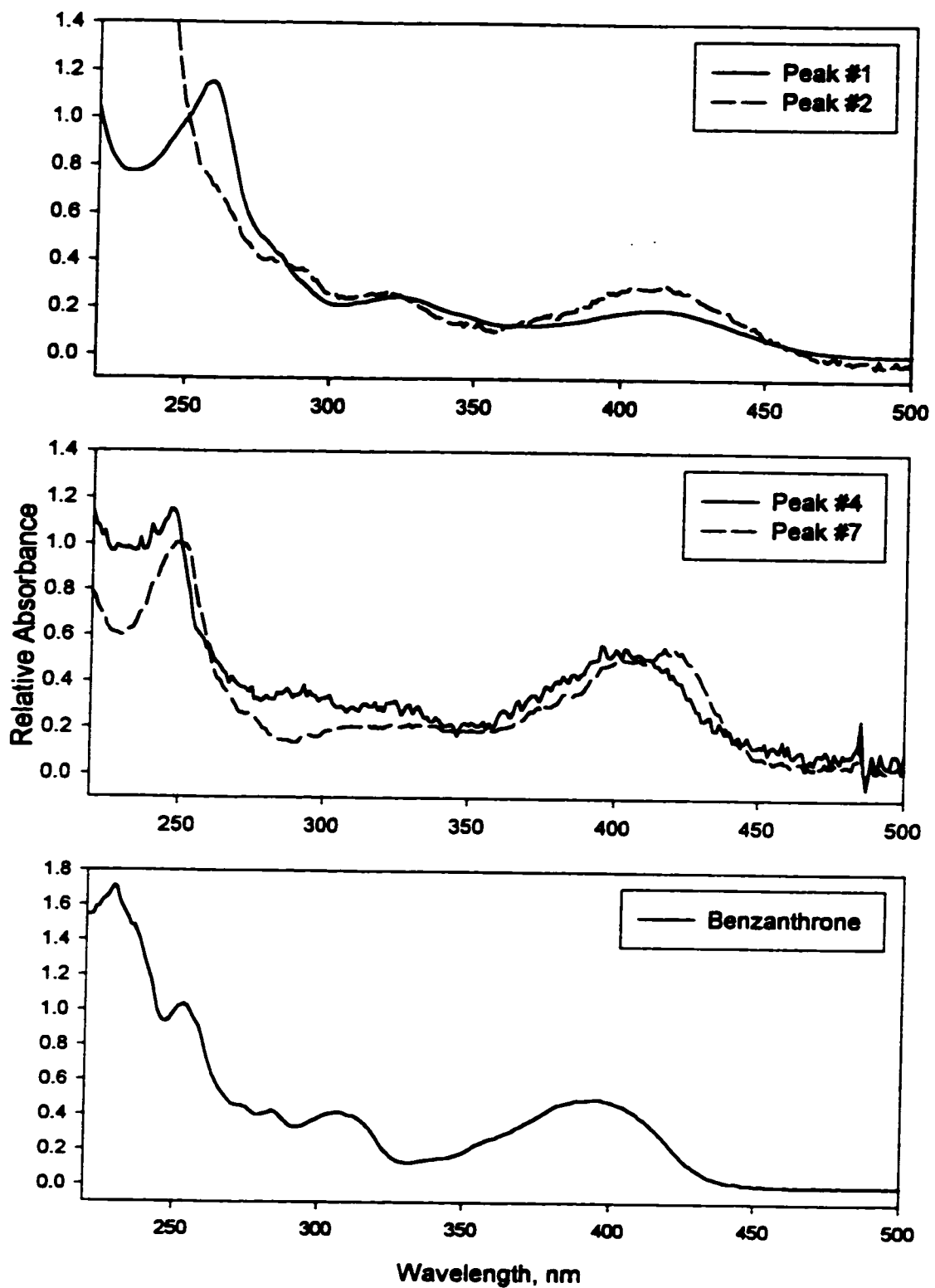
Figure 5.4: Absorbance spectra of peaks #1,2,4, and 7 versus benzanthrone.
Peak numbers correspond to those in figure 5.2.
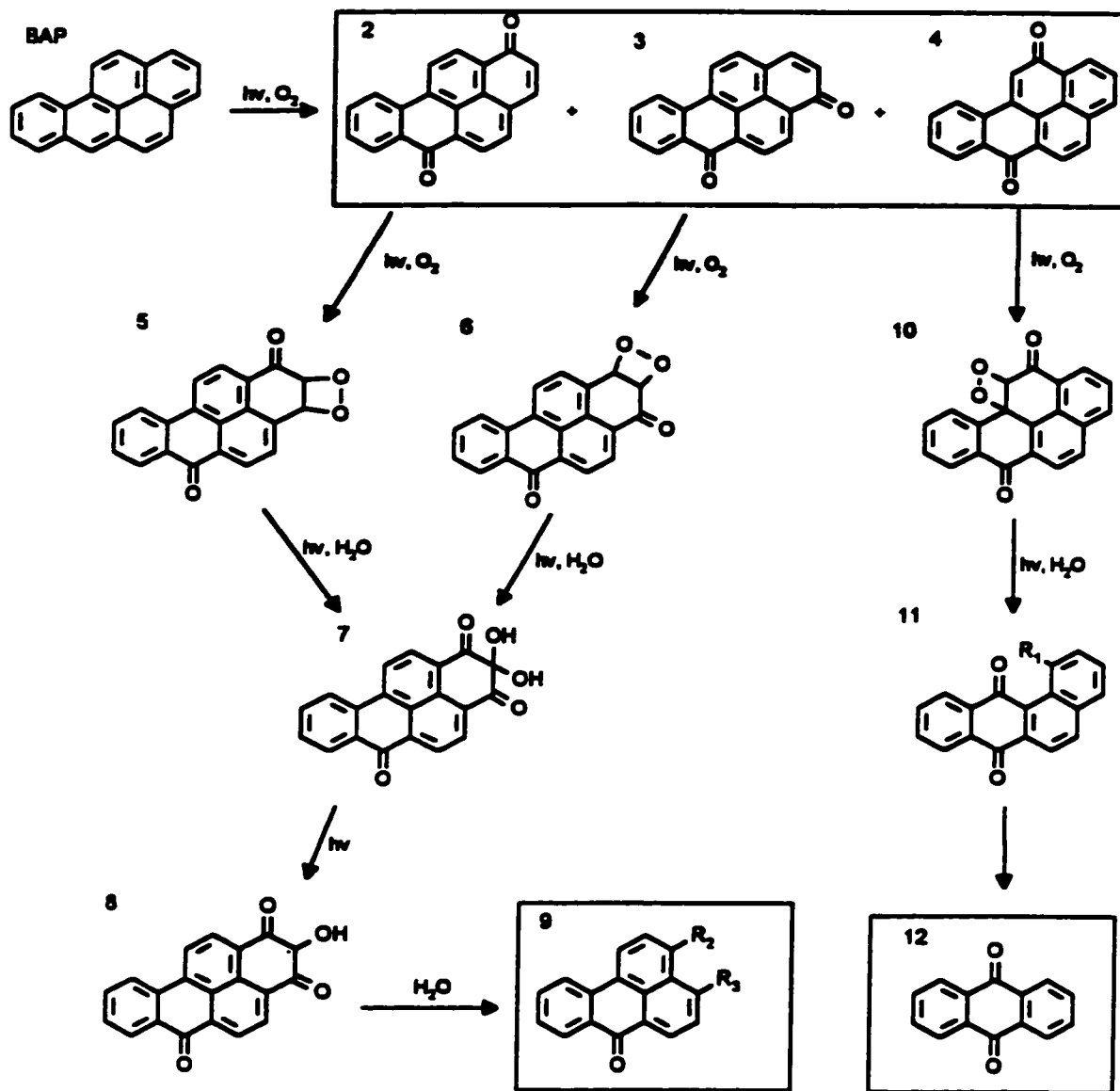
Figure 5.5: Proposed reaction scheme for the degradation of benzo(a)pyrene. After an initial oxidation to form quinones, the quinones undergo an addition of oxygen to the non-resonance stabilized ethenyl bond beta to the carbonyl group. Compounds identified by comparison with standards, or putatively identified, are highlighted in boxes.

Concentrations of BAP were fit to the kinetic model:

$$[BAP] = [BAP]_0 - k_{BAP\ loss}t$$

where [BAP] is the aqueous concentration of BAP, $[BAP]_0$ is the initial concentration of BAP, $k_{BAP\ loss}$ is the zero order rate constant for BAP loss, and t is time in days. It was possible to estimate the rates of formation and degradation of the photoproducts over the first 4 days, using a first order model. The model fit is shown in Figure 5.6. The kinetics data also allow for estimation of the quantum efficiency of formation of the individual quinones from BAP. The model used to fit the experimental data for the quinones was

$$[product_i] = \Phi i\ k_{BAP\ loss}/k_{i\ loss} \cdot \exp(-k_{i\ loss}t),$$

where Φi is the efficiency of formation of product i, and $k_{i\ loss}$ is the first order rate constant for loss of product. Estimates of the yield for product formation Φi and the rate of loss $k_{i\ loss}$ are shown in Table 5.1.

Table 5.1: Yield for rate of BAP quinone formation and first order rates of quinone degradation. Errors are 95% confidence intervals.

Chemical	Φi, yield of formation	k_{loss}, rate of product loss
BAP	-	0.449 ± 0.122 mg/L.d^{-1}
1,6-BAP quinone	0.663 ± 0.047	0.459 ± 0.065 d^{-1}
3,6-BAP quinone	0.373 ± 0.184	0.971 ± 0.411 d^{-1}
6,12-BAP quinone	0.085 ± 0.073	0.124 ± 0.547 d^{-1}
Total Φi	1.121 ± 0.304	

The total yield of quinone formation was approximately one, and thus the three quinones are the main photoproducts formed directly from BAP. It is difficult to compare the rates of loss between BAP and the BAP quinones over the first four days of the experiment, as the quinone rate of loss is concentration dependent and the rate of BAP loss was concentration independent. From four to six days, the rate of BAP loss was approximately first order, and was greater (3.0 d^{-1}) than the rate of

94
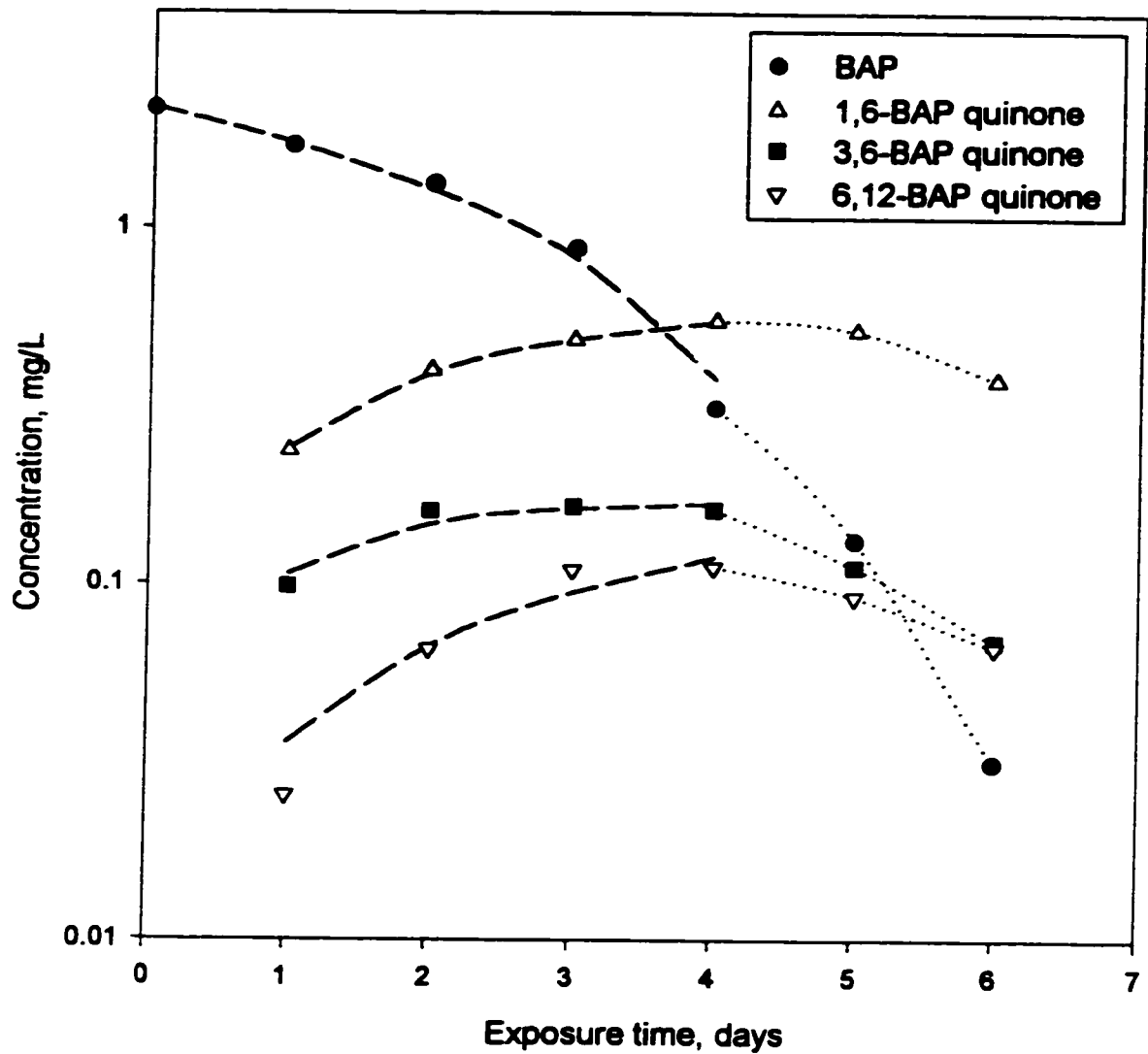
Figure 5.6: Degradation kinetics for benzo(a)pyrene (BAP) and BAP quinones. Dashed lines are the model fit for days 0 to 4 (linear rate of BAP loss) and dotted lines are the model fit for 4 to 6 days (first order rate of BAP loss).

95

quinone loss. The rate of loss of quinones followed a first order rate of loss over the entire six day period.

The sediment bound BAP extracts were also analysed by HPLC, and the same three primary products of photooxidation, the three BAP quinones, were identified in the extracts by comparison with standards. Qualitative analysis of the sediment extracts showed the same initial products of degradation as were observed is the aqueous suspensions. The rate of product formation was much slower from a bound phase, and this was attributed to the sand reducing the exposure of BAP to the light source.

5.3.5. Toxicity of BAP quinones

An assessment of the relative acute toxicities of the BAP quinones and BAP was conducted using the *P. phosphoreum* bioassay. This assay provided a rapid means of assessing whether or not the BAP quinones had a larger toxic impact than the parent PAH, and indicate whether further toxicity testing should be conducted using other organisms. The BAP quinones were isolated from the concentrated six-day sample of photoproducts, and an estimate of the EC_{50} was obtained. The results indicate that the three BAP quinones were more toxic than the parent PAH, and peak #1, the product tentatively identified as a 3,4-dicarboxybenzanthrone, did not exhibit an acute toxic response at the concentrations tested in this experiment. The $EC_{50}s$ of BAP, the BAP quinones, and peak #1 are shown in Table 5.2. The $EC_{50}s$ are expressed as a molar concentration where it was possible to quantify the amount using a reference standard. Each of the quinones identified had a greater toxicity than intact BAP, and for one quinone, 3,6-BAP quinone, the observed toxicity was a minimum of 7 times that of the intact PAH.

Table 5.2. Toxicity of primary components of photooxidized BAP to *P. phosphoreum*. Peak numbers are given in Figure 5.2.

Component	Name	EC_{50}, µmol/L
Peak #1	1,2-dicarboxybenzanthrone[1]	no observed toxicity
Peak #8	1,6-BAP quinone	1.87
Peak #9	3,6-BAP quinone	0.56
Peak #10	6,12-BAP quinone	>> 0.98
Peak #11	BAP	>> 3.97

[1]putative identification only.

5.4 Discussion

The degradation of PAHs in aqueous media has been associated with the production of reactive singlet oxygen (Neff 1979; Zepp and Schlotzhauer 1979; Nikolaou et al. 1984; Newsted and Giesy 1987). In this reaction scheme, light energy is absorbed by the PAH (in this case BAP), which undergoes an intersystem crossing to a triplet state. The excited triplet state PAH then transfers energy or exchanges an electron with ground triplet state oxygen, producing singlet oxygen (Zepp and Schlotzhauer 1979). This singlet oxygen would then react with the PAH, oxidising the compound. Toxicity due to production of singlet oxygen by PAHs in light has also been shown by numerous authors (Bowling et al. 1983; Landrum et al. 1986; Gala and Giesy 1992; Ankley et al. 1994).

The light-mediated oxidation of BAP could proceed by one of three possible reactions: reaction of singlet oxygen with ground state BAP, reaction of excited state BAP with ground state oxygen, or reaction of an excited state BAP with singlet oxygen. Earlier studies (Andelman and Suess 1971; Neff 1979) proposed that the degradation of PAH involved photooxygenation of BAP was mediated by singlet oxygen, formed by excited state energy transfer. The direct dependence of BAP photooxygenation on singlet oxygen has been questioned (Smith et al. 1978; Zepp and Schlotzhauer 1979), based on the theoretical quantum yield for direct photooxygenation. It was determined that the observed rate of photochemical loss was at least two orders of magnitude greater than predicted by a singlet oxygen mediated reaction. Additionally, it has been shown that photochemical transformations

of BAP occur at very low levels of molecular oxygen (Smith et al. 1978).

In the reaction scheme presented in this paper (Figure 5.5) the photooxidation of BAP proceeds by an attack of an oxidizing species at the 6 carbon of BAP. Based on comparison of the electron densities around each carbon (Mezey et al. 1996; Mezey et al. 1998), the 6 position of BAP is structurally similar to the 9 and 10 positions of anthracene. The 9,10 carbon positions of anthracene are known to be very photoactive, and readily undergo chemical reactions (Zepp and Schlotzhauer 1979; Wiberg 1997). As the electron density of carbon 6 of BAP is similar to the reactive site of anthracene, it is expected that it would have similar reactivity as well. Due to steric considerations, a concerted formation of a BAP quinone is not possible. It would follow instead that the reaction occurs in a minimum of two steps, with an oxidative attack at the 6-position carbon followed by a subsequent oxidation at the 1,3,4 or 12 position. These positions would be the most reactive to subsequent oxidations if the reaction intermediate is a radical species, based on the resonance structures of the BAP-6-one radical and the energetic considerations presented in Chapter 3. Three of these species, the 1,6-, 3,6-, and 6,12- BAP quinones, are observed photoproducts.

Subsequent degradation of the BAP quinones resulted in anthraquinone, and other products tentatively identified as substituted benzanthrones. In the presented reaction scheme, the mechanism of degradation of the BAP quinones proceeds via an oxidative attack on the least resonance-stabilized π-bonds within the molecule. Each of the BAP quinones may be divided into four electronic sub-domains: one similar to benzene at the ring including carbons 7,8,9, and 10, one similar to naphthalene incorporating two of the central aromatic rings, two carbonyl regions, and the ethene regions beta to the carbonyl group at carbons 1,3 or 12. The benzyl and naphthyl domains have a high degree of stablility due to resonance stabilization, and are thus unlikely to be the preferred site of further photochemical reactions (see Chapter 3). The resultant products retain the integrity of the benzyl and napthyl domains, and thus the reaction requires a lower energy to proceed, compared to that resulting from fragmentation a benzyl or naphthyl ring (Wiberg 1997).

The carbonyl region may be suseptible to photoreactions, depending on whether its lowest electronically excited state is in a (n,π^*) or (π^*,π^*) conformation (Gilbert and Baggott 1991). The

98

(n,π^*) excited state has similarity to the alkoxy radical, and may undergo α-cleavage reactions. The (π^*,π^*) state is less reactive than the (n,π^*) state, though some reactions are still possible from this state. If the (n,π^*) and (π^*,π^*) are of similar energies, the presence of a polar solvent tends to favor the (π^*,π^*) state and the carbonyl group is less reactive than in a non-polar solvent.

Ethene groups can readily undergo oxidation by singlet oxygen in a a symmetry allowed $(2\pi_s + 2\pi_s)$ cycloaddition to give dioxetanes (Gilbert and Baggott 1991; Malkin 1992), which can further decompose causing ring fission. The main products are ketones, diols, or aldehydes. In the proposed reaction scheme (figure 5.5), the BAP quinones 2, 3 and 4 follow similar degradation pathways, where the ethenyl group beta to the carbonyl is the site of attack of singlet oxygen. As benzo(a)pyrene quinones readily produce active oxygen species (Lesko and Lorentzen 1985; Lesko et al. 1986), oxidation of the quinones by singlet oxygen is an expected mode of degradation. Alternately, the oxygenation of the ethenyl bond could occur by interaction of the excited state quinone with ground state oxygen. Either path will result in the formation of dioxetanes 5, 6 and 10, which will rapidly undergo further photoreactions.

Based on the stability of products, the dioxetane bond in 10 is likely to split to form an aldehyde and a ketone. In aqueous media, the aldehyde can undergo addition of water to the carbonyl bond. The resultant product is a 7,12-benzo[a]anthracenequinone, substituted in the 1-carbon position. One possible structure for this product is shown (11). This and other products are photochemically similar to 7,12-benzo(a)anthracenequinone, which also readily decomposes in the presence of light, forming anthraquinone as one product (Section 3.3.3).

In the presence of light the endoperoxides 5 and 6 can degrade into a trione, which will exist in an equilibrium favouring its gem-diol 7 in the presence of water (Netto-Ferreira and Scaiano 1991). It has previously been shown (Matsuura et al. 1968; Netto-Ferreira and Scaiano 1991) that aromatic 2,2-dihydroxy-1,3-diones readily form hydroxyl radicals in the presence of light, which will then form dimers if no oxygen is present. In the presence of oxygen, this radical species would be rapidly oxidized. The reaction scheme (Figure 5.5) follows this pathway with the formation of an intermediate ketyl radical from the dihydroxydione, which is then oxidized to form a dicarboxylic

acid 9, losing CO_2 in the process. It is likely that other benzanthrones substituted at the 3 and 4 positions are formed as well. Other possibilities for the R- groups at the three and four positions could include hydroxy groups, or a possibly a ring incorporating oxygen. Any of the benzanthrone species may undergo further photooxidation as well.

The degradation products of any PAH or PAH photoproduct are likely to favour the formation of chemical species with a net minimum energy. Thus the degradation of the PAH will favour compounds that retain a large portion of the aromatic structure, and only one ring fission is likely to occur at any given step in the reaction pathway. Additionally, highly symmetrical molecules such as anthraquinone will be favoured products, as the more highly symmetrical electron orbitals will also have minimum energy.

The acute toxicity of the BAP quinones was greater than that of the intact PAH, as determined by the photobacterium assay. This is consistent with what is known about the modes of action of the toxicants; BAP will exhibit some light dependent acute toxicity due to the generation of singlet oxygen (Landrum et al. 1986). The BAP quinones have an additional mode of action, wherein the quinones undergo redox cycling in an organism, leading to oxidative stress (Lesko and Lorentzen 1985; Lesko et al. 1986). The product provisionally identified as the 3,4-dicarboxylbenzanthrone may be a photosensitizer, as it shares the same chromophore as the potent photosensitizer benzanthrone (Newsted and Giesy 1987). It is unlikely to have undergo redox cycling similar to the quinones as it does not share the dione/dihydroxy functionality. As it is an amphipathic molecule, there may be additional toxic effects associated with this structural feature which would require further investigation and characterisation.

Benzo(a)pyrene is a known procarcinogen, undergoing metabolic activation to form potent mutagens. This study has shown that the oxidation products of BAP are also an environmental concern, and the photooxidation products are similar to metabolic products. Some products (benzanthrones) may also be photosensitizers. The major products, the BAP quinones, are more acutely toxic than intact BAP, and are also possible mutagens via redox cycling. Thus, the oxidation products of BAP are a potential environmental hazard.

CHAPTER 6

FRACTIONAL SIMPLEX DESIGNS FOR INTERACTION SCREENING IN COMPLEX MIXTURES

6.1 SUMMARY

In mixture experiments one may be interested in estimating not only main effects, but also some interactions. Main effects and significant interactions in a mixture may be estimated through appropriate mixture experiments, such as simplex-centroid designs. However, for mixtures with a large number of factors, the run size for these designs becomes impractically large. A subset of a full simplex-centroid design may be used, but the problem remains as to which factor level settings should be selected. In this chapter, a solution is proposed that considers design points with either 1 or p individual non-zero factor level settings. These 'fractional simplex designs' provide a means to screen for interactions and to investigate the behavior of many-component mixtures as a whole, while greatly reducing the run size as compared to full simplex-centroid designs. The means of construction of the design arrays is described, and designs for ≤ 31 factors are presented. Some of the proposed methodology is illustrated using generated data.

6.2 INTRODUCTION

The general goal of mixture experiments and mixture-amount experiments is to account for the contributions made to observed responses by main factors and factors in combination. One approach is to test all factors individually, plus all possible combinations of pairs of factors in equal ratios (a second order simplex-centroid). For mixtures containing many components it is frequently impractical to test all

the possible binary combinations of factors, let alone all ternary or more complex combinations, due to the number of experimental runs required. Yet, information regarding interactions that could occur within the mixture is needed. Mixture screening designs have been introduced previously (Snee and Marquardt, 1976), but are generally intended to estimate main factors and not interactions.

Assessment of mixture interactions is being recognised as increasingly important in environmental assessment, where it may be necessary to determine the combined deleterious effect of many factors (Calabrese, 1991; Fay and Feron, 1996; Cassee et al., 1998; Feron et al, 1998). An example to which fractional simplex designs may be applied is the mutagenicity or toxicity of polycyclic aromatic hydrocarbons in environmental systems. Polycyclic aromatic hydrocarbons (PAHs) are very common environmental contaminants, and are major contributors to mutagenicity and toxicity in environmental systems. PAHs also occur almost exclusively as mixtures of many components, making the assessment of interactions a daunting task. A number of established assays may be used to assess the biological effect of single PAHs, and data from single chemical assays used to estimate the response to a mixture. A typical approach is to use single compound estimates with an assumed model such as additive action to predict the mixture effects. The question remains - does the additive model accurately predict the effect for mixtures? PAHs could be assayed individually and in combination, according to a fractional simplex design. The data from fractional simplex design experiments can then be used to isolate the larger interactions occurring within the mixture. Here, the mixtures would be prepared such that each component has an equal expected contribution to the effect. Several dose levels for each combination of PAHs would be prepared to generate a dose-response curve, with the components of each mixture held at constant ratios. From the generated dose-response curves a measure of effect can be used to determine deviations from the assumed model, such as the concentration eliciting 50% response (EC_{50}). The sample data presented in Section 6.5 provides a simpler example than toxicity of PAHs, illustrating the application of the proposed methodology.

As defined previously (Cornell, 1990), a true mixture design is subject to constraints on the mixture proportions. Given a mixture of q components, where x_i represents the proportion of the ith component, the following restrictions apply:

$$0 \le x_i \le 1 \quad \text{and} \quad \sum_{i=1}^{q} x_i = 1, \quad \text{where } i = 1, 2, ..., q \qquad (6.1)$$

Additional constraints, such as upper and lower bounds on any given x_i, may be used for specific experimental designs. A commonly used experimental design for assessing mixture interactions with three or more components is a simplex-centroid design (Scheffé, 1963). Defining a binary combination as a mixture of a pair of factors in an equal ratio based on either concentration or effect, a $\{q,2\}$ simplex-centroid consists of a design point for each pure component and for each possible binary combination, resulting in $q(q+1)/2$ design points. For larger numbers of components, even the testing of all binary combinations becomes unfeasible from an economical or pragmatic perspective (Calabrese, 1991; Cassee et al., 1998). A full simplex-centroid design has 2^q-1 design points, consisting of q pure components, $q(q-1)/2$ binary mixtures with equal proportions, $q(q-1)(q-2)/6$ ternary mixtures with equal proportions, ..., q mixtures of $q-1$ components, and a mixture of all q components in equal proportions (Scheffé, 1963). While it is rarely feasible to test all 2^q-1 design points for seven or more factors, a subset of the full simplex-centroid design may still be used.

In this paper fractional simplex designs for multi-component systems are described. This method is a practical approach for testing for meaningful interactions within a large number of components, and with a minimum number of design points. The basis on which the design arrays were generated and their means of construction are presented. General models appropriate for use with mixture data sets are discussed, and illustrated with a sample data set.

6.3. FRACTIONAL SIMPLEX DESIGNS

The fractional simplex designs presented provide a means of screening for significant interactions present within a mixture, without testing all possible binary combinations. The fractional simplex designs consist of design points containing either 1 or p non-zero factor level settings, where $p \ge 3$, such that all possible binary combinations occur once and only once within the design array. Using a fractional design with $p = 3$ as an example, the design array would contain selected ternary combinations $x_i x_j x_k$ instead of the binary combinations $x_i x_j$, $x_i x_k$ and $x_j x_k$ within a full simplex design. A sample design, for seven factors combined

in ternary mixtures, is shown in Table 6.1. Within this design all binary combinations occur only once and each assembly represents one experimental mixture consisting of three components.

Table 6.1. A {7|3} fractional simplex design. A '+' denotes a component present within an assembly, and '-' denotes absent. For this design '+' = 1/3 and '-' = 0, using the restriction $\Sigma x_i = 1$. Each binary combination appears once within the array. Seven additional assemblies, consisting of the individual components, complete the design array.

Assembly	Component						
	x_1	x_2	x_3	x_4	x_5	x_6	x_7
1	+	+	-	+	-	-	-
2	-	+	+	-	+	-	-
3	-	-	+	+	-	+	-
4	-	-	-	+	+	-	+
5	+	-	-	-	+	+	-
6	-	+	-	-	-	+	+
7	+	-	+	-	-	-	+

Within a set of points comprising a full simplex design, the selection of a subset of higher order design points meeting the once only condition for each pair of factors is not possible for all numbers of factors (though designs with minimal repetition are possible for any number of factors). The simplest example of this is a four-factor mixture, where any two groups of three factors must have a pair of factors in common. Designs without duplication of pairs of factors are termed balanced designs. Given the minimal requirements for the existence of balanced designs, the generation of the design arrays reduces to a problem of combinatorics. The mathematical detail of the fractional simplex design generation has been put in Section 6.7, where an algorithm for the generation of design arrays is presented. The notation $\{q|p\}$ is used to indicate a fractional simplex design of q total factors containing assemblies of p non-zero factors. The number of design points required for selected fractional simplex designs versus a second order simplex-lattice are presented in Table 6.2. The resultant designs meet previously published requirements for symmetric mixture designs (Murty and Das, 1968). Designs meeting these symmetry requirements have associated statistical properties, such as equal variance

estimates for main factors and for interaction terms in the mixture models presented in section 3.

Balanced designs for $q \leq 31$ are presented in section 6.8.

Table 6.2: Number of mixture assemblies required for balanced designs for $q \leq 41$, and where p is the number of factors present within a subgroup. Designs presented in section 6.8 are shown in boldface.

Total number of factors	Number of mixture design points required, where				
	$p = 2$, $\{q, 2\}$ lattice	$p = 3$	$p = 4$	$p = 5$	$p = 6$
7	21	**7**			
9	36	**12**			
13	78	**26**	**13**		
15	105	**35**			
16	120		**20**		
19	171	**57**			
21	210	**70**		**21**	
25	300	100	**50**	**30**	
27	351	117			
28	378		**63**		
31	465	155			**31**
33	528	176			
36	630				**42**
37	666	222	111		
39	741	247			
41	820			**82**	

6.4 MODELS FOR MIXTURE EXPERIMENTS

After obtaining an experimental data set using a fractional simplex design, appropriate models may be used to determine the most significant interactions. The most commonly used parametric mixture models are the canonical polynomials (Scheffé, 1958; Scheffé, 1963). The second degree or binary non-linear model is given by

$$Y = \sum_{i=1}^{q} \beta_i x_i + \sum_{i=1}^{q} \sum_{i<j}^{q} \beta_{ij} x_i x_j + \varepsilon, \qquad (6.2)$$

where Y represents the observed value of the response or effect, β_i is the expected response due to component i, β_{ij} is the quadratic interaction term for the components x_i and x_j, and ε is a normally distributed error term having an expectation of zero and a variance σ^2. The total number of terms in the full quadratic Scheffé model is q linear terms plus $q(q-1)/2$ interaction terms. This will result in a model

with an excessive number of terms if a large number of factors are to be considered. Note that it is not possible to fit the full quadratic model (6.2) using the presented fractional simplex designs, as there are insufficient design points to estimate all terms. Alternate interaction models that are appropriate for use with the screening designs are presented below.

A reduced quadratic model sufficient for isolating the most significant quadratic interactions may be obtained by grouping quadratic terms such that the summed terms have a one-to-one correspondence to experimental points in the fractional design. Considering a fractional design containing ternary design points $x_i x_j x_k$, the quadratic terms $\beta_{ij} x_i x_j$, $\beta_{ik} x_i x_k$ and $\beta_{jk} x_j x_k$ in equation (6.2) are replaced with the summed term $\beta_{ij+ik+jk}(x_i x_j + x_i x_k + x_j x_k)$. While this results in the quadratic factors being aliased in groups of three, the model can be used to isolate the most significant interactions. Each summed term is equivalent to the difference between one assembly in the design and the main factor estimate for that assembly. The reduced quadratic model for $p = 3$ and incorporating all terms is

$$Y = \sum_i \beta_i x_i + \sum_{i \ne j \ne k} \beta_{ij+ik+jk}(x_i x_j + x_i x_k + x_j x_k) + \varepsilon, \qquad (6.3)$$

where the i,j,k are selected to match the mixture design points in the array. This reduces the model to q main factors plus $q(q-1)/6$ interaction terms. For assemblies of p factors within a design array, each interaction term is a sum of $p(p-1)/2$ binary interactions. The reduced quadratic model assumes that there are few interactions present, and the chance of interactions of similar magnitude and opposite sign occurring within a subset is small. Model (6.3) allows hypothesis testing of each mixture design point for statistical significance versus a main factor model. With this particular model, the reduced number of data points used comes at the expense of aliasing the second order terms. In general, the quadratic terms will aliased in groups of $p(p-1)/2$, and quadratic terms within each group are indistinguishable. This model is primarily intended to screen for the largest interactions, by isolating them into a small subset of all possible interactions. If there are a large number of interactions occurring within a mixture, this model will be less effective at identifying the largest interactions, due to the summation of interaction effects within aliased groups.

106

A useful alternate model to the Scheffé quadratic (6.2) and reduced quadratic (6.3) models is a second degree model that expresses the main and second order effects in terms in x_i and $x_i(1-x_i)$, respectively. The interaction terms in this model describe the average deviation from linearity caused by an individual component on mixing with the other components. Starting with the Scheffé model (6.2), the quadratic terms are grouped such that each factor is isolated and all interactions containing that factor are summed, giving

$$Y = \sum_{i=1}^{q} \beta_i x_i + \sum_{i=1}^{q} \beta_i^{(2)} x_i \sum_{j \neq i}^{q} x_j + \varepsilon, \qquad (6.4)$$

where $\beta_i^{(2)}$ is a measure of the average deviation from linearity caused by mixing component x_i with other components. The model contains a total of $2q$ terms. Assuming that the experimental design follows the restriction (6.1), equation (6.4) may be written as a linear and quadratic portion in x_i:

$$Y = \sum_{i=1}^{q} \beta_i x_i + \sum_{i=1}^{q} \beta_i^{(2)} x_i (1 - x_i) + \varepsilon \qquad (6.5)$$

This model provides an estimate of an average non-linear effect of a component within the mixture in terms of individual components only, and has the advantage that the second term vanishes for $x_i = 1$ and $x_i = 0$. This model can act as a descriptor of effects for systems where one component in the presence of any of several other components causes the observed effect to deviate from linearity. An example in toxicology to which this model could be applied is a system where a factor enhances the delivery of toxicants to a target site within an organism.

6.5 SAMPLE DATA

A data set was generated to illustrate the application of the fractional simplex designs. Density of solvent mixtures was used as an experimental endpoint, as it provided an example of a mixture interaction with a straightforward interpretation and few potential confounding factors. The measured density of nine pure solvents and the nine solvents in combination was used as a data set, generated according to a {9|3}

fractional design. The design was used to screen for a significant reduction of volume of the solvents on mixing, as compared to a linear model.

6.5.1 Method

Nine miscible solvents were selected: acetone, acetonitrile, water, methanol, ethanol, propan-2-ol, tetrahydrofuran, dimethylsulfoxide, and dimethylformamide. Ternary mixtures of solvents were prepared according to a {9|3} design, in which equal volumes of solvents were combined in groups of three, resulting in 12 mixture points in the design array. All neat solvents and prepared mixtures were capped in 4 ml glass vials and allowed to equilibrate to 23°C ± 1°C prior to measurement. The densities of solvents and solvent mixtures (Table 6.3) were determined by weighing 1000 μl of solvent using an analytical balance. The errors in measurement for both the neat solvents and the mixtures are derived largely from variability in pipette volumes. The actual variation in density of the solvent mixtures and the accuracy of the balance is negligible compared to the volume error. Thus, it was possible to use two measurements of each neat solvent, in random order within the experimental design, to provide an estimate of measurement error. The error of the mixture estimates has two additional sources: lack of fit of the model, plus a small additional source of error present in the mixtures due to the initial measurement error on preparation. As the mixtures were composed of three independently measured solvent volumes of 1000 μl, a 1000 μl aliquot of the solvent mixture would have an expected error of $(1 + 3^{-3/2})$ times that of the neat mixtures, introducing an additional 19% measurement error. This was considered as an acceptable amount of additional variation compared to the lack of fit and measurement errors, and so was not corrected for during iterative model fitting procedures. Statistical analysis was done using the GLM module of Systat 8.0 (Wilkinson, 1998).

Table 6.3: Measured densities of solvents and solvent mixtures. ACE, acetone; ACN, acetonitrile; H₂O, water; MeOH, methanol; EtOH, ethanol; PrOH, propan-2-ol; THF, tetrahydrofuran; DMSO, dimethylsulfoxide, DMF, dimethylformamide.

Concentration of solvent, nominal v/v of mixture									Density,	
ACE	ACN	H₂O	MeOH	EtOH	PrOH	THF	DMSO	DMF	g/ml	
x_1	x_2	x_3	x_4	x_5	x_6	x_7	x_8	x_9		
1	0	0	0	0	0	0	0	0	0.7721	0.7727
0	1	0	0	0	0	0	0	0	0.7692	0.7740
0	0	1	0	0	0	0	0	0	1.0010	0.9957
0	0	0	1	0	0	0	0	0	0.7828	0.7811
0	0	0	0	1	0	0	0	0	0.7791	0.7803
0	0	0	0	0	1	0	0	0	0.7770	0.7774
0	0	0	0	0	0	1	0	0	0.8700	0.8683
0	0	0	0	0	0	0	1	0	1.0930	1.0943
0	0	0	0	0	0	0	0	1	0.9393	0.9383
1/3	1/3	1/3	0	0	0	0	0	0	0.8659	
0	0	0	1/3	1/3	1/3	0	0	0	0.7794	
0	0	0	0	0	0	1/3	1/3	1/3	0.9602	
1/3	0	0	1/3	0	0	0	1/3	0	0.8887	
0	1/3	0	0	1/3	0	0	0	1/3	0.8326	
0	0	1/3	0	0	1/3	1/3	0	0	0.9008	
0	1/3	0	1/3	0	· 0	1/3	0	0	0.8124	
0	0	1/3	0	1/3	0	0	1/3	0	0.9879	
1/3	0	0	0	0	1/3	0	0	1/3	0.8297	
1/3	0	0	0	1/3	0	1/3	0	0	0.8071	
0	1/3	0	0	0	1/3	0	1/3	0	0.8801	
0	0	1/3	1/3	0	0	0	0	1/3	0.9356	

6.5.2 Fitting of sample data

The measured density of the ternary mixtures was initially fit to a main factor additive model. The residuals for the single chemical and mixture data points for the linear model are shown in Figure 6.1. Four of the mixture points exhibited large deviations from the linear model: $x_1x_2x_3$ (acetone, acetonitrile, water), $x_3x_6x_7$ (water, propan-2-ol, tetrahydrofuran), $x_3x_5x_8$ (water, ethanol, dimethylsulfoxide) and $x_3x_4x_9$ (water, methanol, dimethylformamide). The data was refit to a model including 12 interaction terms according to equation (6.3). Any terms not significantly different from zero at a level of $p = 0.05$ were removed from the model, and the model was iteratively refit to the data. The final iteration resulted in four highly significant interaction terms ($\beta_{12+13+23} = 0.0182$, $p < 10^{-6}$; $\beta_{36+37+67} = 0.0191$, $p < 10^{-6}$; $\beta_{35+38+58} = 0.0307$, $p < 10^{-10}$; $\beta_{34+39+49} = 0.0289$, $p < 10^{-10}$) and two marginally significant interaction terms ($\beta_{14+18+48} = 0.0059$, $p = 0.015$; $\beta_{78+79+89} = -0.0073$, $p = 0.004$). See Table 6.3 for mixture compositions. It should be noted that in using an iteratively fitted model, the testing of parameter values at a level of $p=0.05$ does not guarantee a Type I error rate of 5% but was used instead as a criteria for selection of terms in the model.

Combinations with the largest deviations from linearity could be investigated further by testing binary mixtures from within each combination having a significant interaction. However, as the four most significant interaction terms contained water as a common factor, it was thought that equation (6.5) may be used to provide a good description of the data set, where the model term for water ($\beta_3^{(2)}$) is expected to be the most important interaction. Model (6.5) was fit to the data set, including nine interaction terms (one per solvent). After fitting the model, terms were dropped if they were not significant at $p = 0.05$. The final model fit had two significant interaction terms, $\beta_3^{(2)}$ (water) $= 0.106$, $p < 10^{-9}$, and $\beta_4^{(2)}$ (methanol) $= 0.019$, $p = 0.033$. The residuals from the model fit are shown in Figure 6.1. For the mixtures tested, there was an average increase in density of 2.3% if the mixture contained 1/3 water. This sample data illustrates the utility of fractional simplex designs for screening for mixture interactions within a many-component mixture.
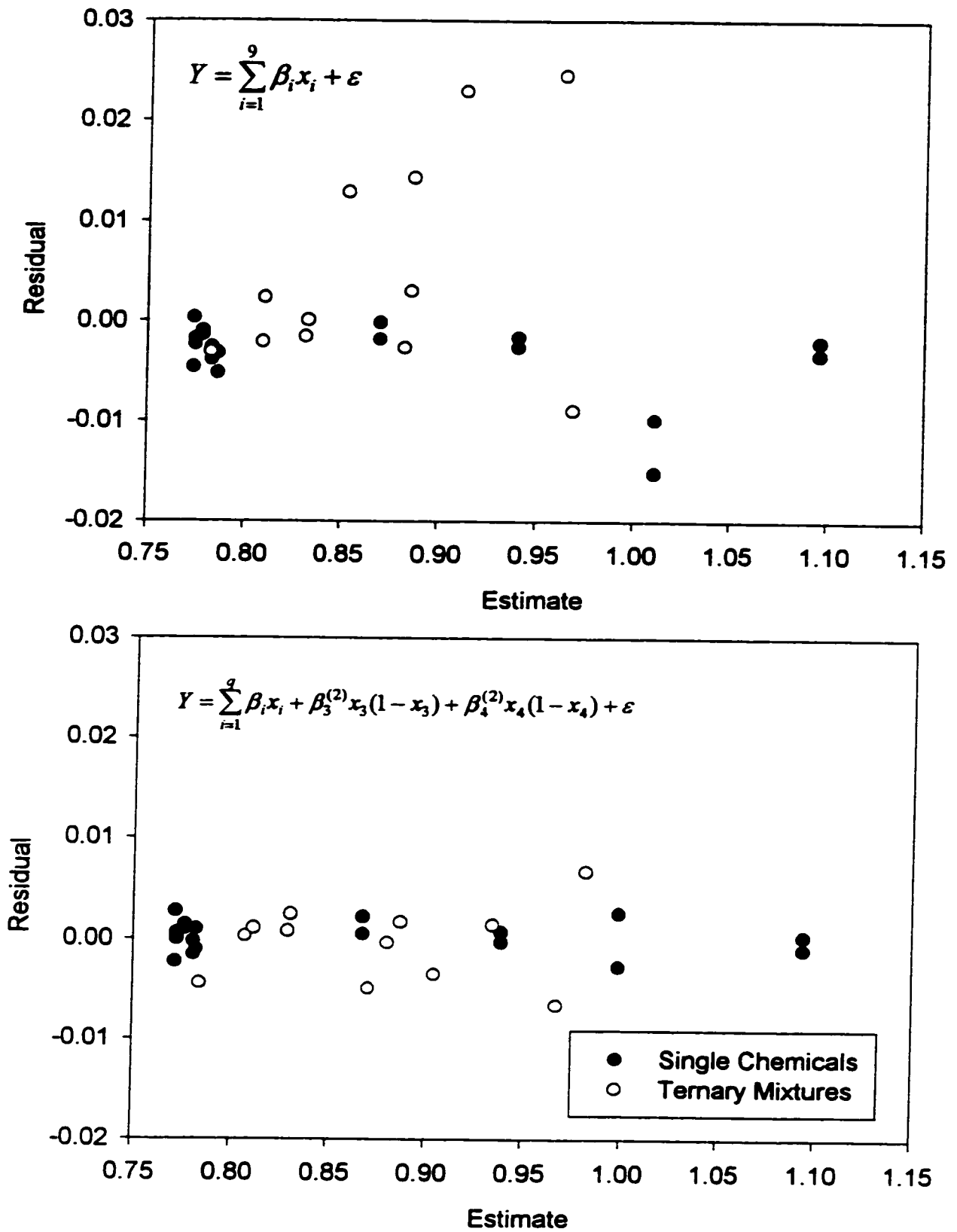
Figure 6.1: Residuals for fitted models. TOP: linear model. Six of 12 observed mixture points deviated significantly from the model. BOTTOM: linear model plus significant interaction terms.

6.6 DISCUSSION

The fractional simplex designs presented here provide a means to fractionate simplex-centroid designs. They are applicable to systems where information on possible interactions within a mixture is required, but extensive data generation is not feasible. Additionally, it provides a means to investigate the behaviour of many-component mixtures as a whole, as well as screening for the largest interactions present. While these designs can be used to provide an empirical means of obtaining mixture interaction models, a more sound interpretation is possible if the designs are used in conjunction with models based on mechanistic data, such as physiologically based pharmacokinetic models in toxicology. Additionally, models based on physical or chemical properties of the constituent factors may provide an accurate description of the response with only a few model parameters.

Estimates of variance within a design may be obtained by replication of a subset of design points, as was done with the sample data in Section 6.5. Alternately, they may be obtained by several replications of the centroid of the design. Other means of variance estimation may be suitable, depending on the experiment of interest. Greater sensitivity to deviations will be achieved using experimental responses with low variance, and this should be considered in the selection of experimental endpoints.

These designs can be applied to toxicity analysis of chemical mixtures within toxicology and pharmacology, and to industrial processes involving mixtures. In particular, the use of these designs will greatly reduce the resources required for investigation of interactions, while retaining reasonable sensitivity in the estimation of parameter values.

6.7 ALGORITHM FOR GENERATION OF FRACTIONAL SIMPLEX DESIGNS

6.7.1. Definitions

Let a design point within the matrix of q factors be represented by $(x_{1u}, x_{2u}, \ldots, x_{qu})$, where x_{iu} represents the proportion of the ith component in the uth experimental assembly (row). Additionally, let p equal the number of non-zero terms within a row, and let that row be called an assembly of order p. All assemblies of the same order can be written as a set A_p of n_p rows. Each design array presented here contains

assemblies in two subsets: A_1, which is composed of q assemblies with one non-zero term in each assembly (corresponding to the q factors), and A_p, containing $n_p = q(q-1)/(p(p-1))$ assemblies of p non-zero factors.

Given the set of integers 1, 2, ..., q, where q is odd, the set defines a one-dimensional finite field $F(q)$, which is closed under addition and multiplication. The field has the property that for any pair within the set, say a and b where a > b, the difference (or distance) between a and b is |a-b|, where |a-b| = a-b and also |a-b| = q+b-a. Defining $D(q-1)$ = 1, 2, ..., $(q-1)$ as the set of possible differences between elements in $F(q)$, any pair of elements within $F(q)$ represent two differences within $D(q-1)$. This property will be applied to the construction of fractional simplex design matrices.

6.7.2 Requirements for balanced design arrays

To construct assemblies with p non-zero factor levels within q factors in a balanced design, the total number of possible binary combinations, $q(q-1)/2$, must be divisible by the number of binary combinations possible within p factors, $p(p-1)/2$. Secondly, in order to group any one factor with all other factors only once, the number of remaining $(q-1)$ factors must be divisible by $(p-1)$. Lastly, selecting one factor in a balanced design of q factors, the selected factor is non-zero in $(q-1)/(p-1)$ assemblies, each containing $(p-1)$ other non-zero factors. To make additional assemblies, only one factor may be selected from each of these groups of $(p-1)$ non-zero factors to avoid duplication of pairs. Thus, there must be p or more groups of $(p-1)$ factors within $(q-1)$ factors and $(q-1) \geq p(p-1)$, excluding the trivial result $q = p$. Summarising the minimum conditions for balanced designs,

$$q(q-1)/\{p(p-1)\} \in I$$

$$(q-1)/(p-1) \in I \tag{6.6}$$

$$(q-1) \geq p(p-1).$$

113

6.7.3 Design generation

The construction of the design matrices were based on rotatable designs, similar to those used previously to construct optimum fractional factorial designs (Plackett and Burman, 1946). The method used to construct the fractional simplex designs is dependent upon both q and p, and may be related to the number of assemblies n_p in the design. Treating the experimental factors 1 to q as elements within a field $F(q)$, if n_p is an integral multiple of q a set of elements within the one-dimensional field $F(q)$ may be selected such that the differences between the elements form the set $D(q-1)$ without duplication. These set(s) of p elements within $F(q)$ form the initial assembly(s) from which the full design array may be generated. The full design array is generated by rotating the initial assembly(s) through $q-1$ steps, by moving the assembly(s) one place to the right $q-1$ times. The resulting design array contains all possible binary combinations of the elements within the set without repetition.

Generation of the design for $q = 13$ and $p = 4$ will be used as an example. Numbering the elements within $F(13)$ as $f = 1$ to 13, the associated difference set D is $\{1, 2, ..., 12\}$. Elements are selected within $F(13)$ using an iterative procedure. As each element assumes all positions in F on rotation of the basis set, the starting position of a given non-zero element is unimportant. Additionally, there must be one adjacent pair of elements within $F(13)$, corresponding to distances of $d=1$ and $d=12$ within D. Thus, the first and second non-zero elements may be chosen as $f_1 = 1$ and $f_2 = 2$ within $F(13)$. Arbitrarily selecting $d = 2$ as another element required within the difference set, there are two possibilities for the third element within F: $d = 2$ is the difference between the third factor and one of f_1 or f_2, or $d = 2$ is the difference between the third and fourth non-zero element. Letting the fourth element be f_4, the two potential sets in F are $(1, 2, 4, f_4)$ or $(1, 2, f_4-2, f_4)$. A value of f_4 is selected by trial such that the set of elements meets the condition that all differences within D appear once. The set $(1,2,5,7)$ meets this requirement, and the initial assembly is

1	2	3	4	5	6	7	8	9	10	11	12	13
+	+	-	-	+	-	+	-	-	-	-	-	-

114

On rotating this assembly through q-1 steps, 13 assemblies are obtained, and all binary combinations occur once within the design.

When the number of assemblies required is not an integral multiple of q, it is not possible to construct the design array using a one-dimensional field. A field of higher dimension can be used, however, if the number of possible elements in each dimension is an odd number. (An even number of elements results in duplication within D for factors a distance of $q/2$ apart, on rotation of the set.) If q is a product of two odd numbers $q = rs$, then $F(r, s)$ is the field from which elements are selected. Here, the difference set is

$$D = \{ \qquad\qquad (0, 1), \qquad \ldots \qquad (0, s\text{-}1)$$
$$(1, 0), \qquad (1, 1), \qquad \ldots \qquad (1, s\text{-}1)$$
$$\ldots \qquad \ldots \qquad \ldots \qquad \ldots$$
$$(r\text{-}1, 0), \qquad (r\text{-}1, 1), \qquad \ldots \qquad (r\text{-}1, s\text{-}1) \quad \}.$$

If $r = p$, then s assemblies may be generated by selecting the column of elements $F(r', 0)$ where $r' = 1$ to p, and rotating the column through s-1 steps within $F(r, s)$. This set of assemblies contains the differences $(1, 0)$ to $(r\text{-}1, 0)$ within D. The remaining assemblies are generated by selecting groups of p elements within $F(r, s)$ such that the distances between the elements comprise the set D, excluding $(1, 0)$ to $(r\text{-}1, 0)$. As with a one-dimensional set, each pair of elements represents two differences within D. Elements are selected using an iterative procedure analogous to that used in a one-dimensional field. The design array is completed by rotating this assembly(s) through both r and s dimensions. Designs generated by this method include the {9|3} and {15|3} arrays. This method can be expanded to fit values of q where q is a product of three or more odd factors.

If $q = 1 + (p\text{-}1)s$, where p is even and s is odd, the design array can be generated in a manner similar to that used where $q = rs$ (r, s both odd). One factor is selected, and placed in s groups containing p-1 other factors per group. The groups are selected so that all other factors are paired with the selected factor once. As the selected factor has been paired with all other factors it is removed from further consideration, and the remaining factors are treated as a set $F(p\text{-}1, r)$ with an associated difference set

$D(p\text{-}2, r\text{-}1)$. Here, the elements $(1, 0)$ to $(p\text{-}2, 0)$ within D are contained within the initial s assemblies. The {16|4} and {28,4} designs were generated using this method.

6.7.4 Designs with repetition of pairs

For designs with a number of factors q that do not meet the requirements (6.6) for balanced designs, arrays which contain some replication of binary combinations may be constructed from the designs generated from one-dimensional fields. Designs for $q = 5$ or 6 can be constructed from the {7|3} design by truncating the final elements '-' of the basis set, then rotating through q-1 steps. Using $q = 6$ as an example, the new basis set is + + - + - -, which is rotated through five steps to give six assemblies. In this example, three pairs are repeated within the design array. In an analogous fashion, designs for $q = 8$ to 11 may be generated from the {13|3} basis set, and designs for $q = 12$ to 17 can be generated from the {19|3} set. Four factor designs for $q = 8$ to 12 can be generated from {13|4}, five factor designs for $q = 13$ to 19 can be generated from {21|5}, and six factor designs for $q = 20$ to 28 can be generated from {31|6}. Thus, design arrays can be constructed for any number of factors from 5 to 28 using the designs provided in section 6.8.

6.8 BASIS ASSEMBLIES FOR BALANCED FRACTIONAL SIMPLEX DESIGNS.

Designs are presented as an initial assembly or assemblies, which on rotation give the full design. A '+' represents a component present at a level $x_i = 1/p$, where p is the number of non-zero factors within one assembly, and '-' represents $x_i = 0$. The factors have been numbered 1 through q. The full designs are obtained by rotating the provided assembly(s) through q-1 steps of one, where q is the total number of factors within the design array. Where designs are presented as blocks of factors, the basis sets are rotated in blocks instead of in steps of one. In addition to the assemblies presented here, the complete esign includes the q factors tested individually. A combination of all factors at a level of $1/q$ may be included as well.

116

Design	number of assemblies	Factors

{7|3}   7

1	2	3	4	5	6	7
+	+	-	+	-	-	-

{9|3}   12

1	2	3	4	5	6	7	8	9
+	+	+	-	-	-	-	-	-
+	-	-	-	+	-	+	-	-
-	+	-	-	-	+	-	+	-
-	-	+	+	-	-	-	-	+

{13|3}   26

1	2	3	4	5	6	7	8	9	10	11	12	13
+	+	-	-	+	-	-	-	-	-	-	-	-
+	-	-	-	-	+	-	+	-	-	-	-	-

{13|4}   13

1	2	3	4	5	6	7	8	9	10	11	12	13
+	+	-	-	+	-	+	-	-	-	-	-	-

{15|3}   35

1	2	3	4	5	6	7	8	9	10	11	12	13	14	15
+	+	+	-	-	-	-	-	-	-	-	-	-	-	-
+	-	-	-	+	-	+	-	-	-	-	-	-	-	-
-	+	-	-	-	+	-	+	-	-	-	-	-	-	-
-	-	+	+	-	-	-	-	+	-	-	-	-	-	-
+	-	-	+	-	-	-	-	-	-	-	+	-	-	-
-	+	-	-	+	-	-	-	-	+	-	-	-	-	-
-	-	+	-	-	+	-	-	-	-	+	-	-	-	-

{16|4}   20
1st column stationary; rotate blocks

1	2	3	4	5	6	7	8	9	10	11	12	13	14	15	16
+	+	+	+	-	-	-	-	-	-	-	-	-	-	-	-
-	+	-	-	-	+	-	-	+	-	+	-	-	-	-	-
-	-	+	-	-	-	+	-	-	+	-	+	-	-	-	-
-	-	-	+	+	-	-	+	-	-	-	-	+	-	-	-

{19|3}   57

1	2	3	4	5	6	7	8	9	10	11	12	13	14	15	16	17	18	19
+	+	-	-	-	-	-	-	-	+	-	-	-	-	-	-	-	-	-
+	-	+	-	-	+	-	-	-	-	-	-	-	-	-	-	-	-	-
+	-	-	-	+	-	-	-	-	-	-	+	-	-	-	-	-	-	-

{21|3}   70

	1	2	3	4	5	6	7	8	9	10	11	12	13	14	15	16	17	18	19	20	21
	+	+	+	-	-	-	-	-	-	-	-	-	-	-	-	-	-	-	-	-	-
	+	-	-	+	-	-	-	-	-	+	-	-	-	-	-	-	-	-	-	-	-
	-	+	-	-	+	-	-	-	-	-	+	-	-	-	-	-	-	-	-	-	-
	-	-	+	-	-	+	-	-	-	-	-	+	-	-	-	-	-	-	-	-	-
	+	-	-	-	+	-	-	-	-	-	-	+	-	-	-	-	-	-	-	-	-
	-	+	-	-	-	+	-	-	-	+	-	-	-	-	-	-	-	-	-	-	-
	-	-	+	+	-	-	-	-	-	-	+	-	-	-	-	-	-	-	-	-	-
	+	-	-	-	-	+	-	-	-	-	+	-	-	-	-	-	-	-	-	-	-
	-	+	-	+	-	-	-	-	-	-	-	+	-	-	-	-	-	-	-	-	-
	-	-	+	-	+	-	-	-	-	+	-	-	-	-	-	-	-	-	-	-	-

{21|5}   21

1	2	3	4	5	6	7	8	9	10	11	12	13	14	15	16	17	18	19	20	21
+	-	-	+	+	-	-	-	-	+	-	+	-	-	-	-	-	-	-	-	-

{25|4}   50

	1	2	3	4	5	6	7	8	9	10	11	12	13	14	15	16	17	18	19	20	21	22	23	24	25
	+	-	-	-	-	-	+	+	-	-	+	-	-	-	-	-	-	-	-	-	-	-	-	-	-
	-	+	-	-	-	-	-	+	+	-	-	+	-	-	-	-	-	-	-	-	-	-	-	-	-
	-	-	+	-	-	-	-	-	+	+	-	-	+	-	-	-	-	-	-	-	-	-	-	-	-
	-	-	-	+	-	+	-	-	-	+	-	-	-	+	-	-	-	-	-	-	-	-	-	-	-
	-	-	-	-	+	+	+	-	-	-	-	-	-	-	+	-	-	-	-	-	-	-	-	-	-
	+	-	-	-	-	+	-	-	-	-	-	-	-	-	-	-	-	+	-	+	-	-	-	-	-
	-	+	-	-	-	-	+	-	-	-	-	-	-	-	-	+	-	-	+	-	-	-	-	-	-
	-	-	+	-	-	-	-	+	-	-	-	-	-	-	-	-	+	-	-	+	-	-	-	-	-
	-	-	-	+	-	-	-	-	+	-	-	-	-	-	-	+	-	+	-	-	-	-	-	-	-
	-	-	-	-	+	-	-	-	-	+	-	-	-	-	-	-	+	-	+	-	-	-	-	-	-

{25|5}   30

	1	2	3	4	5	6	7	8	9	10	11	12	13	14	15	16	17	18	19	20	21	22	23	24	25
	+	+	+	+	+	-	-	-	-	-	-	-	-	-	-	-	-	-	-	-	-	-	-	-	-
	+	-	-	-	-	+	-	-	-	-	-	-	-	-	+	-	-	+	-	-	-	-	-	-	+
	-	+	-	-	-	-	+	-	-	-	+	-	-	-	-	-	-	-	+	-	+	-	-	-	-
	-	-	+	-	-	-	-	+	-	-	-	+	-	-	-	-	-	-	-	+	-	+	-	-	-
	-	-	-	+	-	-	-	-	+	-	-	-	+	-	-	+	-	-	-	-	-	-	+	-	-
	-	-	-	-	+	-	-	-	-	+	-	-	-	+	-	-	+	-	-	-	-	-	-	+	-

{28|4} 63

1ˢᵗ column
Stationary,
rotate
blocks

```
      1  2  3  4  5  6  7  8  9 10 │11 12 13 14 15 16 17 18 19 │20 21 22 23 24 25 26 27 28
      +  +  +  +  -  -  -  -  -  - │ -  -  -  -  -  -  -  -  - │ -  -  -  -  -  -  -  -  -
      +  -  -  -  +  +  +  -  -  - │ -  -  -  -  -  -  -  -  - │ -  -  -  -  -  -  -  -  -
      +  -  -  -  -  -  -  +  +  + │ -  -  -  -  -  -  -  -  - │ -  -  -  -  -  -  -  -  -
      -  +  -  -  +  -  -  -  -  - │ -  +  -  -  -  -  -  -  - │ -  -  -  -  +  -  -  -  -
      -  -  +  -  -  +  -  -  -  - │ -  -  +  -  -  -  -  -  - │ -  -  -  -  -  +  -  -  -
      -  -  -  +  -  -  +  -  -  - │ +  -  -  -  -  -  -  -  - │ -  -  -  -  -  -  +  -  -
      -  -  -  -  +  -  -  +  -  - │ -  -  -  +  -  -  -  -  - │ -  -  -  -  -  -  -  -  +
      -  -  -  -  -  +  -  -  +  - │ -  -  -  -  +  -  -  -  - │ -  -  -  -  -  -  +  -  -
      -  -  -  -  -  -  +  -  -  + │ -  -  -  +  -  -  -  -  - │ -  -  -  -  -  -  -  -  -
      -  +  -  -  -  -  -  +  -  - │ -  -  -  -  -  -  -  +  - │ -  +  -  -  -  -  -  -  -
      -  -  +  -  -  -  -  -  +  - │ -  -  -  -  -  -  -  -  + │ -  -  +  -  -  -  -  -  -
      -  -  -  +  -  -  -  -  -  + │ -  -  -  -  -  +  -  -  - │ +  -  -  -  -  -  -  -  -
      -  +  -  -  -  -  -  +  -  - │ +  -  -  -  +  -  -  -  - │ -  -  -  -  -  -  -  -  -
      -  -  +  -  -  -  -  -  +  + │ -  +  -  -  -  +  -  -  - │ -  -  -  -  -  -  -  -  -
      -  -  -  +  -  -  +  -  -  - │ -  -  +  +  -  -  -  -  - │ -  -  -  -  -  -  -  -  -
      -  -  +  -  +  -  -  -  -  - │ -  -  +  -  -  -  +  -  - │ -  -  -  -  -  -  -  -  -
      -  -  -  +  -  +  -  -  -  - │ -  -  -  +  -  -  -  +  - │ -  -  -  -  -  -  -  -  -
      -  +  -  -  -  +  -  -  -  - │ -  -  -  -  +  +  -  -  - │ -  -  -  -  -  -  -  -  -
      -  -  -  -  -  +  -  +  -  - │ -  +  -  -  -  -  +  -  - │ -  -  -  -  -  -  -  -  -
      -  -  -  -  +  -  +  -  +  - │ -  -  +  -  -  -  -  +  - │ -  -  -  -  -  -  -  -  -
      -  -  -  -  +  -  -  -  -  + │ +  -  -  -  -  -  -  -  + │ -  -  -  -  -  -  -  -  -
```

```
      1  2  3  4  5  6  7  8  9 10 11 12 13 14 15 16 17 18 19 20 21 22 23 24 25 26 27 28 29 30 31
{31|6}  31  +  +  -  +  -  -  -  -  +  -  -  -  +  -  -  -  -  +  -  -  -  -  -  -  -  -  -  -  -  -  -
```

CHAPTER 7

APPLICATION OF FRACTIONAL SIMPLEX DESIGNS TO A MIXTURE OF PAHS AND PAH PHOTOPRODUCTS

7.1 INTRODUCTION

This chapter combines the two primary topics contained within this thesis, namely the photoproducts of photochemical oxidation of PAHs, and the means by which interactions within groups of chemicals may be assessed. The toxicity of a group of seven PAHs and PAH photoproducts, and combinations thereof, was assessed using the fractional simplex designs described in the previous chapter. The organism used for toxicity testing was the luminescent marine bacteria *Photobacterium phosphoreum*. A parametric representation of a sigmoidal curve was used to fit the dose-response curves of individual chemicals. Mixture data sets were graphically compared to dose-response curves predicted by two models of interaction, concentration additivity and response additivity. These are the most frequently occurring types of interactions (Calabrese 1991; Cassee et al. 1998), and form the basis for comparison for mixtures deviating from additivity. A statistical analysis was performed using the set of calculated EC_{50}s to determine significant deviations from additivity at the median response.

When organisms are exposed to a mixture of chemicals, the possible toxic interactions range along a continuum from less than additive, through independent action and strict additivity, to greater than additive toxicity. For any given set of mixture components, the difficulty is to determine where on the continuum the interactions fall. Ideally, this should be done at all dose levels. The effects of the majority of toxicants in combination follow strict additivity (concentration addition), independent action (response additivity), or are intermediate between these two subsets of additive action. The range of response intermediate between these models is similar but not identical to a previously defined 'envelope of additivity' (Loewe 1953; Kodell and Pounds 1988). The most interesting interactions are those in which combinations of two or more chemicals deviate significantly from both additive models,

and the effect is either significantly underestimated or overestimated by the models. While large deviations from additive models occur infrequently, it is not safe to assume that interactions are not present without conducting appropriate tests of the model in question.

Existing methods for assessment of toxicant interactions tend to focus on a given level of response, such as an LC_{50} (50% lethality) or EC_{50} (50% of a measured quantitative response, such as a growth rate, enzyme inhibition, etc.). This has been done partially to provide a readily quantifiable measure of interaction, and also as the point of 50% response is usually near the centre of the range of data points and is thus has minimum error when calculated by regression. However, it is important to consider all dose levels when investigating mixture interactions, especially if one is interested in developing predictive models of response. It is possible that deviations from a predicted model may occur at dose levels other than in the vicinity of 50% response. The deviations from a predictive model may be quantified and a statistical significance determined, or may be assessed by less rigorous but readily interpreted graphical means. Methods for statistical determination of deviations from additivity have been developed for investigating drug interactions (Bliss 1939; Plackett and Hewlett 1963; Unkelbach and Wolf 1985). Graphical methods of interpreting mixture interaction data also have a long history (Loewe and Muischenk 1926; Tammes 1964; Hewlett 1969; Pöch et al. 1996) and are valuable in determining the degree of deviation from additivity.

To investigate possible interactions in a mixture over the entire range or response, it must be possible to describe the dose curve of the toxicants of interest. Dose-response curves are frequently well described by a logistic model of interaction (Sanathanan et al. 1987). A general model of logistic response is

$$P(x) = [\ 1 + \exp\{-\beta \ln \alpha(x)\}]^{-1} \qquad (7.1)$$

where $P(x)$ is the probability of response, β is a measure of the slope of the dose response curve, and $\alpha(x)$ is a measure of the position of the curve on the x-axis. One curve may be compared to another by measuring the relative change in slope, position, or both (Plaa and Vézina 1990).

The degree of interaction may be quantified through use of toxic units (Sprague 1965; Marking 1977), which express the concentration as a fraction of the concentration required to cause a given

effect. Using the concentration required to cause 50% mortality (LC_{50}) as the measure of effect, the concentration of chemical C_i expressed in toxic units is

$$TU_i = [C_i]/(LC_{50})_i \qquad (7.2)$$

where [C_i] is the concentration of chemical C_i and (LC_{50})$_i$ is the concentration of C_i required to cause 50% mortality. Toxic units may also be calculated for other quantitative endpoints, such as an EC_{50}. In this chapter, all TUs were calculated using EC_{50} values. The underlying assumption of concentration additivity is that a given number of toxicants are acting by similar mechanisms within the organism, and can be treated essentially as different forms of the same chemical, adjusted for potency (Calabrese 1991; Pöch et al. 1996). In this model, the median response of the organism to a mixture of toxicants occurs when the sum of toxic units is equal to 1.0:

$$\Sigma_i \, TU_i = \Sigma_i \, [C_i]/(EC_{50})_i = 1.0, \text{ at } EC_{50} \qquad (7.3)$$

It can be assumed that if concentration additivity applies, then the slope of the dose-response curve of a mixture may be represented by an average of the slopes of the contributing components. It is frequently the case that toxicants with similar modes of action will have the same slope of dose response. If this is not so, inspection of the model fit will reveal deviations from the predicted response.

In contrast to the concentration additive model, response additivity assumes that the response is due to different primary mechanisms or sites of action. The responses are thus independent on a cellular level (Plackett and Hewlett 1963; Berenbaum 1985; Kodell and Pounds 1988). For instance, inhibition of respiration and inhibition of protein synthesis are very different mechanisms, but both can lead to inhibition of growth or death of the organism. The predicted response in a response additive model can be represented as the sum of the predicted responses to each of the components:

$$R_{total} = \Sigma_i \, R_i(x_i) \qquad (7.4)$$

In most cases, response addition predicts a lesser effect than concentration addition. However, for assays with shallow sloped dose responses, the two methods of calculation can predict comparable results. In some cases, the response addition model predicts the greater response of the two models (Pöch et al. 1996).

The approach presented in this chapter combines the parametric representation of the dose response curve (7.1) with the additive models (7.2) and (7.4). The logistic response curve (7.1) was used to describe the response of P. phosphoreum to individual toxicants. Mixtures of chemicals were prepared according to a {7|3) fractional simplex design. The observed toxicity of the mixtures was compared to dose response curves predicted by either concentration or response additivity, using the single chemical data in the models to generate the curves. A statistical analysis of the deviations at median response, for each mixture and single chemical, was done to determine the significance of deviations from additivity.

7.2 MATERIALS AND METHODS

7.2.1 Photobacterium phosphoreum toxicity assay

The luminescent bacteria P. phosphoreum (strain NRRL B-11177) were obtained from the Midwest Area National Centre for Agricultural Utilisation Research, Peoria, Ill. Prior to toxicity testing, cultures of P. phosphoreum were grown at room temperature (23 to 25 °C). The growth media was composed of 2.5 g L^{-1} KH$_2$PO$_4$, 30 g L^{-1} NaCl, 5 g L^{-1} glycerol, 1 g L^{-1} yeast extract, 12.5 g L^{-1} Tryptone, and 2.5 g L^{-1} Bactopeptamin, adjusted to pH 7.1 with NaOH. Yeast extract and Tryptone were obtained from BDH Inc., Toronto, ON, and Bactopeptamin was obtained from Difco Laboratories, Detroit, MI. Cultures were harvested when they reached an absorbance of 2.0 to 3.0 at 550 nm, as measured using a spectrophotometer. The culture was diluted to an O.D. of 0.06 in 2% (w/v) saline solution immediately prior to toxicity testing. Twenty-four 500 µl aliquots of cells were added to a 48-well tissue culture (Falcon Safety Products, VWR Scientific Ltd, Toronto, ON, Canada). After 5 min acclimatisation in the 48-well culture plates, the luminescence of the cells was measured. Cells were then dosed with chemical (see below) and incubated for 15 min, after which bacterial luminescence was measured again. Luminescence was measured as total light output from the tissue culture wells using a Cytofluor 2350 fluorescence measurement system (Millipore Ltd., Mississauga, ON, Canada). The excitation lamp of the detector was turned off to eliminate any background fluorescence or scattering. This assay is similar to the Microtox® assay, except that fresh bacterial cultures are used instead of freeze dried cultures.

7.2.2 Delivery of chemicals

Preparations of stock solutions of seven PAHs and oxyPAHs were made in dimethylsulfoxide (DMSO) at the following concentrations: acenaphthenequinone (ACNQ) 10 mg/L, phenanthrenequinone (PHEQ) 2 mg/L, fluorene (FLN) 10 mg/L, fluoranthene (FLA) 4 mg/L, pyrene (PYR) 4 mg/L, 1,2-dihydroxyanthraquinone (dHATQ) 4 mg/L, and phenanthrene (PHE) at 4 mg/L. All chemicals were greater than 98% pure and were purchased from Sigma-Aldrich Chemical Co. (St. Louis, MO, USA). The use of DMSO as a solvent carrier permitted the testing of chemicals at concentrations above their aqueous solubility limit, which aided in obtaining responses over a wider range of dose. Dilutions of the stock solutions were prepared in a dilution series of 1:500, 1:1000, 1:2000, 1:4000, 1:8000, 1:16000, and 1:32000 in a 2% saline solution. 500 μL of these solutions were then each added to 500 μL of the 0.06 OD bacterial suspension in a 48-well plate, resulting in a thousand-fold dilution of chemical at the highest concentration. A control dilution series was also tested using a stock solution containing DMSO only. The concentration of DMSO was ≤0.1% in each of the final mixtures, a concentration not eliciting a response from the bacteria (Environment Canada 1993; McConkey et al. 1997).

7.2.3 Preparation of mixtures for toxicity testing

A {7|3} fractional simplex design, described in the previous chapter, was used to screen for interactions of the above set of chemicals. Two additional mixtures were also tested, one of three PAHs and one of the three oxyPAHs. After obtaining preliminary estimates of the EC_{50} for each chemical, combinations containing three components were prepared in DMSO at concentrations such that each would have comparable expected contributions to the toxicity of the mixture, i.e., the ratio of the concentrations expressed as toxic units was approximately 1:1:1. Pyrene was an exception to this, as it did not elicit a toxic response at the concentrations used. Instead, the concentrations of pyrene used were comparable to concentrations of the other PAHs tested. Each of the final mixtures had a sum of toxic units greater than 1.0 at the highest concentration tested. The highest concentrations tested for each of the mixtures are shown in Table 7.1. Additional concentrations were tested in a diminishing

geometric series, similar to the individual chemicals. Each individual chemical was tested twice, in random order within two separately randomised series.

Table 7.1: Concentrations of toxicants in each mixture at the highest dose level tested. See text for chemical abbreviations. All concentrations are in mg/L. Mixtures M1 to M7 were generated according to a {7|3} fractional simplex design; mixtures M8 and M9 were added to provide additional points consisting of either only PAH photoproducts (M8) or only PAHs (M9).

Mixture #	ANCQ	PHEQ	FLN	FLA	PYR	dHATQ	PHE
m1	4	0.2		2			
m2		0.2	4		2		
m3			4	2		2	
m4				2	2		2
m5	4				2	2	
m6		0.2				2	2
m7	4		4				2
m8	4	0.2				2	
m9			4	2	2		

7.2.4 Quantification of toxicity

Toxicity was measured as percent inhibition of light emission from a treated aliquot, corrected for loss of light in the control as:

$$\% \text{ Inhibition } = 100\left(1 - \frac{L_f \cdot C_i}{L_i \cdot C_f}\right) \qquad (7.5)$$

where L_i is the initial luminescence of the bacteria prior to toxicant exposure, L_f is the luminescence of the bacteria following a 15 min chemical exposure, and C_i and C_f are the initial and final luminescence of the control bacteria.

Calculation of EC_{50}s (the toxicant concentration effective in causing a 50% reduction in light output) and the slopes of the response were based on a logit function for continuous response data (Sanathanan et al. 1987). The data for % inhibition vs. chemical concentration can be fit to the equation

$$R = [1 + \exp\{\beta \ln (x/\mu)\}]^{-1}, \qquad (7.6)$$

where R is the response from zero to one, x is the concentration, μ is the estimate of the EC_{50}, and β is a measure of the slope of the concentration-response curve. This form of the logit equation has a minimum correlation between the parameters β and μ. The expected dependence of the variance on the response is $\sigma^2 \propto (1-R)$, where σ^2 is the variance (Environment Canada 1993). However, as the observed variance was better approximated by a model in which the variance was independent of the response, unweighted least squares was used to fit the response curve. Data analysis and curve fitting was performed with SYSTAT™ 8.0 (Wilkinson 1998). Since all points within a dilution series were tested on bacteria from the same batch and at the same time, there is likely to be some correlation between the data points within a series. For this reason, the data points within a series were not treated as independent measurements; instead the EC_{50} and slope parameters calculated for each replicate set were used in statistical calculations. Error estimates were calculated based upon the parameters estimated from replicate experiments.

7.2.5 Predictive interaction models

The data points obtained from the mixtures were graphically compared to estimated response calculated via two separate interaction models: response additivity and concentration additivity. Deviations from these models would indicate greater than additive or less than additive action. The purpose here is to investigate whether there are significant deviations from the two predictive models used. For concentration additivity, the response was estimated using a variant of the logit equation (7.6). The term (x/μ) in equation (7.6) was replaced by the sum of toxic units $\Sigma \, TU = \Sigma \, x_i/\mu_i$. The slope was replaced by a weighted average according to the formula $1/\beta = \Sigma_i \, (TU_i/\beta_i) / \Sigma_i \, TU_i$. The average is weighted according to the expected contribution of each mixture component at EC_{50}, and the reciprocal of the slope parameter is used to reduce the bias introduced by large slope values, and to provide a

126

more conservative estimate of response at low concentrations. Summarising the full dose response concentration additive model,

$$R_{CA} = [1 + \exp\{\beta' \ln \Sigma TU\}]^{-1},$$ (7.7)

where $\quad \Sigma TU = \Sigma \, x_i/\mu_i$

and $\quad 1/\beta = \Sigma_i \, (TU_i/\beta_i) \, / \, \Sigma_i \, TU_i.$

The response additive model was calculated as the sum of expected responses from each component within the mixture:

$$R_{RA} = \Sigma_i \, [1 + \exp\{\beta_i \ln (x_i/\mu_i)\}]^{-1}$$ (7.8)

Equations (7.7) and (7.8) provide the basis for comparison of the mixture data to the predicted type of interaction. The set of $EC_{50}s$ was compared using a combination of equation (6.5) and the toxic units concept (equation 7.3). The additive model at EC_{50}, expressed as toxic units, is

$$Y = \sum_{i=1}^{q} TU_i + \varepsilon$$ (7.9)

where TU_i is defined in equation (7.3). The additive model at EC_{50} including interaction terms is

$$Y = \sum_{i=1}^{q} TU_i + \sum_{i=1}^{q} \beta_i^{(2)} TU_i (1 - TU_i) + \varepsilon$$ (7.10)

where $\beta_i^{(2)}$ is the second order interaction term for chemical i, expressed in terms of TU_i only. This parameter determines if chemical i induces a net deviation from additivity on combination with other factors.

7.3 RESULTS

7.3.1 Toxicity of individual chemicals

The single chemical toxicity data obtained using the *P. phosphoreum* assay for was fit to equation (7.6) for each replicate data set, and the EC_{50} and slope parameter estimated. The toxicity of each chemical was determined from duplicate samples, and the average parameter estimates calculated (Table 7.2). The single chemical data set was used to estimate the Toxic Units (TUs) which provided the basis for the predictive models of interaction. Several of the chemicals tested had an apparent maximum response, presumably limited by the solubility of the chemicals. In this case, the response at

127

the one or two highest concentration levels deviated from the sigmoidal curve, and these points were omitted from the regression used to obtain estimates of the EC_{50}s and slope parameters.

Table 7.2: EC_{50}s and fitted slope parameters for individual chemicals. See text for chemical abbreviations. EC_{50}s and slope parameters were estimated using the logit equation (7.1). All experiments were performed in duplicate, and errors shown are one standard deviation. The EC_{50}s shown here were used to calculate toxic units for each of the mixtures.

Chemical	EC_{50}, mg/L	Slope parameter β
ANCQ	9.80 ± 2.8	0.82 ± 0.11
PHEQ	0.26 ± 0.11	3.39 ± 0.19
FLN	4.87 ± 0.09	1.02 ± 0.05
FLA	2.31 ± 0.47	1.25 ± 0.25
PYR[1]	-	-
dHATQ	2.08 ± 0.36	0.89 ± 0.05
PHE	1.21 ± 0.01	1.38 ± 0.15

[1] no response was observed in the pyrene toxicity assays.

7.3.2 Toxicity of PAH and photoproduct mixtures

The response to the ternary chemical mixtures was estimated, and interactions investigated as the deviation from the additive interaction models (7.7) and (7.8). Data points were plotted as response versus the sum of toxic units for each mixture, based on the EC_{50}s estimated from the single chemical data set (Table 7.2). The responses predicted by the concentration addition (7.7) and response addition (7.8) models are also plotted. Due to the shallow slope of the response with the *P. phosphoreum* assay, there is not a large distinction between either of the additive models (the distinction between the models would be more apparent for steep-sloped responses). The response to mixtures M1, M2, M3, and M4 are shown in Figure 7.1, M5, M6 and M7 in Figure 7.2, and M8 and M9 in Figure 7.3. Refer to Table 7.1 for mixture composition and concentrations.

For each of M1, M2 and M3, both models adequately describe the observed response. The slope of the curve may have been slightly underestimated in the concentration additive model for M1, possibly due to the larger contribution of PHEQ to the response. M2 had a similarly good fit, except at

Figure 7.1: Percent light inhibition of *P. phosphoreum*, exposed to mixtures M1, M2, M3, and M4. See Table 1 for mixture concentrations. The solid line is the toxicity predicted by a concentration addition model, and the dashed line is the predicted toxicity for a response addition model. The predictive models are based on single chemical data only.

Figure 7.2: Percent light inhibition of *P. phosphoreum*, exposed to mixtures M5, M6, and M7. See Table 1 for mixture concentrations. The solid line is the toxicity predicted by a concentration addition model, and the dashed line is the predicted toxicity for a response addition model. The predictive models are based on the single chemical data only.
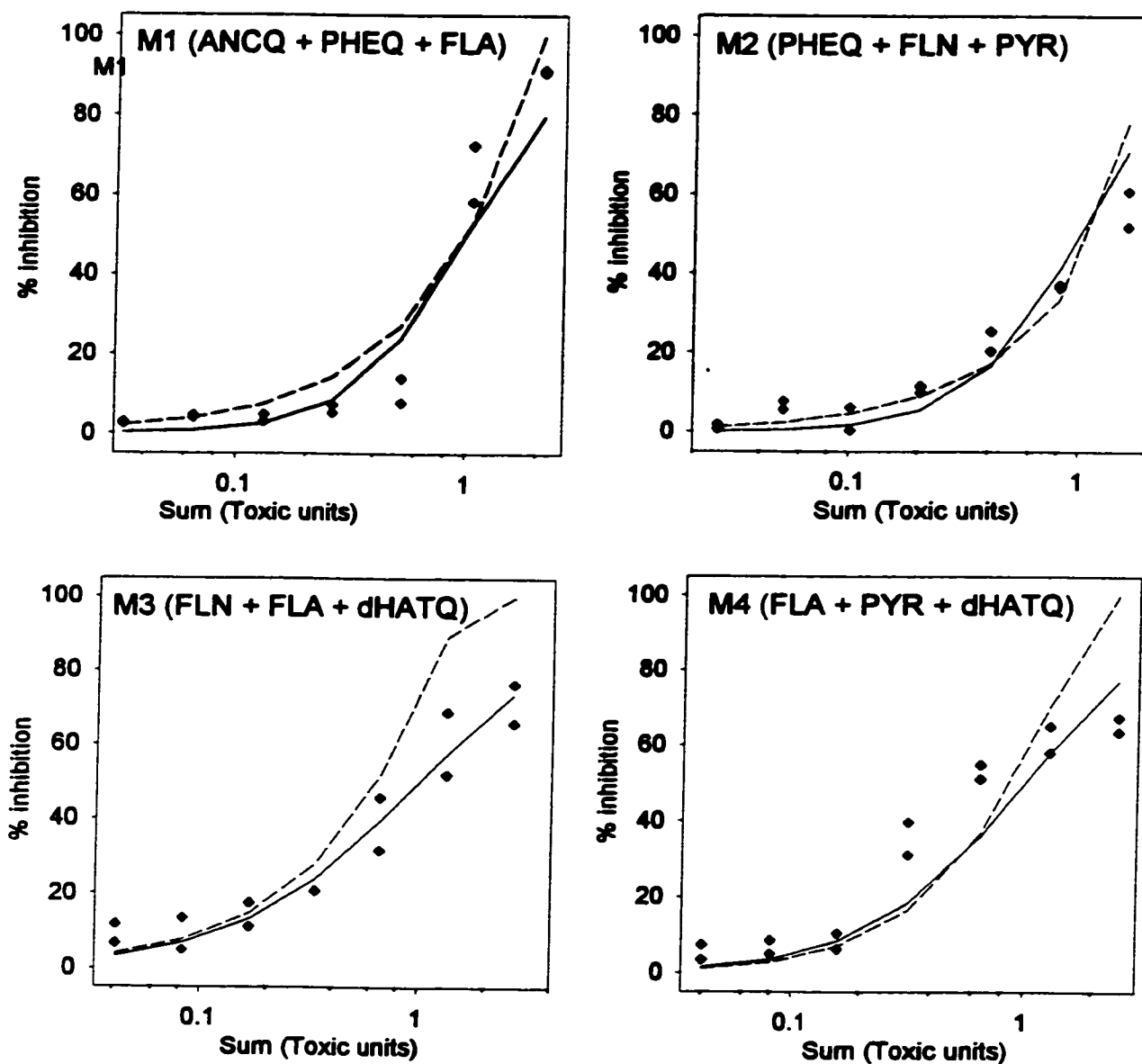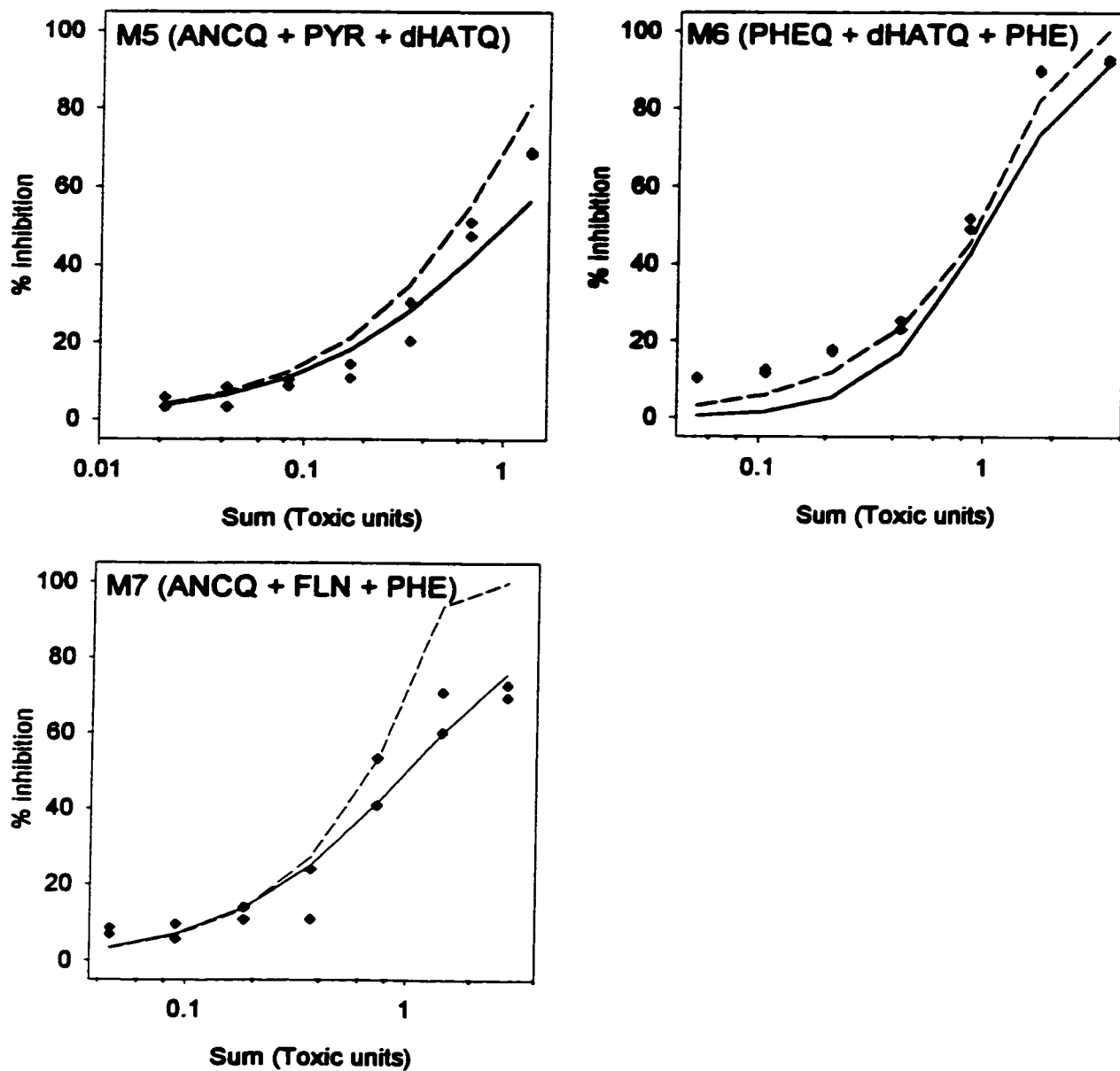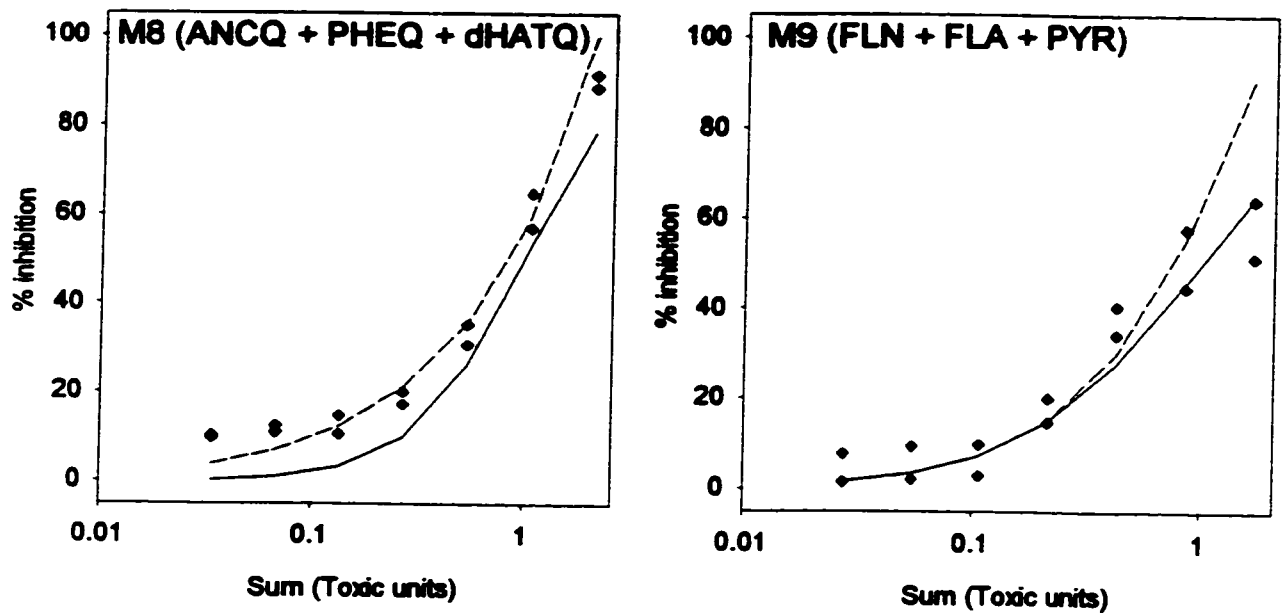
Figure 7.3: Percent light inhibition of *P. phosphoreum*, exposed to mixtures M8 and M9. See Table 1 for mixture concentrations. The solid line is the toxicity predicted by a concentration addition model, and the dashed line is the toxicity predicted by a response addition model. The predictive models are based on the single chemical data only.

the highest concentration level. Mixture M3 was an excellent fit to the concentration addition model, whereas the response addition model overestimates the response somewhat. The response of mixture M4 was interesting, in that there appear to be two simultaneous deviations from the models. The response at higher concentrations is less than predicted, and approaches a maximum inhibition of approximately 70%. The other notable effect is an increase of about 10 to 20% inhibition over the expected response at two of the intermediate doses.

The toxicity of mixtures M5, M6, and M7, and the effect estimated by the response and concentration additive models was determined (Figure 7.2). Both models were reasonable predictors of the observed effect for each mixture. In M6, the RA model was slightly closer to the observed responses. For M7, the concentration additive model was a slightly better predictor. For mixtures M8 and M9 (Figure 7.3), both models were reasonable predictors of effect. For M8 the response additive model is a slightly better fit. Each response was approximately 10% higher than the concentration additive model; one possible cause is a small decrease in the light output of the controls, rather than a consistent increase at all other dose levels.

With the possible exception of mixture M4, there were no apparent large deviations from the response predicted by the additive models in Figures 7.1-7.3. The concentration additive model appears to be a slightly better fit in several cases. On this basis, the concentration additive model was selected to make investigate potential deviations from additivity. The calculated $EC_{50}s$ of the mixtures, expressed as toxic units, will be used as the basis for comparison. The single chemical data was used to estimate the expected toxic units contribution of each chemical to the toxicity of the mixtures, and the EC_{50} of each mixture was expressed as a sum of toxic units. The expected EC_{50} for all mixtures is predicted to occur at $\Sigma TU = 1.0$. The deviation of the experimentally determined responses from the model predictions is shown in Figure 7.4. No large deviations of $EC_{50}s$ were apparent in Figure 7.4, though the predicted response was underestimated in 12 of the 18 mixtures.

A statistical analysis of the EC_{50} data set was performed, approximating the method described in Chapter 6. To determine if there was a net average deviation of the mixtures from the concentration additive model, the average of all $EC_{50}s$, expressed as toxic units, was compared to $\Sigma TU=1.0$.
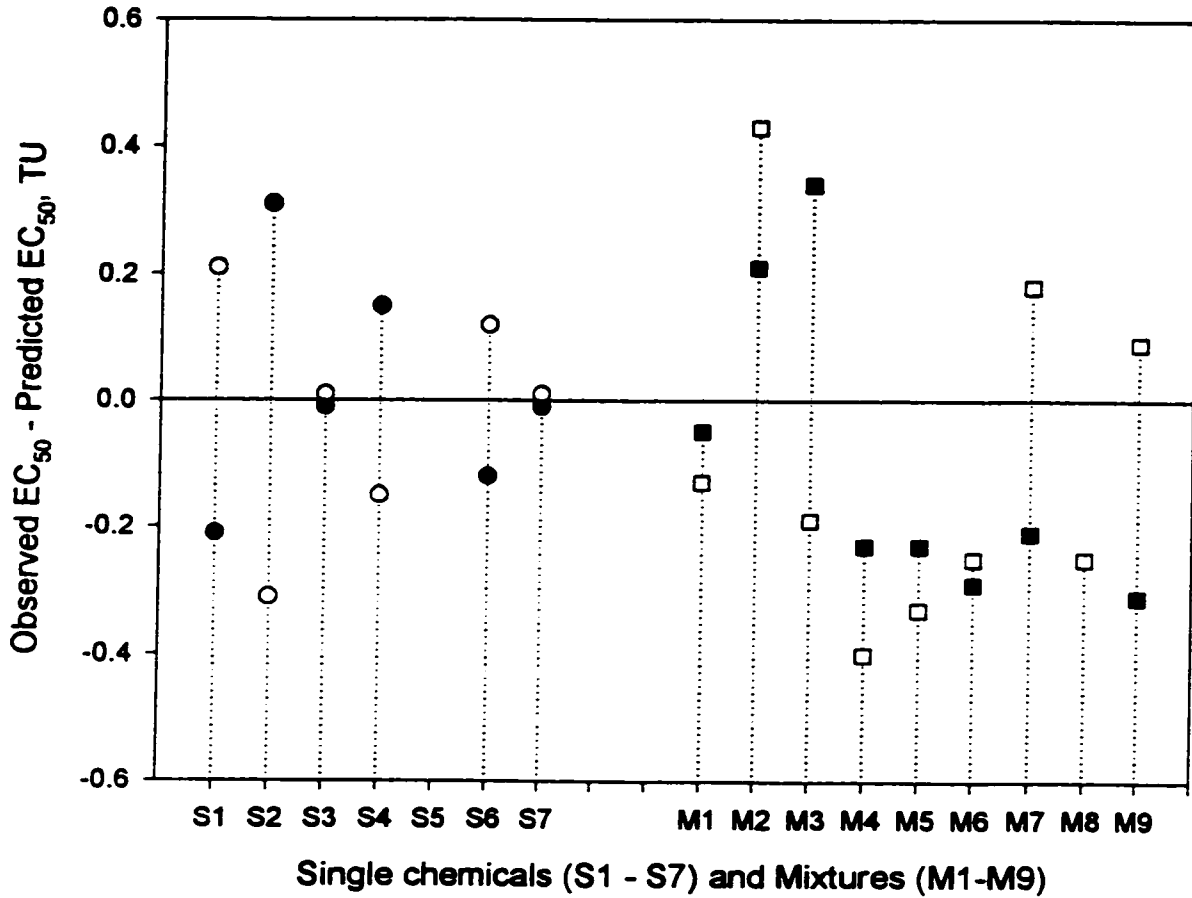
Figure 7.4: EC_{50} residuals (observed - predicted) for concentration additive model. Single chemical data were used to generate the toxic units for each chemical and the model.; Mixture EC_{50}s were compared to model predictions and deviations from the model plotted. There were no significant deviations from the additive model in this data set.

The average EC_{50} was 0.896 TU, with a 95% confidence interval of (0.774, 1.019). As the confidence interval overlapped TU=1.0, the observed greater than additive effect was not significant at a level p=0.05.

Model 7.10 was used to determine if any individual components were causing non-additive effects within the mixtures. The first model fit included the sum of toxic units (the concentration additive model) plus 7 interaction terms. A p-value of 0.05 was used as a criterion for inclusion in the model. It should be noted that p-values used in this manner, while useful for determining relative contributions of model terms, do not provide exact estimates of statistical significance. One term, $\beta_{FLN}^{(2)} = 1.10$ (p = 0.022), was significant when all seven interaction terms were included in the model. However, once non-significant interaction terms were excluded from the model, this term was no longer significant (p=0.457). The next model fit used included the sum of toxic units, plus one interaction term from model 7.10 for all seven terms in sequence (Table 7.3). None of the interaction terms were significant in isolation. Three terms, $\beta_{ANCQ}^{(2)}$, $\beta_{dHATQ}^{(2)}$, and $\beta_{PHE}^{(2)}$ were significant at a level of p < 0.10, but not at the set inclusion limit of p < 0.05. All of the interaction terms except one were also less than zero, indicating a greater than additive, but non-significant, effect for six of seven compounds within the mixtures. Thus, while there is some evidence that there may be some interactions occurring, none were significant within the variance estimate of the experimental system and degree of replication used. Thus, the concentration additive model was a reasonable descriptor of the entire data set.

7.4 DISCUSSION

Mixtures of chemicals were prepared according to a {7,3} fractional simplex design, and tested with the *P. phosporeum* assay. The purpose of this was two-fold: to test for the presence of significant deviations within this set of components, and to illustrate the application of fractional simplex designs to toxicological problems. The seven individual chemicals tested inhibited the production of light output of *P. phosphoreum*, with the exception of pyrene, for which no effect was observed. EC_{50}s and slope parameters were estimated for each of the chemicals (except pyrene). Comparing the EC_{50}s, the

134

Table 7.3. Estimates of interaction coefficients for the concentration additive model, plus one interaction term. In each case, the model used included one interaction parameter for non-additive action of a given mixture component.

Model	Interaction Coefficient, β_i	Standard Error	p (2-tail)
$Y = \Sigma TU_j + \beta_i^{(2)} TU_i(1-TU_i) + \varepsilon$, where			
i = ANCQ	-1.0532	0.5186	0.0582
i = PHEQ	-5.4192	4.0927	0.2030
i = FLN	0.3090	0.4056	0.4566
i = FLA	-0.4674	0.3858	0.2424
i = PYR	-0.0962	0.0921	0.3105
i = dHATQ	-0.7981	0.3815	0.0517
i = PHE	-0.8204	0.4097	0.0614

toxicity estimates may be placed into two groups based on respective potencies. The first group contains chemicals with measured EC_{50}s between 1 and 10 mg/L, and includes all chemicals tested except PHEQ. For very hydrophobic chemicals such as PAHs, this range of EC_{50} is consistent with a non-polar narcosis mode of action (McCarty et al. 1992; Rand et al. 1995). It should be noted that this does not preclude these chemicals from contributing to other possible modes of action as well. The second potency group contained one chemical, PHEQ, which exhibited potency 5 times greater than the next most toxic chemical tested. The slope of the response curve was also greater for PHEQ than for any of the other toxicants, further implying a different mode of action (Calabrese 1991). This is consistent with existing literature on PHEQ, which is known to be a redox cycling agent (Hasspieler and Di Giulio 1994; Di Giulio et al. 1995). While the modes of action of chemicals within organisms are not mutually exclusive, the identification of dominant modes of action can be useful in the interpretation of mixture interactions. Chemicals acting by the same mode of action would be most likely to follow a concentration additive model, whereas chemicals acting by different modes of action would most likely follow a response addition model (Calabrese 1991; Pöch et al. 1996).

Due to the shallow slopes of response typical in the *P. phosphoreum* assay, there was not a large distinction between the concentration additive and response additive models. Thus, this assay may

not be readily used to distinguish between these two types of interaction. It may instead be applied to screen for interactions greater or less than that predicted by either of the additive models, such as synergism and antagonism. A qualitative interpretation of this data set suggests that both models were reasonable descriptors of the data set, but the concentration additive model was a slightly better fit than the response additive model.

If it is assumed that ACNQ, dHATQ, PHE, FLN, FLA, and PYR all act by the same dominant mechanism, it would be expected that these chemicals would follow a concentration additive scenario, and could be treated as different forms of the same toxicant. PHEQ, with a different mode of action, would be expected to interact with this set of toxicants according to response addition. The concentration additive model provided a good description of the data set. On statistical testing of the EC_{50}s, no significant deviations from additivity were found, validating the use of a concentration additive model for this particular set of chemicals tested with this organism. There was a trend to greater than additive action found with 6 of the 7 chemicals, but the effect was not large enough to be statistically significant with the degree of replication used.

One effect that occurred in several of the single and mixture data sets was an upper limit in the observed response, attributed to the solubility of the some chemicals tested. PAHs are only sparingly soluble in water, and although DMSO increases the effective solubility, above a certain concentration the chemical will precipitate from aqueous media. This reduces the concentration of chemical to which the organism is exposed, and so limits the maximum response. This was seen with PYR (no response), in the highest concentrations of PHE, FLA, FLN, and ACNQ, and in mixtures M4, M7, and M9. This may account for the increase in response seen in mixture M4 as well - at intermediate concentrations, PAHs may be less likely to precipitate out of solution if there are several present. This would increase the effective concentration of PAH in solution, and the organism would show a correspondingly greater response. If this is the case, it has environmental implications - having many PAHs present may increase the proportional solubility of the PAHs and hence increase the bioavailability. This suggests that the biological impact of PAHs could be greater than estimated from single PAH assays, if PAHs are present in a mixture.

136

This chapter has illustrated one possible means of applying a fractional simplex design to toxicant mixtures. The toxicants are tested in equipotent mixtures at various levels in a constant ratio of components. The resultant data set is compared to a predictive model, and deviations (if any) are identified. The graphical interpretation presented here is also useful in discussing interactions of the toxicants in question. Statistical treatments of the data may be done at several response levels as well. Comparison of a given response level across all mixtures and single chemicals, as was done with $EC_{50}s$, is useful to directly determine types of interaction. A more mathematical albeit less intuitive approach is to model the response at all dose levels, incorporating terms for slope deviations. The slope deviations would be tested similarly to the EC_{50} parameters. Due to the non-linear nature of dose response curves, statistics appropriate to non-linear data could be used. Of particular appeal is a bootstrap confidence interval for hypothesis testing at given dose levels, as the bootstrap procedure is readily done with existing computer programs (Efron and Tibshirani 1986; Wilkinson 1998).

Fractional simplex designs can provide an empirical assessment of toxicological interactions, and test the applicability of simple models to approximate effect. These designs can also be used in conjunction with models based on theoretical considerations, such as physiologically based pharmacokinetic models, and provide a basis for testing and parameter estimation within these models.

8.0 General Conclusions

PAHs are recognized as important environmental contaminants. Their occurrence is widespread, and the major sources of PAHs are anthropogenic. They exist in environmental compartments almost exclusively as mixtures of many PAHs, and often with other contaminants present as well. They can act as toxicants to organisms via several modes of action, any one of which can be the predominant mode, depending on the organism and its environment. PAHs are also a human health issue, due to their carcinogenic potential. Overall the biological impact of PAHs is a complex problem; there are not only many possible effects, but also many possible causative agents.

The photooxidation of PAHs has been shown to increase the toxicity of PAHs in solution dramatically, and in this thesis some of the products responsible for the observed increase in toxicity were identified. Each of the PAHs investigated in detail (napthalene, phenanthrene, and benzo(a)pyrene) were found to form products that were more toxic than the parent compounds. On reference to the literature, it was found that several of these products could act as redox cycling agents, leading to oxidative stress within an organism. Several products were also identified previously as products of PAH metabolism, and have carcinogenic activity. It was shown here that active carcinogens could also be formed via photoreactions, without requiring metabolic activation.

The relative stability of PAHs and PAH photoproducts was addressed, as it has important implications for environmental concentrations and persistence. The results were not consistent for all photoproducts; some were more stable than the parent PAH, some were less so. Thus some photoproducts are likely to accumulate in environmental compartments, while others will be rapidly degraded. Further oxidation of photoproducts will result in the formation of substituted benzenes and naphthalenes, some of which are inherently resistant to photooxidation as they do not absorb light of the wavelengths present in sunlight.

Given that PAH photoproducts have been found to be toxic in a laboratory setting, the question remains as to whether or not they have significant impact in environmental

compartments. It is almost a certainty that they do under some circumstances, and this possibility is currently being investigated by members of the Greenberg and Dixon laboratories. PAH photoproducts are likely to have a significant toxic impact if PAHs have had exposure to sunlight for a period of time prior to or concurrent with release to the environment. While PAH photoproducts have been found in sediments, it is unlikely that they will accumulate there as light penetration into sediment is minimal. The products of PAH oxidation are more water soluble, and will thus be quickly lost to the overlying water. The result is that while some photooxidation may occur, the soluble products will not stay in the sediment. If the overlying water is shallow and has no outlet, it is possible that oxidation products will accumulate in the water column. A more likely scenario for PAH oxidation product toxicity is that of road run-off or heavy boat traffic on a water body. In the case of road run-off, the PAHs are exposed to full sunlight, and the oxidation products formed will be washed away by rain. The run-off is likely to contain a high concentration of the more water-soluble products. Similarly, boat traffic can introduce PAHs to the uppermost layer of the water column, where they will readily photooxidise. During light exposure some the PAHs can also act a photosensitisers and be highly toxic. The photoproducts can be toxic as well, and the toxicity of the products is no longer dependent upon light activation.

A shortfall identified in the literature was the lack of methods for determining interactions within mixtures. This is highly relevant to PAH and PAH oxidation product toxicity, as PAHs and even the oxidation products of a single PAH occur as mixtures. An idea on how to address mixture interactions without extensive testing was developed, and resulted in the creation of 'fractional simplex designs'. These designs may be used to assess models of interaction, as well as screening for interactions within a mixture. The toxicity of a mixture of PAHs and PAH photoproducts was tested using a fractional simplex design, and the interactions found to be consistent with an additive model of interaction, within the sensitivity limits of the assay used. It is hoped that the generated designs will find use in the environmental assessment of mixtures, and possibly in other fields of study as well.

9.0 REFERENCES

Andelman, J. B. and M. J. Suess (1971). The photodecomposition of 3,4-benzpyrene sorbed on calcium carbonate. Organic Compounds in Aquatic Environments. S. J. Faust and J. V. Hunter. New York, Marcel Dekker: 439-468.

Andino, J. M., J. N. Smith, R. C. Flagan, W. A. Goddard, III and J. H. Seinfeld (1996). "Mechanism of atmospheric photooxidation of aromatics: A theoretical study." Journal of Physical Chemistry 100: 10967-10980.

Ankley, G. T., S. A. Collyard, P. D. Monson and P. A. Kosian (1994). "Influence of ultraviolet light on the toxicity of sediment contaminated with polycyclic aromatic hydrocarbons." Environ. Toxicol. Chem. 13: 1791-1796.

Arey, J., W. P. Harger, D. Helmig and R. Atkinson (1992). "Bioassay-directed fractionation of mutagenic PAH atmospheric photooxidation products and ambient particulate extracts." Mutat. Res. 281: 67-76.

Arfsten, D. P., D. J. Schaeffer and D. C. Mulveny (1996). "The effects of near ultraviolet radiation on the toxic effects of polycyclic aromatic hydrocarbons in animals and plants: A review." Ecotoxicology and environmental safety 33: 1-24.

Bagchi, D., M. Bagchi, J. Balmoori, P. J. Vuchetich and S. J. Stohs (1998a). "Induction of oxidative stress and DNA damage by chronic administration of naphthalene to rats." Res Commun Mol Pathol Pharmacol 101(3): 249-57.

Bagchi, M., D. Bagchi, J. Balmoori, X. Ye and S. J. Stohs (1998b). "Naphthalene-induced oxidative stress and DNA damage in cultured macrophage J774A.1 cells." Free Radic Biol Med 25(2): 137-43.

Barbas, J. T., M. E. Sigman, A. C. Buchanan, III and E. A. Chevis (1993). "Photolysis of substituted naphthalenes on silicon dioxide and aluminum trioxide." Photochem Photobiol 58(2): 155-158.

Basu, D. K. and J. Saxena (1978). "Polynuclear aromatic hydrocarbons in selected US drinking waters and their raw water sources." Environ. Sci. Technol. 12: 795-798.

Baumann, P. C. (1989). PAH metabolites and neoplasia in feral fish populations. Metabolism of polycyclic aromatic hydrocarbons in the aquatic environment. U. Varanasi. Boca Raton, FL, CRC Press: 269-290.

Berenbaum, M. C. (1985). "The expected effect of a combination of agents: the general solution." *J Theor Biol* 114(3): 413-31.

Billington, J. W., G.-L. Huang, F. Szeto, W. Y. Shiu and D. MacKay (1988). "Preparation of aqueous solutions of sparingly soluble organic substances: I. Single component systems." *Environ. Technol. Chem* 7: 117-124.

Bliss, C. I. (1939). "The toxicity of poisons applied jointly." *Ann. Appl. Biol.* 26: 585-615.

Borneff, J., F. Selinka, H. Kunte and A. Maximomos (1968). "Experimental studies on the formation of polycyclic aromatic hydrocarbons in plants." *Environ. Res.* 2: 22-29.

Bowling, J. W., G. J. Leversee, P. F. Landrum and J. P. Giesy (1983). "Acute mortality of anthracene-contaminated fish exposed to sunlight." *Aquat. Toxicol* 3: 79-90.

Boxall, A. B. and L. Maltby (1997). "The effects of motorway runoff on freshwater ecosystems: 3. Toxicant confirmation." *Arch Environ Contam Toxicol* 33(1): 9-16.

Bucheli, T. D. and K. Fent (1995). "Induction of cytochrome P450 as a biomarker for environmental contamination in aquatic ecosystems." *Crit. Rev. Environ. Sci. Technol.* 25: 201-268.

Buhler, D. R. and D. E. Williams (1989). Enzymes involved in metabolism of PAH by fishes and other aquatic animals: oxidative enyzmes (or phase I enzymes). *Metabolism of polycyclic aromatic hydrocarbons in the aquatic environment.* U. Varanasi. Boca Raton, FL, CRC Press: 151-184.

Bulich, A. A. (1986). Bioluminescence Assays. *Toxicity Testing Using Microorganisms.* G. Bitton and B. J. Dutka. Boca Raton, FL, CRC Press Inc. 1: 57-74.

Calabrese, E. J. (1991). *Multiple Chemical Interactions.* Chelsea, MI, Lewis Publishers, Inc.

Cassee, F. R., J. P. Groten, P. J. van Bladeren and V. J. Feron (1998). "Toxicological evaluation and risk assessment of chemical mixtures." *Crit Rev Toxicol* 28(1): 73-101.

Chesis, P. L., D. E. Levin, M. T. Smith, L. Ernster and B. N. Ames (1984). "Mutagenicity of quinones: pathways of metabolic activation and detoxification." *Proc. Nat. Acad. Sci. USA* 81: 1696-1700.

Cody, T. E., M. J. Radike and D. Warshawsky (1984). "The phototoxicity of Benzo[a]pyrene in the green alga *Selenastrum capricornutum.*" *Environ. Res.* 35: 122-132.

Cook, R. H., R. C. Pierce, P. B. Eaton, R. C. Lao, F. I. Onuska, J. F. Payne and E. Vavasour (1983). Polycyclic aromatic hydrocarbons in the aquatic environment: formation, sources, fate and effects on aquatic biota. Ottawa, ON Canada., National Research Council of Canada.

Cornell, J. A. (1990). Experiments with Mixtures. Toronto, Wiley-Interscience.

David, B. and P. Boule (1993). "Phototransformation of Hydrophobic Pollutants in Aqueous Medium I- PAHs Adsorbed on Silica." Chemosphere 26(9): 1617-1630.

Davila, D. R., B. J. Mounho and S. W. Burchiel (1997). "Toxicity of polycyclic aromatic hydrocarbons to the human immune system: Models and mechanisms." Toxicol. Environ. News 4(1): 5-9.

De Guise, S., A. Lagacé and P. Béland (1994). "Tumors in St. Lawrence beluga whales (Delphinapterus leucas)." Vet. Pathol. 31: 444-449.

Di Giulio, R. T., W. H. Benson, B. M. Sanders and V. E. P.A. (1995). Biochemical mechanisms: Metabolism, Adaptation, and Toxicity. Fundamentals of aquatic toxicology: Effects, environmental fate, and risk assessment, 2nd. Ed. G. M. Rand. Washington, D.C., Taylor and Francis.

Doherty, M. D., G. M. Cohen and M. T. Smith (1984). "Mechanisms of toxic injury to isolated hepatocytes by 1-naphthol." Biochem Pharmacol 33(4): 543-9.

Duxbury, C. L., D. G. Dixon and B. M. Greenberg (1997). "Effects of simulated solar radiation on the bioaccumulation of polycyclic aromatic hydrocarbons by the duckweed Lemna gibba." Environ. Toxicol. Chem. 16(8): 1739-1748.

Eadie, B. J. (1984). Distribution of polycyclic aromatic hydrocarbons in the Great Lakes. Advances in Environmental Science and Technology. J. O. Nriagu and M. S. Simmons. New York, NY, Wiley. 14: 195-211.

Edwards, N. T. (1983). "Polycyclic Aromatic Hydrocarbons (PAHs) in the terrestrial environment." J. Environ. Qual. 12(4): 427-441.

Efron, B. and R. Tibshirani (1986). "Bootstrap methods for standard errors, confidence intervals, and other measures of statistical accuracy." Statistical Science 1: 54-77.

England, P. A., C. F. Harford-Cross, J.-A. Stevenson, D. A. Rouch and L.-L. Wong (1998). "The oxidation of Naphthalene and pyrene by cytochrom P450cam." Febs Letters 424(3): 271-274.

142

Environment_Canada (1993). Toxicity testing using luminescent bacteria *(Photobacterium phosphoreum)*. Ottawa, ON Canada, Environmental Protection Publications.

Environment_Canada (1994). Priority Substances List Assessment Report: Polycyclic aromatic hydrocarbons. Ottawa, ON, Environment Canada: 61.

Fay, R. M. and V. J. Feron (1996). "Complex mixtures: hazard identification and risk assessment." Food Chem Toxicol 34(11-12): 1175-6.

Feron, V. J., J. P. Groten, D. Jonker, F. R. Cassee and P. J. van Bladeren (1995). "Toxicology of chemical mixtures: challenges for today and the future." Toxicology 105(2-3): 415-27.

Feron, V. J., J. P. Groten and P. J. van Bladeren (1998). "Exposure of humans to complex chemical mixtures: hazard identification and risk assessment." Arch Toxicol Suppl 20: 363-73.

Flowers-Geary, L., W. Bleczinki, R. G. Harvey and T. M. Penning (1996). "Cytotoxicity and mutagenicity of polycyclic aromatic hydrocarbon ortho- quinones produced by dihydrodiol dehydrogenase." Chem Biol Interact 99(1-3): 55-72.

Forstner, H. J. L., R. C. Flagan and J. H. Seinfeld (1997). "Secondary organic aerosol from the photoxidation of aromatic hydrocarbons: Molecular composition." Environmental Science and Technology 31(5): 1345-1358.

Fort, D. J., E. L. Stover, T. Propst, M. A. Hull and J. A. Bantle (1998). "Evaluation of the developmental toxicities of coumarin, 4- hydroxycoumarin, and 7-hydroxycoumarin using FETAX." Drug Chem Toxicol 21(1): 15-26.

French, A. P. and E. F. Taylor (1978). An Introduction to Quantum Physics. New York, N.Y., W.W.Norton and Company, Inc.

Gala, W. R. and J. P. Giesy (1992). "Photo-induced toxicity of Anthracene to the Green Alga, Selenastrum capricornutum." Arch. Environ. Contam. Toxicol.

Gilbert, A. and J. Baggott (1991). Essentials of molecular photochemistry. Boca Raton, FL, CRC Press, Inc.

Graf, W. and H. Diel (1966). "Concerning the naturally caused normal level of carcinogenic polycyclic aromatic hydrocarbons and its cause." Arch. Hyg. 150: 49-59.

Greenberg, B. M., D. G. Dixon, M. I. Wilson, X.-D. Huang, B. J. McConkey, C. L. Duxbury, K. A. Gerhardt and B. Gensemer (1995). Use of artificial lighting in environmental assessment studies. Environmental Toxicology and Risk Assessment ASTM STP 1262. T. W. LaPoint, F. T. Price and E. Little. Philadelphia, PA., American Society for Testing and Materials. 4.

Greenberg, B. M., X.-D. Huang and D. G. Dixon (1992). "Applications of the aquatic higher plant *Lemna gibba* for ecotoxicological assessment." Journal of Aquatic Ecosystem Health 1: 147-155.

Greenberg, B. M., X.-D. Huang, D. G. Dixon, L. Ren, B. J. McConkey and C. L. Duxbury (1993). Quantitative structure activity relationships for the photoinduced toxicity of polycyclic aromatic hydrocarbons to duckweed- a preliminary model. Environmental Toxiciology and Risk Assessment: 2nd Volume ASTM STP 1216. J. W. Gorsuch, F. J. Dwyer, C. G. Ingesoll and T. W. L. Point. Philadelphia, PA, American Society for Testing and Materials: 369-378.

Griem, P., M. Wulferink, B. Sachs, J. B. Gonzalez and E. Gleichmann (1998). "Allergenic and autoimmune reactions: How do they arise?" Immunol. Today 19(3): 133-141.

Hall, A. T. and J. T. Oris (1991). "Anthracene reduces reproductive potential and is maternally transferred during long-term exposure in fathead minnows." Aquat. Toxicol. 19: 249-264.

Hartman, P. E. and M. A. Goldstein (1989). "Superoxide generation by photomediated redox cycling of Anthraquinones." Environmental and Molecular Mutagenesis 14: 42-47.

Hasspieler, B. M. and R. T. Di Giulio (1994). "Dicoumarol-sensitive NADPH: phenanthrenequinone oxidoreductase in channel catfish (*Ictalurus punctatus*)." Toxicol. Appl. Pharmacol. 125: 184-191.

Hausen, B. M. and M. Schmieder (1986). "The Sensitizing Capacity of Coumarins I." Contact Dermatitis 15(3): 157-163.

Heisenberg, W. (1926). Z. Phys. 39: 499 (as cited in French and Taylor).

Hewlett, P. S. (1969). "Measurement of the potencies of drug mixtures." Biometrics 22: 477-487.

Hoeke, H. and R. Zellerhoff (1998). "Metabolism and toxicity of diisopropylnaphthalene as compared to naphthalene and monoalkyl nalphthalenes: A minireview." Toxicology 126(1): 1-7.

Holst, L. L. and J. P. Giesy (1989). "Chronic effects of the photo enhanced toxicity of anthracene on *Daphnia magna* reproduction." Environ. Toxicol. Chem. 8: 933-942.

Huang, X. D., D. G. Dixon and B. M. Greenberg (1995). "Toxicity of polycyclic aromatic hydrocarbons to the duckweed *Lemna gibba* L. G-3 in natural sunlight." Ecotoxicol. Environ. Saf. **32**: 194-200.

Huang, X.-D., D. G. Dixon and B. M. Greenberg (1993). "Impacts of UV radiation and photomodification on the toxicity of PAHs to the higher plant *Lemna gibba* (duckweed)." *Environ. Toxicol. Chem* **12**: 1067-1077.

Huang, X.-D., S. N. Krylov, L. Ren, B. J. McConkey, D. G. Dixon and B. M. Greenberg (1997). "Mechanistic Quantitative Structure-Activity Relationship Model for The Photoinduced Toxicity of Polycyclic aromatic Hydrocarbons: II. An empirical model for the toxicity of 16 poycyclic aromatic hydrocarbons to the duckweed Lemna gibba L. G-3." Envron. Toxicol. Chem. **16**(11): 2296-2303.

Huang, X.-D., B. J. McConkey, T. S. Babu and B. M. Greenberg (1997). "Mechanisms of photoinduced toxicity of photomodified anthracene to plants: inhibition of photosynthesis in the aquatic higher plant *Lemna gibba* (duckweed)." Environ. Toxicol. Chem. **16**(8): 1707-1715.

Jacobs, M. W., J. A. Coates, J. J. Delfino, G. Bitton and W. M. Davis (1993). "Comparison of Sediment Extract Microtox with Semi-Volatile Organic Priority Pollutant Concentrations." Arch. Environ. Contam. Toxicol. **24**: 461-468.

Jones, K. C., J. A. Stratford, P. Tidridge, K. S. Waterhouse and A. E. Johnson (1989). "Polynuclear aromatic hydrocarbons in an agricultural soil: Long-term changes in profile distribution." Environ. Pollut. **56**: 337-351.

Jordan, V. C. (1994). "Biochemical pharmacology of antiestrogen action." Pharmacol. Rev. **38**: 245-276.

Karcher, W., Ed. (1988). Spectral atlas of polycylic aromatic hydrocarbons. Hingham, MA, Kluwer Academic Publishers.

Karcher, W., R. J. Fordham, J. J. Dubois, P. G. J. M. Glaude and J. A. M. Ligthart, Eds. (1985). Spectral atlas of polycylic aromatic hydrocarbons. Hingham, MA, Kluwer Academic Publishers.

Karrow, N. A. (1998). Chemical mixture immunotoxicity to rainbow trout. Department of Biology. Waterloo, ON, University of Waterloo: 176.

Katz, M., C. Chan, H. Tosine and T. Sakuma. (1979). Relative rates of photochemical and biological oxidation (in vitro) of polynuclear aromatic hydrocarbons. Polynuclear Aromatic Hydrocarbons. P. W. Jones and P. Leber. Ann Arbor, MI, USA, Ann Arbor Science: 171-189.

Kawabata, T. T. and K. L. White, Jr. (1990). "Effects of naphthalene and naphthalene metabolites on the in vitro humoral immune response." J Toxicol Environ Health 30(1): 53-67.

Kawamura, K., I. Suzuki, Y. Fujii and O. Watanabe (1994). "Ice core record of polycyclic aromatic hydrocarbons over the past 400 years." Naturwissenschaften 81: 502-505.

Klein, A. E. and N. Pilpel (1974). J. Chem Soc. Faraday Trans. 70: 1250-1256.

Kodell, R. L. and J. G. Pounds (1988). Assessing the toxicity of mixtures of chemicals. Statistical methods in toxicological research. D. Krewswki and C. Franklin.

Kosian, P. A., E. A. Makynen, P. D. Monson, D. R. Mount, A. Spacie, O. G. Mekenyan and G. A. Ankley (1998). "Application of toxicity based fractionation techniques and structure-activity relationship models for the identification of phototoxic polycyclic aromatic hydrocarbons in sediment pore water." Environmental Toxicology and Chemistry 17(6): 1021-1033.

Krylov, S. N., X.-D. Huang, L. F. Zeiler, D. G. Dixon and B. M. Greenberg (1997). "Mechanistic Quantitative Structure-Activity Relationship Model for The Photoinduced Toxicity of Polycyclic aromatic Hydrocarbons: I. Physical model based on chemical kinetics in a two compartment system." Envron. Toxicol. Chem. 16(11): 2283-2295.

Kuehl, R. O. (1994). Statistical principles of research design and analysis. Belmont CA, Duxbury Press.

Landahl, J. T., B. B. McCain, M. S. Myers, L. D. Rhodes and D. W. Brown (1990). "Consistent association between hepatic lesions in English sole (Parophrys vetulus) and polycyclic aromatic hydrocarbons in bottom sediment." Environ. Health Perspect. 89: 195-203.

Landis, W. G. and M.-H. Yu (1995). Introduction to Environmental Toxicology: impacts of chemicals upon ecological systems. New York, NY, Lewis Publishers.

Landrum, P. F., J. P. Giesy, J. T. Oris and P. M. Allred (1986). Photoinduced toxicity of polycyclic aromatic hydrocarbons to aquatic organisms. Oil in fresh water: Chemistry, biology, technology. J. H. Vandermeulen and S. Hrudy. Elmsford, NY, Permagon Press: 324-328.

Legzdins, A. E., B. E. McCarry, C. H. Marvin and D. W. Bryant (1995). "Methodology for Bioassay-diected Fractionation Studies of Air Particulate Material and Other Complex Environmental Matrices." Intern. J. Environ. Anal. Chem. 60: 79-94.

Lesko, S. A. and R. J. Lorentzen (1985). "Benzo[a]pyrene dione-benzo[a]pyrene diol oxidation-reduction couples; involvement in DNA damage, cellular toxicity, and carcinogenesis." J Toxicol Environ Health 16(5): 679-691.

Lesko, S. A., L. Trpis and R. Zheng (1986). "Somatic mutation, DNA damage and cytotoxicity induced by benzo[a]pyrenedione/benzo[a]pyrenediol redox couples incultured mammalian cells." Mutation Research 161(2): 173-180.

Lipnick, R. L. (1995). Structure-activity relationships. Fundamentals of Aquatic Toxicology: Effects, Environmental Fate, and Risk Assessment, 2nd Edition. G. M. Rand. Washington, DC', Taylor and Francis: 1125.

Livingstone, D. R., M. A. Kirchin and A. Wiseman (1989). "Tissue and subcellular distribution of enzyme activities of mixed-function oxygenase and benzo[a]pyrene metabolism in the common mussel Mytilus edulis." Sci. Tot. Environ. 39: 209-235.

Loewe, S. (1953). "The problem of synergism and antagonism of combined drugs." Arzneim. Forsh. 3: 285-290.

Lorentzen, R. J., S. A. Lesko, K. McDonald and P. O. Ts'o (1979). "Toxicity of metabolic benzo(a)pyrenediones to cultured cells and the dependence on molecular oxygen." Cancer Research 39(8): 3194-3198.

Mackay, D. and W. Y. Shiu (1977). "Aqueous solubility of polynuclear aromatic hydrocarbons." J. Chem. Eng. Data 22: 399.

Malins, D. C., B. B. McCain, M. S. Myers, D. W. Brown, M. M. Krahn, S. L. Chan and W. T. Roubal (1988). "Neoplastic and other diseases in fish in relation to toxic chemicals: an overview." Aquat. Toxicol 11: 43-67.

Malkin, J. (1992). Photophysical and photochemical properties of aromatic compounds. Boca Raton, FL, CRC Press.

Mallakin, A., D. G. Dixon and B. M. Greenberg (1999). "Pathway of anthracene modification under simulated solar radiation." Chemosphere 00: 000-000 (accepted for publication).

Marking, L. L. (1977). Methods for Assessing Additive toxicity of Chemical mixtures. Aquatic Toxicology and Hazard Evaluation ASTM STP 634. F. L. Mayer and J. L. Hamelink: 99-108.

Marshall, C. J., K. H. Vousden and D. H. Phillips (1984). "Activation of c-Ha-*ras*-1 protooncogene by in vitro modification with a chemical carcinogen, benzo(a)pyrene diol epoxide." Nature 310: 586-589.

Matsuura, T., R. Sugae, R. Nakashima and K. Omura (1968). "Photoinduced reactions- XVI. Photopinacolization of tricycloketoindane derivatives." Tetrahedron 24: 6149-6156.

McCarty, L. S., D. Mackay, A. D. Smith, G. W. Ozburn and D. G. Dixon (1992). "Residue-based interpretation of toxicity and bioconcentration QSARs from aquatic bioassays: neutral narcotic organics." Environ. Toxicol. Chem. 11: 917-930.

McConkey, B. J., D.G. Dixon and B. M. Greenberg (1993). Photodegradation pathways of selected polycyclic aromatic hydrocarbons exposed to solar radiation. Ontario Ministry of the Environment and Energy. Tech. Transfer Conference, Toronto, ON.

McConkey, B. J., C. L. Duxbury, D. G. Dixon and B. M. Greenberg (1997). "Toxicity of a PAH photooxidation Product to the Bacteria *Photobacterium phosphoreum* and the Duckweed *Lemna gibba*: Effects of Phenanthrene and its primary Photoproduct, Phenathrenequinone." Environ Toxicol. Chem. 16(5): 892-899.

Meehan, T., A. R. Wolfe, G. R. Negrete and Q. Song (1997). "Benzo[a]pyrene diol epoxide-DNA cis adduct formation through a trans chlorohydrin intermediate." Proc Natl Acad Sci U S A 94(5): 1749-54.

Menzer, R. E., M. A. Lewis and A. Fairbrother (1994). Methods in Environmental Toxicology. Principles and Methods of Toxicology, 3rd ed. A. W. Hayes. New York, NY, Raven Press: 1391-1418.

Mezey, P. G., Z. Zimpel, P. Warburton, P. D. Walker, D. G. Irvine, D. G. Dixon and B. M. Greenberg (1996). "A high-resolution shape-fragment MEDLA database for toxicological shape analysis of PAHs." J. Chem. Inf. Comput. Sci. 36: 602-611.

Mezey, P. G., Z. Zimpel, P. Warburton, P. D. Walker, D. G. Irvine, X.-D. Huang, D. G. Dixon and B. M. Greenberg (1998). "Use of quantitative shape activity relationships to model the photoinduced toxicity of polycyclic aromatic hydrocarbons: electron density shape features accurately predict toxicity." Environ. Toxicol. Chem. 17(7): 1207-1215.

Morgan, D. D., D. Warshawsky and T. Atkinson (1977). "The relationship between carcinogenic activities of polycyclic aromatic hydrocarbons and their singlet, triplet, and singlet-triplet splitting energies of phosphorescence lifetimes." Photochem Photobiol 25(1): 31-8.

Müller, A. M. F., V. Makropoulos and H. M. Bolt (1995). "Toxicological aspects of oestrogen-mimetic xenobiotics present in the environment." Toxicol. Ecotoxicol. News 2: 68-73.

Munkittrick, K. R. and E. A. Power (1989). An evaluation of the sensitivity of microassays relative to trout and daphnid acute lethality tests. Ottawa, ON, Canada., Environment Canada, River Road Environ. Technol. Centre.

Murty, J. S. and M. N. Das (1968). "Design and Analysis of Experiments with Mixtures." The Annals of Mathematical Statistics 39(5): 1517-1539.

Neff, J. M. (1979). Polycyclic aromatic hydrocarbons in the aquatic environment. London, Applied Science Publishers.

Neff, J. M. (1985). Polycyclic aromatic hydrocarbons in the aquatic environment. Fundementals of aquatic toxicology. G. M. P. Rand and S. R. Petrocelli. Washington, D.C., Hemisphere Publishing Co.

Netto-Ferreira, J. C. and J. C. Scaiano (1991). "Photochemistry of 1,2,3-indanetrione." Photochemistry and Photobiology 54(1): 17-21.

Newsted, J. L. and J. P. Giesy (1987). "Predictive models for Photoinducted Acute Toxicity of Polycyclic Aromatic Hydrocarbons to Daphnia Magna Strauss (Cladocera, Crustacea)." Environ. Toxicol. Chem. 6: 445-461.

Nikolaou, K., P. Masclet and G. Mouvier (1984). "Sources and Chemical Reactivity of Polynuclear Aromatic Hydrocarbons in the Atmosphere - A Critical Review." The Science of the Total Environment 32: 103-132.

Oris, J. T. and J. P. Giesy (1985). "The photoinduced toxicity of anthracene to juvenile sunfish (Lepomis Spp)." Aquatic Toxicol 6: 133-146.

Oris, J. T. and J. P. Giesy (1986). "Photoinduced Toxicity of Anthracene to Juvenile Blugill Sunfish (Lepomis Macrochirus Rafinesque): Photoperiod Effects and Predictive Hazard Evaluation." Environ. Toxicol. Chem. 5: 761-768.

Palisade Corporation (1990). Wiley registry of mass spectral data. Newfield, NJ, Palisade Corporation.

Pauli, W. (1924). Z. Phys. 31: 373, 765 (as cited in French and Taylor).

Payne, J. F., L. L. Fancey, A. D. Rahimtula and E. L. Porter (1987). "Review and perspective on the use of mixed function oxidase enzymes in biological monitoring." Comp. BNiochem Physiol 86 C: 233-245.

Payne, J. R. and C. R. Phillips (1985). "Photochemistry of petroleum in water." Environ. Sci. Technol. 19: 569.

Plaa, G. L. and M. Vézina (1990). Factors to consider in the Design and Evaluation of Chemical Interaction Studies in Laboratory Animals. Toxic Interactions. R. S. Goldstein, W. R. Hewitt and J. B. Hook. Toronto, Academic Press, Inc.: 4-30.

Plackett, R. L. and J. P. Burman (1946). "The design of optimum multi-factorial experiments." Biometrika 33: 305-325.

Plackett, R. L. and P. S. Hewlett (1963). "A unified theory for quantal responses to mixtures of drugs: The fitting to data of certain models for two non-interactive drugs with complete positive correlation of tolerances." Biometrics 23: 27-44.

Pöch, G., D. A. Dawson and R. J. Reiffenstein (1996). "Model Usage in Evaluation of Combined Effects of Toxicants." Ten 3(2): 51-59.

Rand, G. M., P. G. Wells and L. S. McCarty (1995). Introduction to aquatic toxicology. Fundamentals of aquatic toxicology: Effects, environmental fate, and risk assessment, 2nd. Ed. G. M. Rand. Washington, D.C., Taylor and Francis.

Ren, L., X. D. Huang, B. J. McConkey, D. G. Dixon and B. M. Greenberg (1994). "Photoinduced toxicity of three polycyclic aromatic hydrocarbons (fluoranthene, pyrene, and naphthalene) to the duckweed Lemna gibba L. G-3." Ecotoxicol Environ Saf 28(2): 160-71.

Ren, L., L. F. Zeiler, D. G. Dixon and B. M. Greenberg (1996). "Photoinduced effects of polycyclic aromatic hydrocarbons on Brassica napus (Canola) during germination and early seedling development." Ecotoxicol. Environ. Saf 33: 73-80.

Robinson, J. and J. M. Cooper (1970). "Method of determining oxygen concentration in biological media, suitable for calibration of the oxygen electrode." Anal. Biochem. 33: 390-399.

Saito, I. and T. Matsuura (1979). . Singlet oxygen. H. H. Wasserman and R. W. Murray. New York, NY., Academic Press: 511.

Sakai, M., D. Yoshida and S. Mizusaki (1985). "Mutagenicity of polycyclic aromatic hydrocarbons and quinones on Salmonella typhimurium TA97." Mutat Res 156(1-2): 61-7.

Sanathanan, L. P., E. T. Gade and N. L. Shipkowitz (1987). "Trimmed logit method for estimating the ED50 in quantal bioassay." Biometrics 43: 825-832.

Sanders, G., K. C. Jones, J. Hamilton-Taylor and H. Dörr (1993). "Concentration and deposition fluxes of polynuclear aromatic hydrocarbons and heavy metals in the dated sediments of a rural English lake." Environ. Toxicol. Chem. 12(1): 1567-1581.

Santodonato, J. (1997). "Review of the estrogenic and antiestrogenic acitivity of polycyclic aromatic hydrocarbons: Relationship to carcinogenicity." Chemosphere 34(4): 835-848.

Sasaki, J. C., J. Arey, D. A. Eastmond, K. K. Parks and A. J. Grosovsky (1997). "Genotoxicity induced in human lymphoblasts by atmospheric reaction products of naphthalene and phenanthrene." Mutat Res 393(1-2): 23-35.

Scheffé (1963). "The simplex-centroid design for experiments with mixtures." Journal of the Royal Statistical Society, B. 25: 235-263.

Scheffé, H. (1958). "Experiments with mixtures." Journal of the Royal Statistical Society, B.: 344-360.

Schirmer, K., D. G. Dixon, B. M. Greenberg and N. C. Bols (1998). "Ability of 16 priority PAHs to be directly cytotoxic to a cell line from the rainbow trout gill." Toxicology 127(1-3): 129-41.

Schoeny, R., T. Cody, D. Warschawsky and M. Radike (1988). "Metabolism of mutagenic polycyclic aromatic hydrocarbons, by photosynthetic algal species." Mutat. Res. 197: 289-302.

Siegl, W. O., R. H. Hammerle, H. M. Herrmann, B. W. Wenclawiak and B. Luers-Jongen (1999). "Organic emissions profile for a light-duty diesel vehicle." Atmospheric Environment 33(5): 797-805.

Silkworth, J. B., T. Lipinskas and C. R. Stoner (1995). "Immunosuppressive potential of several polycyclic aromatic hydrocarbons (PAHs) found at a Superfund site: new model used to evaluate additive interactions between benzo[a]pyrene and TCDD." Toxicology 105(2-3): 375-86.

Silverstein, R. M., G. C. Bassler and T. C. Morrill (1991). Spectrometric Identification of Organic Compounds. Toronto, John Wiley and Sons, Inc.

Smith, J. H., W. R. Mabey, N. Bohonos, B. R. Holt, S. S. Lee, T.-W. Chou, D. C. Bomberger and T. Mill (1978). Environmental pathways of selected chemicals in freshwater systems: Part II. Laboratory studies. Athens, GA, U.S. Environmental Protection Agency.

Smith, M. T. (1985). "Quinones as mutagens, carcinogens, and anticancer agents: introduction and overview." J Toxicol Environ Health 16(5): 665-72.

Smolarek, T. A., S. L. Morgan, C. G. Moynihan, H. Lee, R. G. Harvey and W. M. Baird (1987). "Metabolism and DNA adduct formation of benzo[a]pyrene and 7,12- dimethylbenz[a]anthracene in fish cell lines in culture." Carcinogenesis 8(10): 1501-9.

Snee, R. D. and D. W. Marquardt (1976). "Screening concepts and designs for experiments with mixtures." Technometrics 18: 19-29.

Spiegel, M. R. (1981). Applied differential equations. Toronto, Prentice-Hall of Canada, Ltd.

Sprague, J. B. (1965). "Lethal levels of mixed copper-zinc solutions for juvenile salmon." J. Fish Res. Bd. Can. 22: 425-432.

Stevens, B., S. R. Perez, J. A. Ors and M. L. Pinsky (1974). "The photoperoxidation of unsaturated organic molecules. O_2 $^1\Delta_g$-acceptor re-encounter probabilities." Chem. Phys. Lett. 27: 157-160.

Suess, M. J. (1976). "The environmental load and cycle of polycyclic aromatic hydrocarbons." Science of the Total Environment 6: 239-250.

Tammes, P. M. L. (1964). "Isoboles, a graphic representation of synergism in pesticides." Neth. J. Plant Pathol. 70: 73-80.

Thornton, S. C., L. Diamond and W. M. Baird (1982). "Metabolism of benzo[a]pyrene by fish cells in culture." J Toxicol Environ Health 10(1): 157-67.

Timbrell, J. A. (1991). Principles of Biochemical toxicology. Washington, D.C., Taylor and Francis.

152

Tingle, M. D., M. Pirmohamed, E. Templeton, A. S. Wilson, S. Madden, N. R. Kitteringham and B. K. Park (1993). "An investigation of the formation of cytotoxic, genotoxic, protein- reactive and stable metabolites from naphthalene by human liver microsomes." Biochem Pharmacol 46(9): 1529-38.

Unkelbach, H. D. and T. Wolf (1985). "Dose-response analysis of combination preparations." Stat. Med. 4: 77-85.

van Brummelen, T. C. (1995). Distribution and ecotoxicity of PAHs in forest soil. Faculteit der biologie. Amsterdam, Netherlands, Vrije Universiteit van Amsterdam: 173.

van Brummelen, T. C. (1998). Bioavailability and Ecotoxicity of PAHs. The Handbook of Environmental Chemistry Vol. 3 Part J

PAHs and related Compounds. A. H. Neilson. Berlin, Springer-Verlag. 3: 203-263.

Van Brummelen, T. C., C. A. M. Van Gestel and R. A. Verweij (1996). "Long-term toxicity of five polycyclic aromatic hydrocarbons for the terrestrial isopods Oniscus asellus and Porcellio scaber." Environ. Toxicol. Chem. 15: 1199-1210.

Van der Oost, R., F. J. Van Schooten, F. Ariese, H. Heida, K. Satumalay and N. P. E. Vermeulen (1994). "Bioaccumulation, biotransformation, and DNA binding of PAHs in feral eel (Anguilla anguilla) exposed to polluted sediments- a field survey." Environ. Toxicol. Chem. 13: 859-870.

van Wezel, A. P., D. A. de Vries, D. Sijm and A. Opperhuizen (1996). "Use of the lethal body burden in the evaluation of mixture toxicity." Ecotoxicol Environ Saf 35(3): 236-41.

Varanasi, U. (1989). Metabolism of polcyclic aromatic hydrocarbons in the aquatic environment. Boca Raton, FL, CRC Press.

Wan, M. T. (1994). "Utility right-of-way contaminants: Polycyclic aromatic hydrocarbons." Journal of Environmental Quality 23: 1297-1304.

Wiberg, K. B. (1997). "Properties of Some Condensed Aromatic Systems." J. Org. Chem. 62: 5720-5727.

Wilkinson, L. (1994.). SYSTAT, Version 5.05 for Windows. Evanston, IL, USA., Systat Inc.

Wilkinson, L. (1998). SYSTAT 8.0. Evanston, IL, SPSS Inc.

Wilson, A. S., C. D. Davis, D. P. Williams, A. R. Buckpitt, M. Pirmohamed and B. K. Park (1996). "Characterisation of the toxic metabolite(s) of naphthalene [published erratum appears in Toxicology 1997 Jun 6;120(1):75]." Toxicology 114(3): 233-42.

Zafiriou, O. C. (1977). "Marine organic photochemistry previewed." Mar. Chem. 5: 497.

Zepp, R. G. and P. F. Schlotzhauer (1979). Photoreactivity of Selected Polycyclic Aromatic Hydrocarbons in Water. Polynuclear Aromatic Hydrocarbons. P. W. Jones and P. Leber. Ann Arbor, MI, Ann Arbor Science Publishers: 141-158.

Zheng, J., M. Cho, A. D. Jones and B. D. Hammock (1997). "Evidence of quinone metabolites of naphthalene covalently bound to sulfur nucleophiles of proteins of murine Clara cells after exposure to naphthalene." Chem Res Toxicol 10(9): 1008-14.